



**NTNU – Trondheim**  
Norwegian University of  
Science and Technology

# Link Budget for NTNU Test Satellite

**Brenda Lidia Escobar  
Mendez**

Master of Science in Communication Technology

Submission date: July 2013

Supervisor: Torbjørn Ekman, IET

Co-supervisor: Roger Birkeland, IET

Norwegian University of Science and Technology  
Department of Electronics and Telecommunications



## **Problem statement**

Link Budget results an essential tool not only for the establishment of communication. Designing of components, setting-up of the Earth station, analyzing quality of downloaded data, for instance, require knowing information of the link capacity. It has derived in different calculations to obtain Link Budget since the NUTS project started, made from different subsystems perspectives that once had been done and link information was used calculation remained with the initial theoretical values and assumptions. Taking in account updates, and even components installed, in conjunction with a tracking analysis, will lead to more realistic results and then let introduce more complex concepts on transmitted message in order to improve the performance, modulations schemes and error control will be treated. Combinations of those transmission techniques should be within restrictions of NTNU Test Satellite.



## **Preface**

This thesis is the result of the participation on NUTS project during spring 2013. The satellite student project is developed at NTNU that involves to the Norwegian Center for Space related to Education, NAROM and. Students from different departments of the University take a part on the different subsystems and within the complete process, they are involved on designing, analysis, testing until launching, it let to take experience on-hands and work in their master's thesis at the same time.

The interdisciplinary characteristic of the project turns it interesting and challenging as well, it implied acquiring knowledge related to the different involved areas due to direct implications with the communication systems, and even in general terms about satellites technologies, so, weekly meetings with NUTS teamwork resulted profitable. Furthermore, develop a practical work of thesis implies a painstaking judgment of results to make inferences in addition to theoretical comprehension; launching is planned for 2014 and results obtained henceforth will have impact in the performance of NUTS in orbit.

Achieve the objective of this work entailed the participation of different people. I would like to thank my supervisor Torbjørn Ekman for his proposal and conduct me to this thesis topic according to my interests, to be patient and take the time for technical explanations, beyond this work his support and orientation has resulted fruitful on my academic formation. Participation with NUTS team has been rewarded, I am grateful with them for their contribution to acquire practical knowledge about satellites and to understand the project, the disposition to provide data needed in this work is valued as well. I should thank to other students that have taken a part previously; results of their works are also reflected here. Special thanks to Roger Birkeland, the project manager, for let me join in the group and supply with all the essential information for this thesis, his comments and suggestions has been useful along this time.

I also would like to thank my family, to my parents for the effort they have done over the years, for the gift of education, their advices and confidence; this achieved goal is also yours; to my sisters and niece for their enthusiasm and unconditional support in each plan traced. Finally but not less important, I thank my master's colleagues from Universitat Politècnica de València (Polytechnic University of Valencia) for the mutual aid and fellowship, and for the long and profitable hours at Student's Home.



## Abstract

The NTNU Test Satellite, NUTS, is the project of Norwegian University of Science and Technology developed in the academic ambience of CubeSat scheme. Outset had placed three years ago and the plan is to be launched by 2014. Communication system has been previously studied and frequencies allocations were defined on VHF and UHF bands, the channel will carry information of TT&C, commands from station and response from satellite besides transferring of data generated by the payload. Then, analysis in this work was focused on down direction, in terms of power results more critical since transmitted power at spacecraft is restricted.

At first, Friis formula was adapted to obtain the basic equation which leads to the power transmitted, then, losses were introduced to figure out the performance along the trajectory of NUTS. Satellite link is vulnerable to different factors, ionospheric and atmospheric attenuation and its influence on wave polarization, losses resulting from misalignment of antennas, free space loss depending on the slant range that makes crucial a geometric analysis of the track. It was included to determine the impact of satellite motion along the orbit in the parameters of link budget equation. In addition noise system directly related with temperature and noise figure of the different elements is determinant on final results. Characteristics of devices in the receivers at each end were taken into consider to model the equivalent noise circuit, then, equations for NUTS noise system at each end were obtained.

A simple spreadsheet was first used to know the energy per bit received at Earth station when both antennas are straight pointing each other. Nevertheless, obtain the values under tracking implied more variables, like antenna radiation pattern and its respective gain, that is not as reachable to reckon on simple calculus. In this point, a template in Matlab was used which involves different functions as parameters varying through spacecraft trajectory. Once energy per bit to noise ratio was obtained measurement of link quality was depicted by introducing error probability as the most appropriate parameter on digital communications. Link margin by using binary modulation schemes on frequency and phase were calculated, theoretical probability and simulations by means iterations of bit error probability were compared for the energy per bit received in a range of elevation angles. Furthermore, the fading conditions prompted implementation of forward error control; combinations under the NUTS constraints were studied by using block codes. Bit Error Probability by transmitting a coded message was obtained involving codes Hamming and Reed Solomon, scenario was varied for different bandwidth and symbol rate. Those parameters had an important role for this student satellite and restrictions implied.

Finally, visibility time was obtained, defined parameters for transmission and devices chosen complaining with link budget results were used as input data on Satellite Tool Kit software, simulations of tracking were done in a period of one week, data generated related to access time was read in Matlab script and visibility time for different height computed. A previous study of the radio packet with AX.25 protocol was used as a base to estimate the transferred images per day that can be reached when different elevation angles are chosen as minimum. Link margin decreases at low elevation angles, then, a balance between modulation and error control, should be found. Different suitable scenarios are proposed here.





# Contents

<b>Chapter 1. Introduction.....</b>	<b>1</b>
1.1 The NUTS Project.....	1
1.2 Outline.....	2
<b>Chapter 2. NUTS Specifications .....</b>	<b>4</b>
2.1 Satellite Classification .....	4
2.2 The CubeSat Standard.....	4
2.3 NUTS Overview .....	5
2.3.1 Radio Specifications .....	5
2.3.2 Antennas .....	6
2.3.3 ADCS .....	6
2.4 Orbital elements .....	7
<b>Chapter 3. Propagation Theory .....</b>	<b>11</b>
3.1 Ionospheric Effects .....	11
3.1.1 Faraday rotation .....	12
3.1.2 Group delay.....	12
3.1.3 Dispersion .....	12
3.1.4 Ionospheric Scintillation .....	13
3.2 Antenna Parameters .....	13
3.2.1 Power flux density .....	14
3.2.2 Gain.....	14
3.2.3 Radiation pattern and angular beamwidth .....	15
3.2.4 Polarization .....	15
3.2.5 Polarization loss factor.....	15
3.2.6 Pointing loss.....	16
3.3 The dipole antenna.....	17
3.4 The Friis equation .....	17
3.5 Radio Noise.....	17
3.5.1 Thermal Noise.....	18
3.5.2 Noise Figure and Noise Temperature .....	18
3.5.3 Antenna noise temperature .....	19
<b>Chapter 4. Modulation Schemes .....</b>	<b>21</b>
4.1 Digital baseband signals .....	21
4.2 Digital carrier modulation.....	22
4.3 Modulation schemes .....	22

4.3.1 FSK.....	22
4.3.2 PSK.....	23
4.3.3 Bit Error Probability .....	24
<b>Chapter 5. Link Budget.....</b>	<b>26</b>
5.1 Link budget basic equation.....	26
5.2 Additional losses .....	27
5.3 Noise System .....	28
5.3.1 LNA and line noise temperature .....	30
5.3.2 Antenna noise temperature .....	31
5.4 Carrier to Noise Ratio.....	32
5.5 Tracking analysis.....	33
5.5.1 Pointing loss .....	34
5.5.2 Propagation losses .....	35
5.5.3 Polarization Loss Factor .....	37
5.6 Link Budget Calculation.....	37
5.6.1 Downlink .....	38
5.6.2 Uplink.....	38
5.7 Link Margin.....	38
5.8 Error control .....	41
5.8.1 Gain coding .....	42
5.8.2 Block code.....	42
5.9 Results and discussion.....	45
<b>Chapter 6. Communications System Overview .....</b>	<b>48</b>
6.1 NUTS Communication Layer.....	48
6.2 Earth Communication System.....	48
6.3 On board Communication System.....	49
6.4 Communication Protocol.....	51
6.5 Downlink Capacity .....	53
<b>Chapter 7. Software Tools .....</b>	<b>56</b>
7.1 Matlab Implementation .....	56
7.2 Satellite Tool Kit Simulation.....	58
7.2.1 Losses and propagation models.....	59
7.2.2 Equipment Considerations .....	60
<b>Chapter 8. Conclusions and Future Work .....</b>	<b>63</b>
8.1 Conclusions .....	63
8.2 Future Work.....	64
<b>A Link Budget.....</b>	<b>69</b>
<b>B Matlab Scripts .....</b>	<b>71</b>
B.1 Bit Error Probability .....	71
B.2 Link Budget .....	75
B.3 Visibility time .....	82
B.4 Link Data Text File.....	85
<b>C STK Link Budget.....</b>	<b>87</b>

<b>D Datasheets .....</b>	<b>88</b>
---------------------------	-----------

# List of Figures

2.1 NUTS in its Coordinate system .....	7
2.2 NUTS points to the center of the Earth .....	7
2.3 Satellite orbital elements .....	8
3.1 Misalignment between receiver and transmitter antennas.....	16
4.1 FSK Modulation and demodulation diagram .....	23
4.2 PSK Modulation and demodulation diagram .....	23
5.1 Diagram of NUTS Earth station receiver .....	29
5.2 Equivalent diagram for NUTS Earth station receiver .....	29
5.3 Equivalent diagram for NUTS Satellite receiver.....	30
5.4 Geometry of elevation angle.....	33
5.5 NUTS elevation angle for height of 600 km .....	35
5.6. Losses due to Scintillation and Cloud&Fog for NUTS system.....	37
5.7 Bit error rate as a function of $E_b/N_0$ .....	40
5.8 Block diagram for a coded message with FEC.....	41
5.9 $E_b/N_0$ vs BER for different codes and modulations .....	44
5.10 $E_b/N_0$ vs BER for 4-PSK.....	44
5.11 $E_b/N_0$ received at 600km .....	46
5.12 Link Margin along NUTS trajectory .....	46
6.1 NUTS Communication System layers.....	48
6.2 NUTS Satellite communication system diagram.....	50
6.3 ADF7020-1 FSK Correlator/Demodulator Block Diagram .....	50
6.4 ADF7020-1 FSK Modulator Block Diagram .....	51
6.5 NUTS AX.25 Radio Packet.....	52
6.6 Visibility time at 145.9 MHz.....	53
7.1 $E_b/N_0$ vs Bit Error Probability for FSK and PSK modulation.....	56
7.2 Output graphs generated by <code>link_budget.m</code> .....	57
7.3: Elevation angle vs. $E_b/N_0$ .....	58
7.4: NUTS satellite tracking simulated on STK .....	60
7.5: $E_b/N_0$ along the pass for height of 600 km.....	61
7.6: $E_b/N_0$ vs elevation angle at height of 600 km .....	61

# List of Tables

2.1 Satellite classification by mass criterion .....	4
2.2 Specification summary of dipole antenna .....	6
5.1 Passive losses at Satellite receiver .....	28
5.2 Passive losses at Earth station receiver .....	28
5.3 Empirical atmospheric losses for frequencies below 2 GHz .....	36
5.4 Ionospheric losses for NUTS system .....	36
5.5 Combinations of polarizations with RHCP at NUTS Earth station .....	37
5.6 Typical combinations for Hamming and Reed Solomon codes .....	43
5.7 Values reached with Binary and 4-ary modulation .....	43
5.8 Proposed combinations for NUTS system .....	43
5.9 Link Margin for NUTS using uncoded binary modulation .....	45
5.10 Link Margin for NUTS using 4-PSK and Hamming code .....	45
6.1 Data budget with a rate of 9600 bps .....	54
6.2 Data budget with a rate of 1800 bps .....	54
6.3 Images transferred per day for different minimum elevation angles .....	54
7.1 Sample file of Antenna Noise Temperature .....	59

# List of Acronyms

ADCS	Attitude Determination Control System
AR	Axial Ratio
ARQ	Automatic Repeat Request
AWGN	Additive White Gaussian Noise
BER	Bit Error Rate
BFSK	Binary Frequency Shift Keying
BPSK	Binary Phase Shift Keying
CRC	Cyclic Redundancy Check
CSP	CubeSat Space Protocol
DPCM	Differential Pulse Code Modulation
EIRP	Effective Isotropic Radiated Power
FEC	Forward Error Correction
FSK	Frequency Shift Keying
FSPL	Free Space Path Loss
GEO	Geostationary Earth Orbit
GISM	Global Ionospheric Scintillation Model
HiN	Narvik University College
HMAC	Hash-based Message Authentication Code
IARU	International Amateur Radio Union
IF	Intermediate Frequency
IR	Infrared
ISI	Intersymbol Interference
ITU	International Telecommunication Union
LEO	Low Earth Orbit
LHCP	Left Hand Circular Polarized
LM	Link Margin
LNA	Low Noise Amplifier
MCU	Microcontroller Unit
MEO	Medium Earth Orbit
NAROM	Norwegian Centre for Space related Education,
NASA	National Aeronautics and Space Administration
NF	Noise Figure
NRZ	Non Return to Zero
NTNU	Norwegian University of Technology and Science
NUTS	NTNU Test Satellite
OBC	On Board Computer
PLF	Polarization Loss Factor
PLL	Phase Locked Loop
P-POD	Poly Pico-Satellite Orbital Deployer
PSK	Phase Shift Keying

RAAN Right Ascension of the Ascending Node  
RF Radio Frequency  
RHCP Right Hand Circular Polarized  
RRC Root Raised Cosine  
RZ Return to Zero  
SNR Signal to Noise Ratio  
SR Stack-run  
STK Satellite Tool Kit by Analytical Graphics, Inc.  
TEC Total Electron Content  
TT&C Telemetry, Tracking and Command  
UHF Ultra High Frequencies  
UiO University of Oslo  
VHF Very High Frequencies





# Chapter 1

## Introduction

### 1.1 The NUTS Project

The NTNU Test Satellite is a CubeSat project developed by students from different areas in the Norwegian University of Science and Technology. It is also managed by the Norwegian Centre for Space related Education, NAROM and takes a part of the national student satellite program which also involves the University of Oslo (UiO) and Narvik University College (HiN). Following the standard, NUTS will be a double CubeSat and launching is planning by 2014. One of the main goal is education since is performed as a part of the student's project and master thesis, furthermore establishing and keeping two-ways communication, transmit a beacon signal receivable for radio amateurs, implementation of an internal RF communication link, observing the atmospheric gravity waves located at mesosphere [3] are part of the aims for NUTS satellite as well.

Analysis of communications system and performance of the link results critical in this project and on satellite scenarios, in general. The mere fact of setting up communication between Earth Station and NUTS will mean an important successful of the project that take relevance for data transmission generated by the payload. Communication system has been analyzed before this work and previous link budget were calculated as well since the beginning of NUTS project such is required, nevertheless, they were done before Earth station were installed and the last documented work about was realized for design of spacecraft antenna [6], thus that calculation does not involves parameters resulting of that master project. The present work intent to update all the variables, constraints and conditions implicated on communication NUTS system and calculate the link budget along tracking trajectory, once results of energy per bit is obtained, an analysis of modulation schemes with and without FEC are included that yield on proposals for satellite system and finally the downlink capacity is calculated depending on visibility time and taking in account the distribution of radio packet on AX.25 protocol.

## 1.2 Outline

Chapter 2 gives a brief reference of CubeSat standard, then defined parameters for NUTS are indicated, these have been separated by subsystem and just relevant for link budget are mentioned.

Chapter 3 introduces the phenomena that affect radiowave propagation on satellite communication. Concepts related to noise system and modulation schemes are also included from theoretical perspective, in addition, basic terms related to modulation and digital transmission are introduced in Chapter 4.

Chapter 5 contains the procedure followed to obtain the energy per bit ratio received on downlink direction. Analysis of the tracking and how it affects the parameters of link budget is also explained, then, error probability and bit error rate are compared for different modulations schemes by using block codes.

Chapter 6 offers an overview of NUTS Communications Systems from the layers model perspective. Commercial devices for spacecraft are proposed and process for link communication is analyzed focused on modulator and demodulator of these components. Then AX.25 protocol is introduced and, based on previous works, a distribution of the radio packet is presented to calculate the downlink capacity.

Chapter 7 includes a description of scripts implemented in Matlab and how they were used throughout this work. Results from Satellite Tool Kit simulations and criteria for input data are in this section as well. Finally Chapter 8 submits conclusions of the complete work and proposals for future work.



# Chapter 2

## NUTS Specifications

NUTS project comes up in the framework of CubeSat standard. At first a reference of sizes of satellites is given to locate the CubeSat in the world of satellites and also to stand out the importance of picosatellites in academic environment, some specifications related to the standard are included. Then, subsystem and general characteristics of NUTS are summarized; information included provides useful data for calculus in posterior Chapters.

### 2.1 Satellite classification

At the beginning of the space industry, satellites were small, because of necessity. Then, during the next two decades, custom designs for a particular mission led to methods with rather long times for requirements before implementation, subsystems designed separately which required important modifications for one satellite to another. Although it implies spacecraft extremely capable to fulfill its mission, modular, low cost and small designs are the current trend. It represents an opportunity for academic institutions and small organizations access to space.

Artificial satellites have many different ways to be classified, by function, type of orbit, cost, performance, size, and this last has a bearing in the cost, such that in academic ambit is the most relevant factor. The Table 2.1 shows a version of satellite classification by mass criterion [1].

Table 2.1: Satellite classification by mass criterion

Satellite class	Mass
Large Satellite	>1000 kg
Minisatellite	100-1000 kg
Microsatellite	10-100 kg
Nanosatellite	1-10 kg
Picosatellite	0.1-1 kg
Femtosatellite	1-100 g

### 2.2 The CubeSat Standard

The CubeSat, in the category of picosatellite, was developed in an academic ambit, to provide a standard reduced in cost and development time. Furthermore,

as an option to students acquire some experience in satellites process, designing, testing and launching. According to the standard, a single CubeSat must have dimensions of 10x10x10 cm, a cube with a mass of up to 1.33 kg, each triple CubeSat shall not exceed 4.0 kg mass. It must fulfill general requirements, as well, during launch all parts shall remain attached to the CubeSats, pyrotechnics is not permitted, and not be used hazardous materials. For the main structure and the rails, aluminum shall be employed. Other mechanical specifications are detailed in [2].

### **2.3 NUTS Overview**

The system of NUTS is distributed in hardware, meaning different subsystems, such as the OBC, ADCS and radio subsystem, will have their own MCUs, the generic and modular design chosen allow supporting different payloads. To meet the goal of observing gravity waves, an IR camera as a payload will be installed. It should provide images, enough in quality and quantity that let analyzes the properties of the waves. Images compression was analyzed at [4] finding out the video coding with three-dimensional DPCM combined with a dead-zone quantizer and SR coding can provide 0.83 bits per pixel. A different backplane will be implemented in order to enhance the power and data buses, cards can be slotted to provide access to the different subsystems, the OBC, ADCS and radio subsystem. The on-board OBC is a 32-bit AVR32 UC3 micro controller whose computing capacity also supports payloads in other missions. As another novelty, the structure of the NUTS will be made on composite material instead of aluminum typically used on this kind of projects [5].

#### **2.3.1 Radio Specifications**

Practically every CubeSat in operation are in the range of UHF and VHF being enough for currently missions. Transmission in higher frequencies would demand a larger transmit power because of the losses along the path, in addition antennas can be relatively small. On this project, amateur radio frequencies will be used. Links will transmit with less than 1 watt of power. In addition, some other restrictions like the region must be considered to select the central frequencies, and is that Norwegian amateur radio bands corresponds the segment between 144-146 MHz for VHF and 432-438 MHz for UHF. It is planned that NUTS satellite communication will be established by two transceivers, so, central frequencies in the mentioned range has been selected in this work, 145.9 MHz and 438 MHz. Spacecraft antennas were analyzed in previous work using different central frequencies, for VHF band a tolerance of 0.2 MHz to obtain the same performance is allowed and for UHF if a new central frequency within the IARU UHF range is chosen, it does not alter the antenna efficiency [6], frequencies chosen are in the range of tolerance and the change does not represent a drawback. Is not yet defined which band will be used for uplink and downlink, here, calculations have been done in both bands for downlink of housekeeping and payload data, use of AX.25. The Amateur Packet Radio Link Layer Protocol is proposed to send the packet information, it accept and reliably deliver data in communications link between two points. Detailed conformation of the frame will be covered in the last part of this work. A bandwidth of 25 KHz was defined and used for antenna

design [6 7], so, it will be the same in the present link budget although it was found that the mismatch loss remains the same in a 7 MHz bandwidth.

### 2.3.2 Antennas

From the three types of antennas analyzed in [6], performance of the VHF turnstile and VHF dipole were similar along the trajectory for different elevations angles although turnstile presents a higher link margin than dipole, so it was suggested for NUTS in that previous work. Nevertheless, dipoles patterns share characteristics with an analytical pattern and it was used for simulations, even there is a slightly deformed respect to the real model. Design of dipoles is less complex than turnstile and its gain is near-isotropic. Monopoles antennas were also analyzed and its performance yielded low link margin results for low elevations angles. A comparison graph between link margin with different antennas can be found in [6] simulated with theoretical parameters, it was done just as a tool for the antenna design. So, a single dipole antenna was chosen as a feasible option for NUTS in the present job. In addition, mismatch and excess insertion from were obtained from antenna design work where dipole link margin were calculated before design and analysis, assuming passive losses of 1.1 dB. Nevertheless, a summary of these losses were figure out for turnstile antenna once simulations were done. Considering that, for an elevation angle of  $90^\circ$  there is a difference of 3 dB corresponding to passive losses between dipole and turnstile antenna, characteristic values for dipole are indicated in the Table 2.2.

Table 2.2: Specification summary of dipole antenna

Parameter	VHF	UHF
Center Frequency	145.9 MHz	438 MHz
Wavelength	206 cm	69 cm
Radio bandwidth	25 kHz	25 kHz
Passive losses	5.9 dB	6.7 dB

### 2.3.3 ADCS

The Attitude Determination Control System, ADCS, is required in the satellite to maintain the correct orbit and attitude with respect to the Earth for continuous communication. ADCS-system version of NUTS is similar to other systems; it will employ magnetic torquers in the form of coils wound inside the frame [12]. The sensors used are a gyro, magnetometer and the solar panels will be used as sun sensors [13]. Different estimator algorithms and regulators are currently developed and tested [14 15]. Most recent results [16] have yielded an estimated accuracy of 1-2 degrees off and tracking accuracy of  $\pm 5$ ,  $\pm 5$ ,  $\pm 10$  in Euler angles which is the result of selected combinations of rotations about X, Y and Z axes [17]. Time to adjust the pointing direction around 3-4 orbits depends on the initial angular velocity. A representation of NUTS body in the coordinate system is shown in figure 2.1.

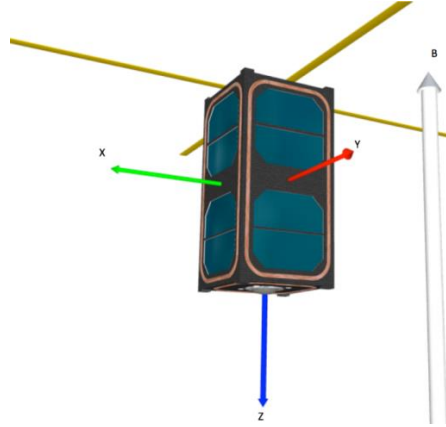


Figure 2.1: NUTS in its Coordinate system, B refers to magnetic field vector. From [15]

Another interesting point for communication establishment is the concern of spinning of satellite, ADCS design consider that spacecraft pointing to Earth center around the entire trajectory [16], as is illustrated in figure 2.2; so, in the tracking analysis it let avoid outages and fading during visibility due to antenna rotation that would occur if satellite will be rolling on it.

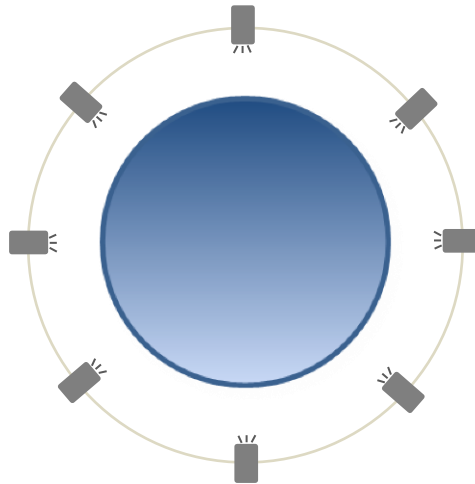


Figure 2.2: NUTS points to the center of the Earth along the trajectory.

## 2.4 Orbital elements

Satellite rotation can be described by the relative movement of two point bodies considering that the mass of the spacecraft is smaller than the mass of the earth and also assuming that there are on free space. Movement is analyzed by using Newton's second law and Newton's law of gravitation [9]. Applying mathematical procedures, an equation that defines the radius of the satellite is obtained; it corresponds to the orbit  $r_0$ .

$$r_0 = \frac{p}{1 + e \cos(\theta - \theta_0)} \quad (1.1)$$

Where  $\theta_0$  is a constant that takes the value of zero when the radius is oriented with respect to the orbital plane axes.  $p$  is a focal parameter that determines the size of the orbit.  $e$  refers to eccentricity. Orbit is an ellipse if  $e$  has a value

between 0 and 1,  $e$  is equal to 1 orbit is a parabola and for values higher than 1 it is a hyperbola. When  $e$  is equal to zero the orbit is circular. To describe the orbital parameters of communications satellites some elements have been defined and wide explained in specialized text [9 10 11], for NUTS satellites, they had been determined and link performance has been analyzed maintaining some and varying other ones to expose the difference and the reached capacity varying those elements. Orbits, in general terms, are considered as ellipses whose shape are described by *Semi-major axis* and *eccentricity*, for NUTS satellite that will describe a Polar Orbit, eccentricity is considered as zero since corresponds to a circular trajectory, major semi-axis corresponds to mean Earth radius plus height satellite, around 6971 km if 600 km height is selected. Polar orbit are used on sensing and collecting data services due to the satellite can scan, along the trajectory, all the Earth on a period cycle.

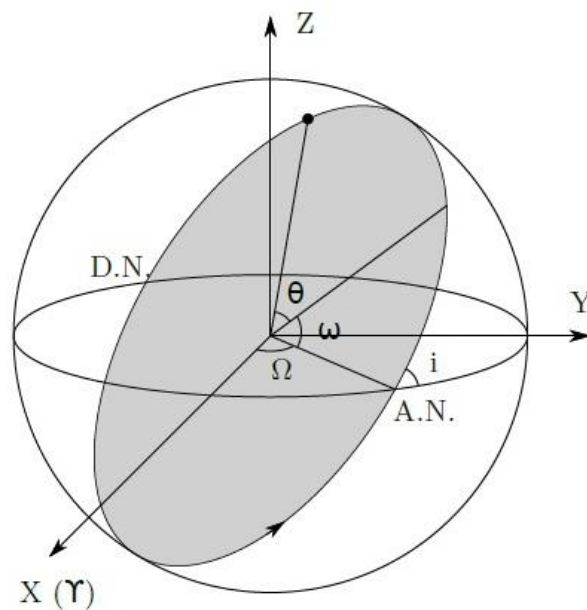


Figure 2.3: Satellite orbital elements. From [6]

Position of the orbit plane in space is specified by the *inclination*  $i$  and the *Right Ascension of the Ascending Node* also denoted as RAAN or  $\Omega$ . Both parameters are indicated in the figure 2.3 where one can observe that  $i$  refers to the angle at the ascending node counted positively in the forward direction between normal to the line of nodes in the orbital plane and to the line of nodes in the orbital plane [9], a polar orbit has an inclination close to  $90^\circ$ , more exactly  $98^\circ$  if one considers the oblateness of the Earth. When inclination is greater than  $90^\circ$ , like in NUTS case, orbit is called a retrograde because satellite is rotating westward in the contrary direction to the Earth. RAAN, refers the angle taken measured from  $0^\circ$  to  $360^\circ$  in the forward direction between the reference direction and that of the ascending node of the orbit [9], describing the rotation of the plane along the z axis. If perturbations are not taken in account, the orbital plane will be rotating around the Earth covering all with around 12 or 14 passes per day [6], remained in a fixed orbital plane. In addition, *time of perigee* and *argument of perigee* ( $\omega$ ) are elements in the orbital definition. Perigee specifies the closest approach to the Earth; in a circular orbit it can acquire relevant importance if one considers the



oblateness of the Earth, external forces and conditions that modifies the circular shape.

NUTS will be positioned in a Low Earth Orbit, although range of height for LEO orbit is not exactly defined values are roughly 160 to 2500 km, and some remarkable advantages is that due to are near of the Earth, talking in spatial terms, path losses are lower than other orbits, MEO or HEO for instance, besides, propagation delay is less for the same reason. It means that in this orbits signal transmitted and received is strength, images with adequate quality could be sent. It is also suggested for covering locations in high altitudes like polar zones. Nevertheless its period of time is short due is sweeping across the space all the time, this movement let contact the satellite and reach a theoretical value between 8 to 10 minutes per access [11]. In summary, small power, small antenna size and less energy to be inserted in this orbit result suitable for low cost spacecraft.



# Chapter 3

## RF Propagation Theory

The analysis of performance of link satellites results a complex process by the fact that many parameters are involved in ends, reception, transmission and the media with its special conditions. Each of these variables requires a certain compromise to obtain the best link performance. This chapter introduces the factors that affect the signal along the path from the transmitter until it reaches the receiver and yields to some useful assumed values for NUTS link budget.

### 3.1 Ionospheric Effects

Along the trail followed by the signal, between earth station and a satellite, radiowave suffers different modifications cause to environmental conditions and variety of propagation phenomena, path cross the different atmospheric and ionospheric layer which produces variations in the signal most of them uncontrolled although possible to predict by means propagation models and numerical methods. Variations and distortions produced in amplitude, phase, polarization, time delay, are also influenced by the frequency of operation and elevation angle causing greater impact at highest frequencies and lower elevations.

The frequency is an important parameter which determines impacts on satellite-earth links. Ionosphere is divided in layers D, E and F, regions depends on the altitude, and in the case of signal below about 30 MHz space communications is not possible due to absorption and reflection. Increasing frequency above about 30 MHz permit propagation although properties of the signal will suffer modifications and here location, time and epoch of year are variables implied. For frequencies higher than 3 GHz ionospheric effects does not have an important influence.

ITU R-P.531-11 describes four different ionospheric effects, rotation of the polarization and as secondary consequences, time delay and direction of arrival also changes, random ionospheric patches which are nondeterministic processes, group velocity dispersion caused by no linearity of electron density with frequency and the main effect called scintillation produced due to performance of irregularities as lens that distortion the amplitude, phase and angle of arrival of the wave. The ionosphere is a layer that contains gas and charged particles, located around 50 to 2000 km above earth's surface, such that the parameter defining the degradation entailed by this layer is the electron

concentration or total electron content, TEC. Free electrons and positive ions are contained in the ionosphere and in the lower region only a part of the molecules are ionized and most of them are neutral so that free electrons bias radiowave propagation.

TEC amount varies with the altitude, for each D, E, or F layer, quantity increases at higher altitudes although not linearly since also depends on sunspot cycle and solar activity. Geomagnetic storms and latitude also carry weight being mid latitude the most homogeneous region and high latitudes a fitful zone due to proximity to aurora region. Nevertheless a method to find out the electron concentration has been developed [20].

Total electron content can be defined as the number of electrons presents along a column having a cross section of  $1 \text{ m}^2$  [20] which has the same position that the path between two points.

$$N_T = \int_s n_e(s) ds \quad (3.1)$$

where:

$s$  is the propagation path [m]

$n_e$  is the electron concentration [el/m<sup>3</sup>]

Ionospheric alterations on propagation are mainly proportional to TEC amount.

### 3.1.1 Faraday rotation

Geomagnetic field and anisotropy of the medium produces that a wave crossing the ionosphere present a rotation in its polarization sense. This phenomenon depends on frequency operation being more relevant on VHF band and waves linearly polarized, and is directly proportional to TEC along the path. In order to minimize the Faraday rotation effects electric or mechanic adjustment of the polarization is done, also using a circular polarization is a common solution. This last option will be used for NUTS and had been taken in account for link budget calculations and simulations in the present work.

### 3.1.2 Group delay

Group delay refers to the additional time that takes the radiowave to be propagated through the ionosphere due to the presence of charged particles, propagation velocity suffers a reduction and trail time increases reciprocally to the frequency squared and proportional to electron concentration. Graph included on [20] depicts the ionospheric time delay in a range of 0.1 to 3 GHz. For frequencies close to 130 MHz variation group delay is between 0.08  $\mu\text{s}$  to 8  $\mu\text{s}$ , and in the case of 450 MHz band, time delay is range 0.006  $\mu\text{s}$  to 6  $\mu\text{s}$ , electron concentration given of  $10^{16}$  to  $10^{19}$  el/m<sup>2</sup> in both cases.

### 3.1.3 Dispersion

Dispersion is produced by propagation delay in a radiowave with significant bandwidth; it is a function of frequency and represents the difference in the time delay between the lower and upper frequencies of the spectrum which signal is transmitted. It is proportional to TEC amount and inversely proportional to

frequency cubed, it means that delay decreases when frequency increases and also with decreasing pulse width transmitted. A concept introduced on this point refers to coherence bandwidth described as the channel capacity that the RF carrier can support due to ionospheric dispersion, common values are in the order of some gigahertz. Coherence bandwidth is not a design parameter,

### 3.1.4 Ionospheric Scintillation

Irregularities in electron density along the path in the ionosphere cause rapid amplitude and phase fluctuations of the microwave, apparent direction of arrival is changed as well. Scintillation index denoted as  $S_4$  is the parameter used to measure these fluctuations.

$$S_4 = \left( \frac{\langle I^2 \rangle - \langle I \rangle^2}{\langle I \rangle^2} \right)^{1/2} \quad (3.2)$$

Where  $I$  is the signal intensity and is proportional to the square of the signal amplitude.  $\langle \rangle$  denote average value. Intensity distribution determines the scintillation index and is described by the Nakagami distribution for a range of  $S_4$  values. For values less than 0.3  $S_4$  is frequency dependent  $f^{1.5}$ . For values between 0.3 to 0.6 and higher, amplitude is according to log normal distribution.  $S_4$  follows a Rayleigh distribution when is close to unity. Even in polar region, measurements have demonstrated that  $S_4$  index rarely exceed 1. ITU P.531-11 Recommendation presents indices taken at 3 different polar stations in the VFH and UFH bands, highest value was 1.5 measured at 400 MHz, in the VHF case highest value was just above 1 during some minutes. Nonetheless station Kokkola closest to Trondheim in latitude presents an index value below 1 during the measuring period. Peak to peak fluctuations can be approximated as follow.

$$P_{fluc} = 27.5S_4^{1.26} \quad (3.3)$$

Where  $P_{fluc}$  is the peak-to-peak power fluctuation in dB. This approximation is based on empirical measurements and according to it for scintillation index of 1.0 corresponds a fluctuation of 27 dB!. Scintillations have demonstrated being more intense at high latitudes and also in the zone of the magnetic equator in a range of  $\pm 20^\circ$ , and for high frequencies in the order of gigahertz and up, scintillation is severe. Global Ionospheric Scintillation Model (GISM v.P531-11) is recommended by ITU to predict the scintillation index, depth of amplitude fading, rms phase and angular deviations depending on satellite and ground station locations as well. Software is available on ITU website section although a license is required to obtain useful data.

### 3.2 Antenna Parameters

Antennas, defined as the structure between the guided wave and the free space [21] on satellite communications, make up the link between Earth station and spacecraft. Several variables define its performance based on the isotropic radiator and reciprocity theorem, the most influential on link budget are now introduced.

### 3.2.1 Power flux density

Concept of power flux density is easier to understand by considering a theoretical source which radiates the same power,  $P_t$  watts, in all directions. In practice this isotropic radiator does not exist but let suppose that is located at the center of a sphere whose radio is  $r$  meters. Power flux density is defined as the power radiated by the source outward per unit surface, given in Watts/m<sup>2</sup> as follow.

$$F = \frac{P_t}{4\pi r^2} \quad (3.4)$$

### 3.2.2 Gain

In the practice, power radiated by the antenna varies with direction ( $\theta$ ). Gain is a concept that relates the power radiated per unit solid angle in  $\theta$  direction to total power radiated per unit solid angle.

$$G(\theta) = \frac{P(\theta)}{P_0/4\pi} \quad (3.5)$$

Theta indicates the direction of maximum radiated power and is also called boresight direction, so that  $G(\theta)$  ratio corresponds to peak antenna gain.  $P_0$  indicates the total power radiated by the antenna. Losses, like dissipative or impedance mismatch loss, are not considered in this form, such as power fall upon all the aperture area  $A$  of the antenna. Nevertheless, antennas absorb a part of the incoming energy on the aperture and reflect it away, besides lossy components. These losses between incident power and the one in the output are represented as aperture efficiency by

$$A_{eff} = \eta_A A_r \quad (3.6)$$

The efficiency usually ranging from 50% to 80% and it takes in account losses like spillover, illumination law, diffraction effects and mismatch losses

$$\eta_A = \eta_i \eta_s \eta_f \quad (3.7)$$

$\eta_i$  relates the illumination law of the reflector respect to uniform illumination. The spillover efficiency  $\eta_s$  describes the ratio of the energy radiated that is intercepted by the reflector to the total energy radiated, an acceptable value is roughly 80%, and it increases as the angle under which the radiator views the reflector increases.  $\eta_f$ , the surface finish efficiency, refers to the effects that surface roughness has on the gain, and in this case the most suitable value must be reach between best performance and manufacturing cost. All those terms included lead let find out  $A_{eff}$  and then formulate another fundamental relationship for antenna gain.

$$\frac{A_{eff}}{G} = \frac{\lambda^2}{4\pi} \quad (3.8)$$

Knowing physical dimensions of the antenna and assuming an efficiency of 0.7, for instance, an estimated gain could be obtained.

### 3.2.3 Radiation pattern and angular beamwidth

Variations of gain depending on direction are represented in the radiation pattern. Two ways to depict are common, in polar or Cartesian coordinate form. The maximum radiation corresponds to the main lobe, and side lobes should be as less as possible. In other words, radiation pattern is equal the gain normalized respect to the maximum value  $G_{max}$  and is expressed as a function of azimuth  $\theta$  and elevation  $\varphi$  angles.

$$g(\theta, \varphi) = \frac{G(\theta, \varphi)}{G_{max}} \quad (3.9)$$

The beamwidth of the antenna is defined as the angle between two directions where the gain falls a certain value respect to the maximum; a fall of the half is denoted as 3 dB beamwidth.

### 3.2.4 Polarization

Electric and magnetic field that composed the waves have the characteristic to be orthogonal and perpendicular to the direction of propagation, and depending on the frequency, they present variations. Polarization of the wave transmitted or received by the antenna is defined by the variation on time of the electric field vector. If one observes along the direction of propagation, the vector describe a figure that varies on the time, this shape traced corresponds the instantaneous electric field which describe polarization. According to it, three different polarizations are distinguished, linear, circular and elliptical. If the electric wave describes a vector directed line polarization is linear. When the figure is an ellipse, corresponds to elliptical polarization. Circular polarization is obtained when ellipse turn into circle, so, circular and linear are considered as special cases of elliptical polarization. The parameters that characterized polarization are direction, axial ratio AR and inclination  $\tau$ . First of them refers to the direction of rotation respect the direction of propagation and can be right-hand also called clockwise, or left-hand known as counter-clockwise. The second parameter is the axial ratio AR defined as the relation between the major to the minor axis, and finally  $\tau$  which refers to inclination of the ellipse. As was mentioned before, for NUTS satellite circular polarization has been chosen to avoid Faraday rotation effects. This polarization is obtained when the two orthogonal components of field are equals in magnitude and have a time-phase difference that is odd multiple of  $\pi/2$ , in terms of AR, it is equal to unity. The rotation sense is determined by the forward phase component and considering the field rotation as if wave moves away from the observer being right-hand circularly polarized for clockwise rotation or left-hand if rotation is counterclockwise.

### 3.2.5 Polarization loss factor

Ideally the receiving antenna is oriented according to the polarization of the received wave, nevertheless, along the path, radiowave is affected by atmospheric

conditions that changes its polarization. Expressing polarization loss as a factor, PLF, it is a term that indicates the portion of the power actually picked up by the receiver antenna. This concept is defined as

$$P_r = PLF \cdot P_i \quad (3.10)$$

where  $P_i$  is the incident power and  $P_r$  is the power coupled into the receiving antenna. An alternative form to calculate PLF in terms of axial ratio is given in [22].

$$PLF = \frac{(1+AR_w^2)(1+AR_r^2)+4AR_wAR_r+(1-AR_w^2)(1-AR_r^2)\cos(2[\tau_w-\tau_r])}{2(1+AR_w^2)(1+AR_r^2)} \quad (3.11)$$

where  $AR_w$  and  $AR_r$  correspond to the axial ratio of the incident wave polarization vector and receive antenna polarization vector respectively, in the same way,  $\tau$  corresponds to the angle between the wave polarization and the receive antenna polarization and conversely. Observing the equation one can see that for AR equal to 1 and even if  $\tau$  is unknown, PLF is founded to be 1. That is the case of circular polarization whose axial relation is equal to unity. In a communication system with circular polarization in one end and linear polarization in the other one, PLF is assumed as 3 dB regardless of the orientation of the linearly polarized wave. This value is for ideal circularized antenna or wave, when it is not ideal PLF value can be above or below 3 dB according to orientation and the axial ratio. PLF is also calculated as the square of the cosine of the angle between the unit vectors of incident wave and antenna, this method is used on Satellite Tool Kit software, for instance.

### 3.2.6 Pointing loss

Pointing losses are the result of the misalignment of angles of transmission and reception due to a not lined-up boresights between Earth station and satellite antennas, such that the received signal is outside the peak of the antenna beam at reception. Next figure shows it graphically where angle in the transmitter is named  $\theta_R$ , and  $\theta_T$  is used for the angle in the receiver.

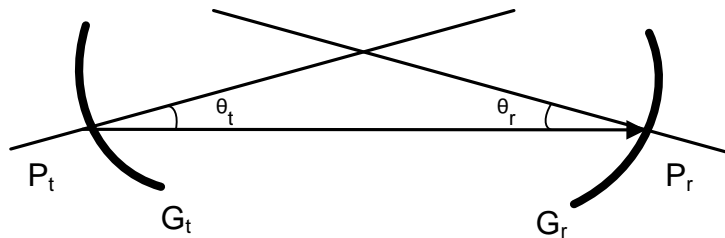


Figure 3.1 Misalignment between receiver and transmitter antennas

Figure above represents the satellite link at  $90^\circ$  of elevation angle nonetheless  $\theta_R$  and  $\theta_T$  changes depending on time and orbit. Losses can be obtained as a function of the mentioned angles, as follow [9]



$$L_T = 12(\theta_T/\theta_{3dB})^2 \quad (3.12a)$$

$$L_R = 12(\theta_R/\theta_{3dB})^2 \quad (3.12b)$$

$\theta_{3dB}$  is the angle where gain fall down half respect its maximum value. The main causes of misalignment on NUTS link are due to inaccuracy on Earth tracking system and ADCS of the satellite, then, an additional analysis is carried on Chapter 5 to obtain the losses along trajectory.

### 3.3 The dipole antenna

The dipole is a basic antenna consists of two segments, and in the case of the half-wave dipole, each segment is one-quarter of wavelength with the feed in the center. Dipole radiates in all directions out of its own axis describing a pattern quasi omnidirectional. Properties that characterize the half-wave dipole are a theoretical gain of 2.15 dB also expressed as directivity 1.64, impedance of 73 ohms, effective aperture equal to  $0.13 \lambda^2$  and beamwidth of  $78^\circ$ . When the dipole is located along the  $z$  axis, the maximum radiation occurs in the  $xy$  plane and a cut in this plane would show the gain as a circle. Another characteristic refers to symmetry such as the radiation pattern only varies with  $\theta$ .

$$g(\theta) \propto \left[ \frac{\cos\left(\frac{kl}{2}\cos\theta\right) - \cos\left(\frac{kl}{2}\right)}{\sin\theta} \right]^2 \quad (3.13)$$

### 3.4 The Friis equation

Let suppose a system with two antennas whose polarizations are matched and a distance  $r$  separates them, drawing on equation 3.4, and being  $P_t$  the power in the radiator antenna the power incident on receptor antenna is defined by the *Friis transmission formula* as follow

$$P_r = \frac{P_t G_t A_{eff}}{4\pi r^2} \quad (3.14)$$

This form exhibits that the power received not depends on frequency when  $G_t$  and  $A_{eff}$  are constant in a certain band. Using receiving antenna gain instead effective area, from equation 2.6, and substituting in Friis form, gives

$$P_r = \frac{P_t G_t G_r}{(4\pi r^2/\lambda)^2} \quad (3.15)$$

This final expression is essential in the link budget equation on wireless communication system and will be clawed back in Chapter 5.

### 3.5 Radio Noise

Several sources of noise are presented along the path of the satellite link and the main contribution came from thermal noise that is a critical situation in the reception end due that it produces noise power in the information bandwidth. Space conditions lend noise to the signal power, and, in addition, physical

elements such as mixers, converters, switches, combiners and multiplexers represent other noise sources. Altogether are the most significant noise power which directly affects the performance receiver system.

### 3.5.1 Thermal Noise

Electrons thermal motion in every conductor that is not at zero temperature produces a voltage difference between the terminals of the conductor and it can be measured defining the equivalent noise temperature  $T_e$ .  $T_e$  is useful to determine the noise produced by the components in the receiver, and is defined as the noise power generated by a device having a noise temperature  $T_n$  being equal to the noise power produced by a passive resistor at the same temperature  $T_n$ . In communications receivers, thermal noise is modeled as an Additive White Gaussian Noise process, AWGN. Next equation defines this concept and involves the bandwidth where electrical noise is generated.

$$N = kT_e B_n \quad (3.15)$$

where:

$k$  is the Boltzmann's constant =  $1.39 \times 10^{-23}$  J/K = -228.6 dBW/K/Hz.

$T_e$  is the equivalent noise temperature of noise source in K.

$B_n$  corresponds to noise bandwidth in which the noise power is measured given in Hertz.

And here, other useful concept is introduced, the noise power spectral density, which corresponds to the noise power in a 1-Hz bandwidth  $B$ , following the relation

$$N_0 = \frac{N}{B} \quad (3.16)$$

Noise power depends on the ambient temperature of the source, and derives in the effective noise temperature which includes several sources, sky, atmospheric, interfering signals that are not necessary thermal. So, effective noise system temperature refers to hypothetical thermal noise source and additional interfering sources.

### 3.5.2 Noise Figure and Noise Temperature

Noise Figure is a relation used to express the noise produced by a device and refers to the ratio between the SNR at the input to SNR at the output of a system, given by

$$NF = \frac{(S/N)_{in}}{(S/N)_{out}} \quad (3.17)$$

This ratio shows that at the output of the device the signal obtained includes the noise already present at the input plus additional noise introduced by the device. Nevertheless on satellite communications systems using noise temperature is more practical and following the steps given in [11] results the expression.

$$T_e = T_0(NF - 1) \quad (3.18)$$

Where  $T_0$  is a reference temperature, usually 290 Kelvin, K. If NF is given in dB it must be converted to a ratio in lineal dimension. This form results relevant and performing the adequate adjusts is useful for active and passive elements that have certain attenuation. A note respect to  $T_0$  is that it corresponds to mean environment temperature which results difficult to measure directly. Equation 3.19 gives an approximation to obtain it, based in a model atmosphere [23]

$$T_m = 1.12T_s - 50 K \quad (3.19)$$

where  $T_m$  is the environment temperature and  $T_s$  corresponds to surface temperature, both in K.

### 3.5.3 Antenna noise temperature

The noise present at the terminals of the antenna is called noise temperature of the antenna,  $T_a$ , and it is due to losses that came from the radio path and losses caused by the physical structure of the device. It is obtained from the convolution of the brightness temperature  $T_b$  of a radiating body located in a direction  $(\theta, \varphi)$  and the radiation pattern of the antenna with a gain  $G(\theta, \varphi)$  [9]

$$T_a = (1/4\pi) \iint T_b(\theta, \varphi)G(\theta, \varphi)\sin\theta d\theta d\varphi \quad (3.20)$$

In the case of uplink design, satellite antenna picks up the noise from the earth and from the space being the beamwidth of the satellite antenna similar to angle of view of the Earth from the satellite, temperature also depends on the frequency and covered area,

Oceans or continents for instance, besides, is not equal for all satellites and at least that one has the exact data  $T_a = 290 K$  is a good approximation on basic designs for on board antenna [9]. In the downlink analysis, a great deal of factors affects  $T_a$ , phenomena and conditions which can be summarized in frequency, elevation angle, atmospheric conditions and galactic noise. Several methods have been development [9 24 25 24] to simplify the calculus of  $T_a$ , due to not all variables of NUTS system implied in those forms are known a method exposed by Kraus [21] has been selected for noise system calculations.



# Chapter 4

## Modulation Schemes

Digital communications links requires techniques to processing signal. FSK and PSK as possible modulation schemes for NUTS system are briefly treated in this Chapter, understanding these concepts is essential to estimate the link margin and error probability of the link.

### 4.1 Digital baseband signals

Three essentials points should be take into account in a modulator, a symbol generator, a mapper and a signal carrier. Binary digital format is the basis on digital communications. Unipolar NRZ, polar NRZ or RZ, Manchester and Alternate Mark Inversion bipolar are different waveforms to represent the digital information transmitted. Bit period  $T_b$  results a basic term in digital communications and is defined as the inverse of bit data rate  $R_b$

$$R_b = \frac{1}{T_b} \quad (4.1)$$

Bits can be combined to cut down the bandwidth, so, a group of two bits corresponds to a quaternary encoding, three bits form a group of 8 level coding, and for a group of  $N_b$  binary digits corresponds a  $m$ -ary signal where  $m$  denotes the number of possible levels defined as

$$m = 2^{N_b} \quad (4.2)$$

From above equation and if signal level is defined, one can found the number of bits per symbol  $N_b$  doing the inverse operation.  $N_b$  times the bit duration results in the symbol duration and according to 4.2 the symbol rate corresponds to

$$R_s = \frac{R_b}{N_b} \quad (4.3)$$

To express the symbol rate, also are used unit of baud, as baud rate which is equal to the bit rate when  $N_b=1$ .

## 4.2 Digital carrier modulation

The digital modulator in a system is in charge of carrier a digital bit stream on radio waves to be transmitted over the RF channel through using a modulation scheme. Channel is affected by noise and when the bit stream arrives at the input of demodulator also bit errors are present. Coherent detection refers when the demodulator has RF carrier phase information, but if it is not available means non-coherent detection. Depending on which is used, noise will affect differently. In the first case distortions are produced by the in-phase component of the noise, and for non-coherent detection both noise components will have influence.

## 4.3 Modulation schemes

Several modulations techniques exist; some are derived from others or are an evolution of basic schemes. A useful classification for satellite communications is according to sensitivity characteristic on nonlinear distortion as constant and variable envelope modulation schemes. Let describe the carrier as a sinusoidal signal, amplitude, frequency or phase are the parameters that can be manipulated in the signal defining the scheme modulation and, they are called Amplitude Shift Keying ASK, Frequency Shift Keying FSK or Phase Shift Keying PSK.

### 4.3.1 FSK

Frequency Shift Keying is the basic form of digital signals modulation implemented in the high frequency radio spectrum. It is based in the principle of shifting the frequency of a carrier in two states of nominal frequencies,  $\omega_1$  and  $\omega_2$  where each one corresponds to a binary state, such as

$$\omega_1 = \omega_0 - \Delta\omega \quad (4.4a)$$

$$\omega_2 = \omega_0 + \Delta\omega \quad (4.4b)$$

Where  $\Delta\omega_0$  is the frequency deviation. Then, the FSK signal can be described as follow

$$v(t) = \cos \omega_0 t, \quad \omega_0 = \begin{cases} \omega_1 & \text{for } m(t) = 1 \\ \omega_2 & \text{for } m(t) = 0 \end{cases} \quad (4.5)$$

If the bit period of the binary data is considered as  $T$ , effective bandwidth is defined by  $B = 2\Delta f + 2/T$  where the difference in carrier frequencies is  $2(\Delta f) = 2(\Delta\omega_0)/2\pi$ . Figure 4.1a shows the modulator circuit to generate an FSK signal, employing a tunable oscillator to switch between  $\omega_1$  and  $\omega_2$ . When the binary symbols are orthogonal, frequencies are chosen such as to meet orthogonality criteria as well [26], and then, at the output one channel will present the maximum and the other one will be zero.

Orthogonality in the sinusoids is obtained only if they are integrated over all the time, when it is done in a short time accuracy of recognizing the difference between the two frequencies has a restriction that limits the rate at which different frequencies can be changed. It could be improved transmitting more bits by using more than two frequencies, information rate would increase. Nevertheless, it would imply a multilevel technique demodulation, a complex circuit demodulator

where probability of misdetection in noise increases as number of levels increase. Shannon Theorem consider as an eventual limit when level spacing is of the order of the noise density [27]. Figure 4.1b depicts the synchronous demodulator using two coherent local oscillators operating at  $\omega_1$  and  $\omega_2$ .

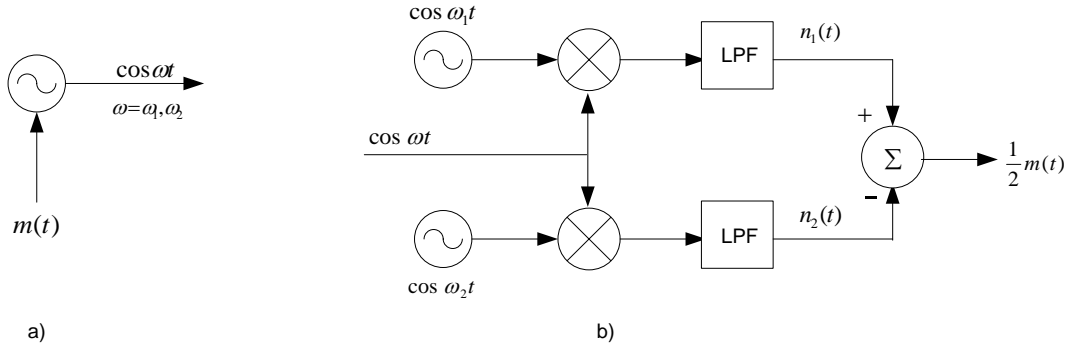


Figure 4.1: FSK Modulation and demodulation diagram.

### 4.3.2 PSK

Phase Shift Keying involves switching the carrier wave between two phases, waveform can be described as

$$v(t) = m(t)\cos \omega_0 t \quad 4.6$$

Where  $m(t)$  takes the value of 1 or -1. Figure 4.2a illustrates the scheme to generate the PSK waveform, using a local oscillator to mix a polar NRZ version of the binary data. Demodulator is shown in figure 4.2b.

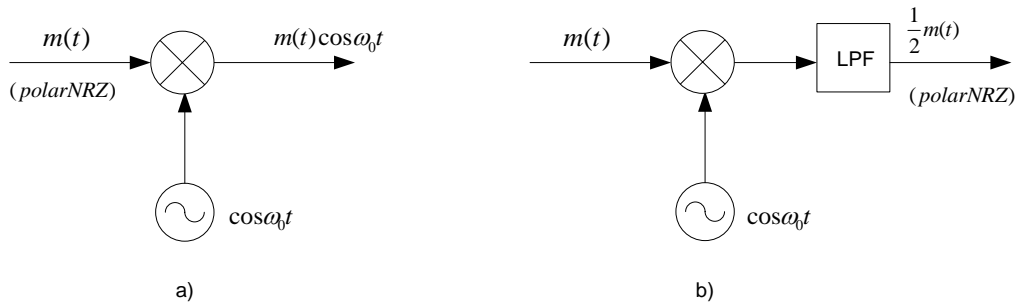


Figure 4.2 PSK Modulation and demodulation diagram.

The output of the mixer is the result of combine the PSK signal with the local oscillator [27]

$$v_1(t) = v(t) \cos(\omega_0 t) = \frac{1}{2} m(t)[1 + \cos(2\omega_0 t)] \quad 4.7$$

A low pass filter is used to limit the spectrum to the main lobe region being the output voltage proportional to the original polar-NRZ.

$$v_0(t) = \frac{1}{2} m(t) \quad 4.8$$

### 4.3.3 Bit Error Probability

Bit Error Probability  $P_e$  is the indicator of quality in a digital radio link and is defined as the likelihood that a bit sent over the link will be received incorrectly.  $P_e$  occurs because a symbol error occurs, the link noise produce spurious in the stream causing that the decision circuitry cannot identify the original sent data. In non-differential modulation one symbol error formed by  $N_b$  bits can produce 1, 2 or  $N_b$  bit errors. Using differential modulation one error in one symbol will produce that the next symbol be misinterpreted and as a consequence, the number of bit error could be more than the number of bits per symbol. As thermal noise increase, symbol rate also increase. A valid assumption for analyze the bit error probability in satellite links where noise is not due to interference from another communication link, is that noise have an AWGN voltage distribution. Let consider a noise voltage  $n_o(t)$  at the output of the demodulator, that will be added to signal voltage  $V$ , different noise values per instant sample could yield to change the sign of  $v(t)$ , the sum of both voltages, producing error on decision circuit. So, an error occurs when a  $+V$  is transmitted and  $n_o < -V$ , the sum of the signal and noise is less than zero volts, or, when a  $-V$  is sent and  $n_o > +V$ , the sum is greater than zero. Then, error probability can be figure out considering that in the sampled instant, noise voltage at the receiver output exceeds the value, in the wrong direction, of the signal sample voltage. Or in mathematical terms,  $P_e = P(n_o > +V)$ , and is described by integrating the Probability Density Function of AWGN

$$P_e = \frac{\sigma}{\sqrt{2\pi}} \int_{+V}^{\infty} \exp\left[-\frac{\lambda^2}{2\sigma^2}\right] d\lambda \quad 4.9$$

Where  $\sigma$  is the rms noise voltage. The given expression is solved by numerical or approximation solutions.  $Q$  function,  $Q(z)$  or complementary error function  $erfc(x)$ , are used. Following the condition that  $V$  should be greater than  $\sigma$  to reach small error probability values, the assumption  $V > 3\sigma$  yields to an approximation probability in a sample instant expressed as

$$P_e = Q[V/\sigma] = \frac{1}{2} erfc[V/\sigma\sqrt{2}] \quad 4.10$$





# Chapter 5

## Link Budget

This Chapter describes the way that link budget was figure out. Calculations imply several variables due to spatial conditions and satellite trajectory, so, assumptions and considerations are also mentioned in this chapter. Design of link communications requires meeting certain target, for digital systems this aim is usually defined by the Bit Error Probability which let establish the required signal to noise ratio at the receiver. Difference between actual and required signals generates the link margin LM that shows how robust the link is, a higher margin a more robustness. Link margin put up with those parameters that in certain moment have been taken as assents or approximations which result quite to achieve an accurate value, atmospheric conditions, attenuation, intermittently on ionospheric scintillation or non-ideal components that derive on assumed scenarios. Then LM for different modulations schemes is included with or without Forward Error Control.

### 5.1 Link Budget basic equation

Link budget is a method to evaluate the received power and noise power in a radio link and is the result of the summary of all gain and losses that affect the signal along the path, such as decibel units are more practical for those quantities.

#### Effective Isotropic Radiated Power

Denoted as EIRP, this parameter is taken from de fact that power radiated per unit solid angle by an antenna is equivalent to the relation between transmission gain in certain direction by power generated and  $4\pi$ . The product gain by power radiated is defined as EIRP, using variables introduced in chapter 2 and in dB units result in a sum.

$$[EIRP] = [P_t] + [G_t] \quad (5.1)$$

Terms in brackets express that units are given in the logarithm form, as in this case,  $P_t$  is in dBW and  $G_t$  in dBi.

#### Power flux density

This parameter refers to received power density on a surface located at a distance  $r$  from the transmitting antenna. It is expressed in  $W/m^2$ .

$$\Phi = \frac{P_t G_t}{4\pi r^2} \quad (5.2)$$

Substituting 5.1 in the numerator, power flux density can be expressed in terms of EIRP, obtaining the expression

$$\Phi = 10 \log \left( \frac{EIRP}{4\pi r^2} \right) \quad (5.3a)$$

$$[\Phi] = [EIRP] - 20 \log(r) - 10.99 \quad (5.3b)$$

### Free space loss

From Friis formula introduced in Chapter 3, and substituting EIRP form in 3.14 which involves antenna efficiency is easy to see that

$$P_r = \frac{(EIRP)(G_r)}{(4\pi r^2/\lambda)^2} \quad (5.4a)$$

The new form for received power is composed by three terms that can be arranged using dB units to obtain the equation

$$[P_r] = [EIRP] + [G_r] - 20 \log \left( \frac{4\pi r}{\lambda} \right) \quad (5.4b)$$

In this point  $r$  is considered as the distance between earth station and spacecraft, for a perfect pass at  $90^\circ$ , then it corresponds to the height of the satellite. Nevertheless  $r$  changes along the orbit and corresponds to the slant range parameter. EIRP and  $G_r$  add a positive amount to received power whereas that last term represents a loss denoted as Free Space Loss, rewriting the equation

$$[P_r] = [EIRP] + [G_r] - FSL \quad (5.4c)$$

Being FSL the free space loss. A first observation that one can deduce is that increasing frequency will enhance the received power, nevertheless, from equation 3.8 is clear that gain is inverse to the square of wavelength, so, using an operation frequency on VHF or UHF band does not represent an improvement on received power. This equation can be considered as the basic one for the link budget although it corresponds to an ideal case where no additional losses are taking into consider.

### 5.2 Additional losses

Additional losses due to several causes must be added to reach more realistic results. Attenuation due to ionospheric conditions, polarization losses and mismatch losses were described in theory part of this work. In addition, losses associated with transmitting and receiving equipment need to be considered. Basic link budget equation is determined by all these terms

$$P_r = EIRP + G_r - FSL - L_a - L_i - L_{pol} - L_{pt} - L_{ta} - L_{ra} \quad (5.4d)$$

Where:

$L_a$  is the atmospheric attenuation  
 $L_i$  is the ionospheric losses  
 $L_{pol}$  is the polarization losses  
 $L_{pt}$  is the pointing losses  
 $L_{ta}$  and  $L_{ra}$  are losses due to transmitting and receiving equipment.

All terms are in dB, and it is known that some losses change as slant range changes. This analysis will be treated later in order to determine which parameters are affected along tracking satellite and how much the affectation is. Nevertheless, passive losses are included in this section, values for a turnstile antenna were obtained in [6] and an additional loss of 3 dB for the dipole has been added according to recommendations in that work. Passive losses on Earth station receiver have been obtained according to specifications on datasheet of installed devices, although an assumed excess insertion loss of 1 dB was added. Values are indicated in next tables.

Table 5.1: Passive losses at Satellite receiver

Loss	Unit	VHF	UHF
Mismatch loss	[dB]	0.2	1
Assumed cable loss	[dB]	0.2	0.2
Excess insertion loss	[dB]	2	2
Excess polarization loss	[dB]	0.5	0.5
Dipole consideration	[dB]	3	3
Total passive loss	[dB]	5.9	6.7

Table 5.2: Passive losses at Earth station receiver

Loss	Unit	VHF	UHF
Connection loss	[dB]	2	2
Cable loss	[dB]	2.76	4.98
Excess insertion loss	[dB]	1	1
Excess polarization loss	[dB]	0.5	0.5
Total passive loss	[dB]	6.26	8.48

### 5.3 Noise System

Drawing on noise power concept introduced in Chapter 3 is feasible determine the total noise power in the receiver by adding noise sources as many elements are in the front end, like in a chain. It leads in the System Noise Temperature that let analyze how the noise power is affecting the signal power delivered by the antenna. Figure 5.1 indicates devices that compose the receiver at laid Earth station. The most significant noise in the system is the one at the front end section in the receiver since signal coming from space is low, then noise generated by the RF amplifier must be as small as possible. A Low Noise Amplifier LNA is used in this part of configuration.

Four sources of noise can be distinguished in figure 5.1,

- 1) Sky noise
- 2) Antenna noise
- 3) Front end noise (LNA)
- 4) Connecting elements

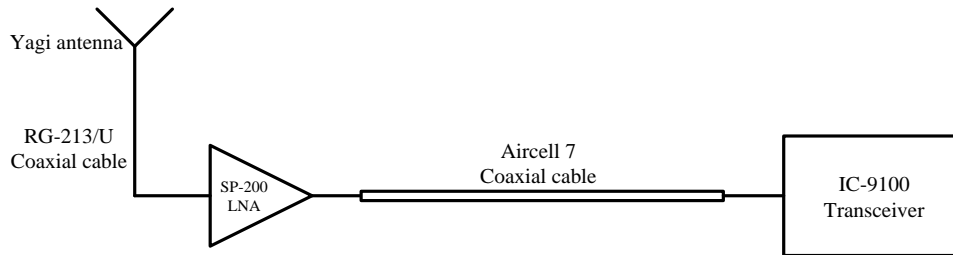


Figure 5.1: Diagram of NUTS Earth station receiver.

The first two sources are external noise injected to the system via the antenna and the last one is generated internally, by the electronic components, lines and connector, thus that design has a critical importance for both ends, Earth Station and On board. NUTS receiver system for downlink has been designed and ground terminal is already installed, then, in this work noise system has been calculated directly using parameters found in the datasheets of physical laid devices on ground station. In the case of satellite it was made a first calculus and Matlab simulations using most typical values for each element, basing on the obtained results, it has been proposed commercial components. Values corresponding to proposed devices were used as input data on STK simulations.

The total noise power at the input of the transceiver results of the collection of all noise contributions that each device represents. Deduction of noise power let obtain the system noise temperature which will be used to evaluate the link performance. Figure 5.2 depicts an equivalent circuit for Earth station receiver just to noise analysis. Devices have been replaced by a noise source and an amplifier with the same gain, so that, receiver has the same gain in its equivalent diagram.

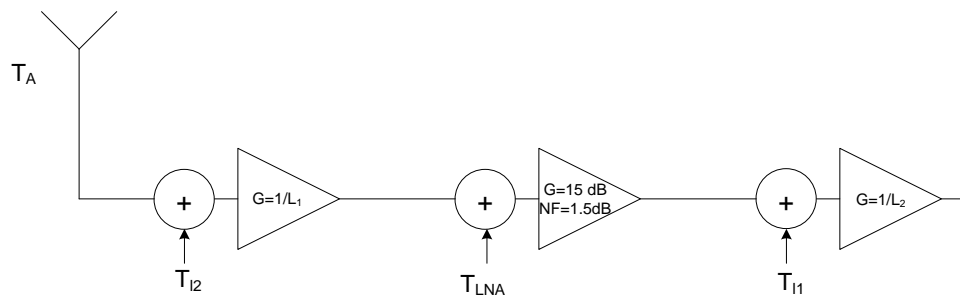


Figure 5.2: Equivalent diagram for NUTS Earth station receiver.

From the equivalent circuit and using equation 3.15 for noise power the expression for the NUTS receiver system is deduced as a chain of noise powers connecting in cascade.

$$P_n = G_{l1}kT_{l1}B + G_{l1}G_{LNA}kT_{LNA}B + G_{l1}G_{LNA}G_{l2}kB(T_{l2} + T_a) \quad (5.5a)$$

Where  $P_n$  is the noise system power,  $G_{l1}$  and  $G_{l2}$  are the gains of the lines,  $G_{LNA}$  the gain of the low noise amplifier,  $T_{l1}$ ,  $T_{l2}$  and  $T_{LNA}$  denotes the lines and LNA noise temperatures, and alike for the antenna,  $T_a$ . Rewriting equation 5.5

$$P_n = kB G_{l1} G_{LNA} G_{l2} \left( \frac{T_{l1}}{G_{l1} G_{l2}} + \frac{T_{LNA}}{G_{l2}} + T_{l2} + T_a \right) \quad (5.5b)$$

Considering that the complete system has a temperature  $T_s$ , in order to obtain the same noise power in both sides of equation, one can express.

$$kBT_s = kB \left( \frac{T_{l1}}{G_{l1} G_{l2}} + \frac{T_{LNA}}{G_{l2}} + T_{l2} + T_a \right) \quad (5.5c)$$

Where left hand term represents the noise power at the input of transceiver and right term corresponds to noise power generated due to chain of elements in the Earth station receiver. Last equation shows that noise system temperature at Earth station is given by

$$T_{s,ea} = kB \left( T_a + T_{l2} + \frac{T_{LNA}}{G_{l2}} + \frac{T_{l1}}{G_{l1} G_{l2}} \right) \quad (5.6a)$$

In the same way, analysis for Satellite system yields to

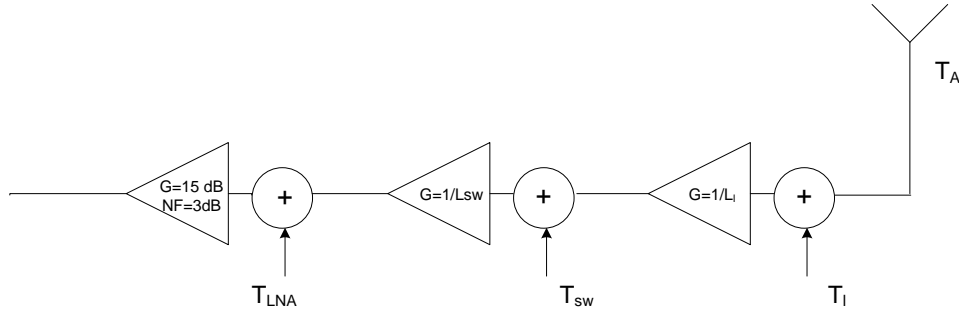


Figure 5.3: Equivalent diagram for NUTS Satellite receiver.

$$T_{s,sat} = kB \left( T_a + T_l + \frac{T_{SW}}{G_l} + \frac{T_{LNA}}{G_{l1} G_{SW}} \right) \quad (5.6a)$$

An intermediate switch with a noise temperature  $T_{SW}$  has been placed between antenna and LNA; it will commute states for reception or transmission. Terms are in linear form. The script `noise_system.m` was implemented in Matlab to acquire noise system values for each link budget. Next section describes how each term in equations 5.6 was defined.

### 5.3.1 LNA and line noise temperature

Modeling a LNA as an active device is deduced that its noise temperature, and also for all active devices which possess a gain  $G$  and a noise figure  $NF$ , could be defined applying the concept described in section 3.5.2, so that noise contribution for LNA is

$$T_{LNA} = T_0(NF_{LNA} - 1) \quad (5.7a)$$

Where  $T_{LNA}$  is the LNA noise temperature,  $T_0$  the reference temperature and  $NF_{LNA}$  the noise figure of the device. For passive devices, in this case the line connection, the influence on the signal power is determined by a relation that depends on the loss factor. So, for the line transmission, gain corresponds to the inverse of loss,  $G = 1/L$ , such that the noise contribution corresponds to

$$T_{line} = T_0(L_{line} - 1) \quad (5.7b)$$

The equation is given in linear form. Nonetheless, most of cases, losses are given by the fabricant as attenuation  $A$  in dB per meter that increases as the frequency rises. Then, one can use the next relation that involves  $A$ .

$$T_{line} = T_0 \left( 10^{\frac{A[dB]}{10}} - 1 \right) \quad (5.7c)$$

Above equation results useful even for attenuation implied along the path like the one due Cloud and Fog, it is applied on STK software, for instance.

In the present work and so as to procure more realistic results  $T_0$  was calculated by equation 3.19 as depending of surface temperature. This last parameter,  $T_s$ , was obtained by taking samples from the NASA online application [28] which provides global data imagery related to weather and environmental parameters. Data from 2001 until 2010 were used to obtain an average between nights and days temperatures per month, the final mean quantity gave a temperature surface of 274.02 K and a value of 256.9 K for environment surface which was replaced by  $T_0$  for noise system temperature calculations.

### 5.3.2 Antenna noise temperature

In the third chapter was introduced how the antenna noise temperature is defined. In this section, is presented an approximation for calculate it based on procedure developed on [21]. Assuming an antenna efficiency  $\eta$  of 70%, equation 3.20 is integrated resulting in three terms, noise contribution due to main-lobe  $T_a^{ml}$ , to side-lobe  $T_a^{sl}$  and to back-lobe  $T_a^{bl}$ .

$$T_a^{ml} = \frac{1}{\Omega_a} (T_{sky} \times \eta \Omega_a) \quad (5.8a)$$

$$T_a^{sl} = \frac{1}{\Omega_a} [T_{sky} \times (1 - 0.3) \times (1 - \eta) \Omega_a] \quad (5.8b)$$

$$T_a^{bl} = \frac{1}{\Omega_a} [T_o \times 0.3 \times (1 - \eta) \Omega_a] \quad (5.8c)$$

So that, antenna noise temperature corresponds to

$$T_a = T_a^{ml} + T_a^{sl} + T_a^{bl} \quad (5.9)$$

All terms are given in Kelvin.  $T_{sky}$  corresponds to sky temperature, it was taken as a constant value obtained from graphs [29].  $T_{sky}$  for VHF band was found roughly 1000 K and for UHF band of 150 K. About the ground temperature,  $T_o$ , its influence varies depending of elevation angle of the side and back lobes. A

useful list of approximate values for different elevation ranges is given in [9], where the best case corresponds to a contribution of 10 K for lobes located at an elevation angle between 10° to 90°, and the worst one is 290 K for elevations less than -10°, it means back lobes. This last amount was taken to figure out noise antenna contribution as the worst case. For VHF band, antenna noise temperature resulted in 1229 K, most noise amount is introduced by the lobes that aim to sky, main and back lobe which represents around 93% of the total since in these frequencies sky noise has a peak in the range of thousands due to cosmic noise. Reducing back and side lobe would represent a decrease just on 18.5% of total noise. In the case of UHF main contribution comes from main lobe and side lobe, this last one picks up noise from ground. Nevertheless, noise picked up by side and back lobes represents an important contribution of 41%, so that, reduction of these lobes would mean reduction in the antenna noise temperature, in the same percentage.

#### 5.4 Carrier to Noise Ratio

Also denoted as  $C/N$ , refers to the ratio of carrier power to the noise power at the antenna output terminals or demodulator input in the receiver. It was described that NUTS receiver system introduces noise due to LNA and connections, then  $C/N$  will be calculated at transceiver input. Carrier to noise ratio is then given by

$$\frac{C}{N} = \frac{P_r}{P_n} \quad (5.10a)$$

Here,  $P_n$  denotes the noise power at the demodulator input and  $P_r$  the received signal power. Replacing equivalent equations from previous sections for both powers,  $C/N$  can be expressed in linear form as

$$\frac{C}{N} = \frac{EIRP}{L} \left( \frac{G_r}{T_s} \right) \left( \frac{1}{kB_n} \right) \quad (5.10b)$$

FSL and additional losses have been grouped in  $L$ . In dB,

$$\frac{C}{N} = EIRP + \left( \frac{G_r}{T_s} \right) - L - k - B_n \quad (5.10c)$$

$C/N$  is a key parameter which defines the performance of satellite communications link. A large  $C/N$  will mean a better performance, is proportional to figure of merit  $G_r/T_s$ , or just  $G/T$  of the receiving equipment with units in dB/K.

#### Carrier to Noise Density

Involving noise power density concept, carrier to noise density is given by

$$\frac{C}{N} = \left( \frac{C}{N_o} \right) \frac{1}{B_n} \quad (5.11a)$$

Rewriting and expressing in dB.



$$\frac{C}{N_o} = \left(\frac{C}{N}\right) + B_n \quad (5.11b)$$

### 5.5 Tracking analysis

Until here, link budget analysis has been focused in the case when satellite is just above the Earth station, pointing straight toward the antenna. Nevertheless, the movement of the satellite along the trajectory and how it influences in the link budget parameters must be analyzed. Although a circular orbit is considered for NUTS trajectory, the distance between the satellite and Earth station varies with elevation angle  $El$ . This angle refers the measured degrees upward from the local horizontal plane at the Earth station to the satellite path and determines in pairs with the azimuth  $Az$  the look angle. At very low elevations angles propagation of the signal will be highly affected by environment effects that also depends on the frequency. Azimuth is measured eastward from geographic north to the projection of the satellite path on a horizontal plane at the Earth station, its exact geometry results more complex thus commercial software are employed to compute. Then, tracking position will be represented by elevation angle  $El$ , the vector from the center of the Earth to the satellite  $r$ , and the nadir angle  $\alpha$ . Figure 5.4 depicts the geometry of elevation angle calculation where the plane of the paper is the plane defined by the center of the Earth, the satellite, and the earth station, such as a horizontal dipole perpendicular to this plane will present a radiation pattern as is illustrated.

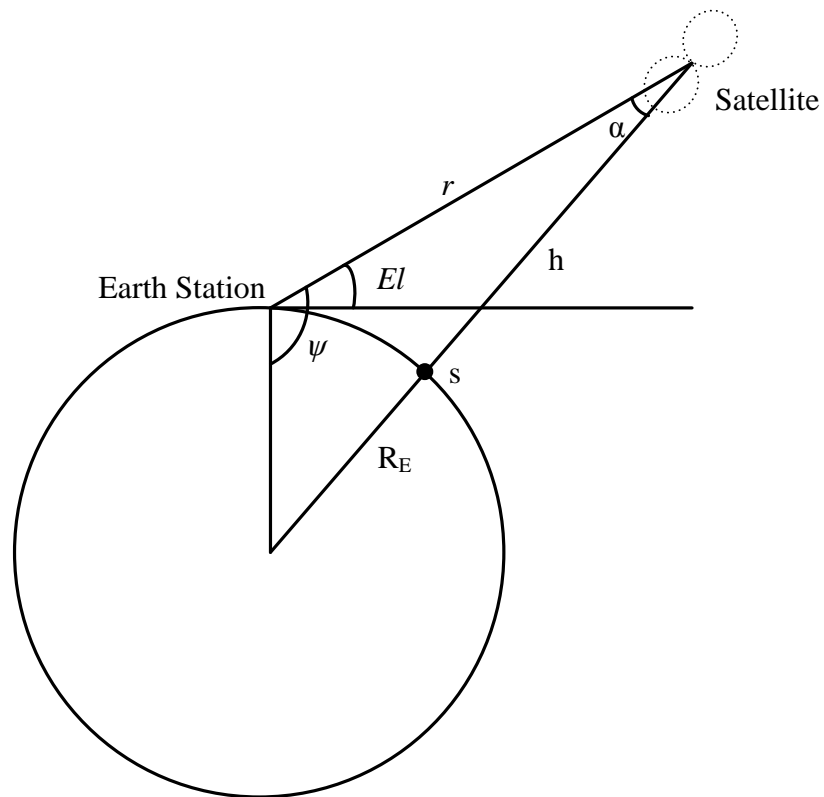


Figure 5.4: Geometry of elevation angle

The point on the surface of the Earth, located in the line between the satellite and the center of the Earth is denoted as subsatellite point  $s$ , then, the nadir refers the direction from the satellite to the subsatellite point. When the beamwidth of satellite antenna points a location on the Earth different to the subsatellite point, the direction corresponds to an angle away from nadir. Nadir angle, can be found by the law of sines,

$$\frac{\sin(\psi)}{R_E + h} = \frac{\sin(\alpha)}{R_E} \quad 5.12a$$

Since  $\psi = 90^\circ + El$ , nadir angle can be expressed as

$$\alpha = \arcsin\left(\frac{R_E}{R_E + h} \cos(El)\right) \quad 5.12b$$

Where  $R_E$  is the mean radius of the Earth and  $h$  corresponds to the altitude. As can be seen, the other parameter which varies with the time is  $r$ , and again, by geometry, it corresponds to

$$(R_E + h)^2 = R_E^2 + r^2 - r^2 - 2R_E r \cos(\psi) \quad 5.12c$$

$$r = \sqrt{(R_E \sin(El))^2 + 2R_E h - h^2} - R_E \sin(El) \quad 5.12d$$

From last expression, and relating it with 5.4, is clear that FSL depends on slant range. This function is included in the Matlab script `los_vs_elevation.m` for the link budget along the trajectory.

### 5.5.1 Pointing loss

In the case of nadir angle expression, it can be seen that there is one unpredictable degree which depends on the antenna coordinate system. Considering that the antenna polarization is defined by the directions  $(\theta, \varphi)$  and assuming that dipole is oriented along z-axis, perpendicular to the nadir,  $\theta$  in the pattern expression 3.13 takes the value of  $90^\circ$  and is affected by the nadir angle and the inaccuracy  $\theta_R$  due to tracking system on the Earth Station that is of  $10^\circ$  in the worst case [6]. Then,

$$\theta = 90^\circ - \alpha - \theta_R \quad 5.13$$

Now, from dipole pattern expression, and with the knowledge that the wavenumber corresponds to  $k = 2\pi/\lambda$  and that even if the length of the dipole  $l$  varies, pattern does not varies, it means  $l \approx \lambda/2$ , such that 2.15 is reduced to

$$G \propto \left[ \frac{\cos\left(\frac{\pi}{2} \cos\theta\right)}{\sin\theta} \right]^2 \quad 5.14$$

Then, for an elevation angle of  $15^\circ$ , and height of 600 km corresponds a nadir angle of  $62^\circ$  which yields to  $\theta = 28^\circ$  and a gain of -8.19 dB. The inaccuracy of  $10^\circ$  introduces a reduction, so,  $\theta = 18^\circ$  that gives -12.09 dB. Such as, polarization

loss under these considerations for on board end is the result of the difference between those values and yields to  $L_{pnt} = 3.8 \text{ dB}$ .

Previous analysis has been done assuming a defined value for elevation. Nevertheless if  $El$  changes with time, a further mathematical analysis, that involves the Earth rotation and the location of the Earth station respect the satellite in each instant of time along the trajectory, is required. A simplified procedure to figure out the elevation-time relation was developed on [6], where those movements were leaving out, the results were also improved on [18] and implemented in the `elevation_vs_time()` function, results give an approximation of the pass behavior and the code was used in this work to generate elevation angles for NUTS. However, in practical terms, a perfect pass does not occur and in order to know more real values STK is here a useful tool. NUTS scenario was simulated in this software; the elevation angles reached in a period of time are traced in Figure 5.5.

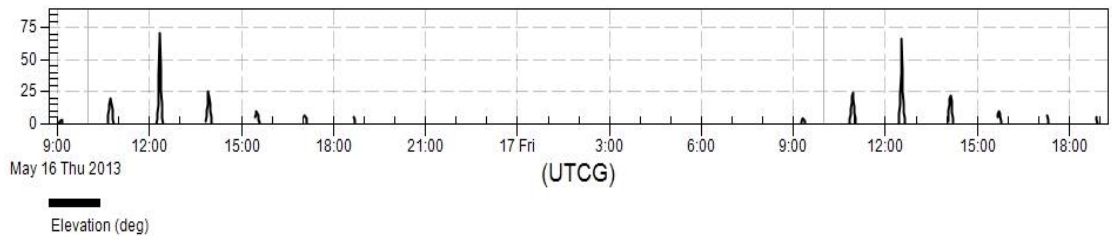


Figure 5.5: NUTS elevation angle for height of 600 km.

### 5.5.2 Propagation losses

In Chapter 2 losses that affect the signal propagation due to ionospheric conditions were introduced. Since the behavior of each phenomenon is unpredictable, they can be analyzed by combining mathematical and statistical models, observations, and tools software, like GISM for scintillation, for instance. Several procedures are wide described on different ITU recommendations documents [20 31 32 33]. In addition, specialized documents resulting of depth analysis are available; reference [34] for example, is a good review of all ionospheric affectations at VHF and UHF bands. In this assignment, empirical values from [35] are used, Table 5.1 indicates atmospheric losses for different elevations angles, values are considered valid for frequencies below 2 GHz, and in addition a value for 2.5 degrees was added in [36] and included here.

In the case of ionospheric losses, the same reference [35] provides a value of 0.7 dB at 146 MHz and 0.4 dB at 438 MHz. By interpolating those amounts for 145.9 MHz, a loss of 0.8 dB is obtained for NUTS VHF center frequency. Nevertheless, a dependence of elevation angle is not provided. Different methods have demonstrated that scintillation is the factor with most influence on ionosphere and results critical at low elevation angles [20 37 38], then, from STK simulation, data of scintillation was generated and added to values proportionated on [29]. Cloud and fog loss was founded as influential factor as well, it was also included in the ionospheric losses, and total values are indicated in next tables 5.2 for both frequency bands. Last two angles,  $80^\circ$  and  $90^\circ$ , and respective losses were just added here STK uses Tropospheric scintillation model P.618-8 by ITU-R to figure out those losses, input data were,

Surface temperature: 274.02 K  
Tropo fade outage: 0.10 %  
Percent time refractivity: 10.00 %

Table 5.3: Empirical atmospheric losses for frequencies below 2 GHz

Elevation [°]	$L_{atm}$ [dB]
0	10.2
2.5	4.6
5	2.1
10	1.1
30	0.4
45	0.3
90	0

Graphics of Scintillation and Cloud&fog losses are included as well, where is clear that in the range from 0° to 10° scintillation reaches the highest values. Two peaks are observed in the range of 0° to 5°, this is due to discontinuities in the ITU-R model present in this lapse [37]. Other methods have been developed, and a unified model based on ITU recommendation is treated in [39], it achieves removing of discrepancies. However the important fact for NUTS scenario is that, for elevation angles upper 20°, P.618-8 is stable. Results obtained can be used; operation above 20° of elevation corresponds to  $L_{ion}$  not higher than 1.3 dB.

Table 5.4: Ionospheric losses for NUTS system at a)145.9MHz and b) 438MHz

Elevation [°]	$L_{ion\_VHF}$ [dB]
0.10	44.18
2.12	11.17
4.12	0.90
6.10	1.65
7.98	1.52
10.13	2.01
20.14	1.36
29.68	1.23
40.27	1.07
49.70	1.04
63.39	1.02
70.87	1.01
80.00	1.01
90.00	1.01

a)

Elevation [°]	$L_{ion\_UHF}$ [dB]
0.10	47.95
2.12	15.05
4.12	1.72
6.10	1.33
7.98	1.17
10.13	0.93
20.66	1.26
31.75	0.95
40.27	0.82
51.11	1.56
63.39	1.42
70.87	1.30
80.00	1.30
90.00	1.30

b)

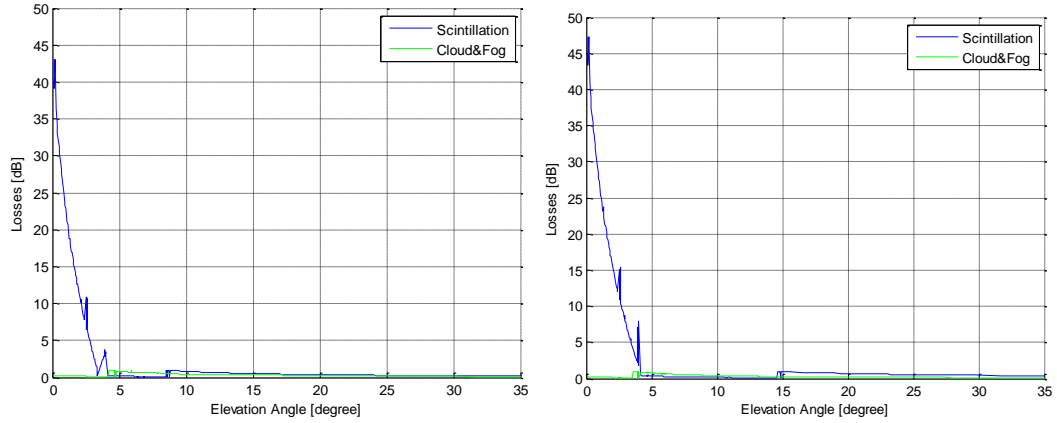


Figure 5.6: Losses due to Scintillation and Cloud&Fog for NUTS system. Left trace corresponds to simulation to 145.9 MHz of frequency and right plot to 438 MHz.

### 5.5.3 Polarization Loss Factor

In free space communications where the polarization state of the received wave is the same as that of the transmitter antenna with same directions, PLF yields to be zero [19]. A turnstile antenna is laid at Earth station, and is planning to have a circular polarization on right hand direction, RHCP. It suggests that the best option for the antenna on board should be RHCP as well, where a PLF of 0 dB is obtained. Nevertheless, is known that the media produce changes in the wave polarization, then, when signal arrives to antenna on Earth it will not have the initial RHCP. Considering that a circular polarization is the result of elliptical and lineal polarization, arriving signal will fall in those cases, where the worst PLF values result of the next combinations for NUTS scenario

Table 5.5: Combinations of polarizations with RHCP at NUTS Earth station

Polarization combination	PLF [dB]
Circular-lineal	3
Circular-circular (opposite handedness)	$\infty$
Circular-elliptical (opposite handedness)	(3, $\infty$ )

Infinitum value is a drawback here, to avoid it, use of circular polarization in both directions, RHCP and LHCP at the Earth station have been proposed, then the useful signal will be the result of combine both. With those implementations, a PLF of 3 dB as worst case can still be considered valid for link budget calculation. Taking into account this and described considerations for losses in this section, a more realistic link budget can be accomplished.

### 5.6 Link Budget Calculation

Uplink and Downlink are the two signals paths involved in the satellite link such that each one must present the performance necessary to meet the objective of margin for digital signals.

### 5.6.1 Downlink

Based on link equation defined at the beginning of this Chapter, the present section expose the power received in the Earth station from NUTS satellite in the ideal case when on board antenna is straight down to the earth station antenna, it means an elevation angle of  $90^\circ$ , additional losses are included since even at  $90^\circ$  misalignments and atmospheric conditions occur and affect the signal power. NUTS satellite is considered to be in the polar orbit located at a medium height for LEO, 600 km. As operation frequency 145.9 MHz has been selected. A power of 1 Watt at the output of satellite transceiver equivalent to 0 dBW added to a gain of 2.15 dB of the half dipole antenna corresponds to an EIRP of 2.15 dB, nonetheless, passive losses of 5.9 dB must be taking into account which gives an EIRP of -3.75, a low value emitted which free space loss and inevitable losses that occurs trough the path are added. Path length of 600 km gives a FSL of 131.18 dB which added to polarization, pointing and atmospheric losses result in an isotropically received power of -139.44 dB. These losses were obtained as Section 5.5 describes. At Earth station, there is an antenna with a gain of 13.1 dB, datasheet is included in Appendix D. In addition, connection losses that belong to receiver system are included resulting in a received signal power of -133.33 dB. Noise system was calculated according to considerations in Section 5.3. With these values, the  $C/N$  results in 24.58 dB within a noise bandwidth of 25 KHz. This quantity of power to noise must be compared with a target value for digital signals.

### 5.6.2 Uplink

In this case, power is not as restricted as in downlink case, as is shown in the next results. Taking parameters installed on earth station, where transceiver emits 20 dBW of power, EIRP radiated to satellite corresponds to 26.84 dBW. Then, following the same steps to obtain carrier to noise ratio

$$\frac{C}{N} = 26.84 \text{ dBW} + 2.15 \text{ dB} - 24.17 \text{ dBK}^{-1} - 142.29 \text{ dB} + 228.6 \frac{\text{dBW}}{\text{HzK}} - 43.98 \text{ dBHz}$$

$$\frac{C}{N} = 47.15 \text{ dB}$$

$C/N$  and energy per bit to noise density  $E_b/N_0$ , are the relevant parameters to evaluate the link performance and its feasibility; and one of them is used to know how the link responds within an acceptable range of errors and how strong the signal is respect to the noise.

### 5.7 Link Margin

In previous Chapter, a function to figure out the error probability was introduced. Extracting equation 4.10, and using the form  $V^2/2R$  to describe the power in the symbol at the decision circuit with a resistance of 1 ohm, the energy per symbol  $E_s$  in Joules is given by the signal voltage  $V$  and the symbol duration  $T_s$ , related as

$$E_s = \frac{1}{2}V^2xT_s \quad (5.15)$$

Differential schemes propagate an error to the next symbol, and then non differential schemes result suitable in NUTS project. Since BFSK and BPSK are constant-envelope signaling, a constant amplitude  $V$  has been assumed and effects of Nyquist RRC filters on pulse shape are not taken into account. Then the noise power  $N$  at the demodulator output is  $\sigma^2$  watts for a resistance of 1 ohm. Since it has the AWG noise characteristics, noise power spectral density  $N_o$  can be described by 3.16, and considering the noise bandwidth as the inverse of period of symbol  $T_s$ , a valid expression for  $N_o$  is like

$$N_o = \sigma^2 x T \quad (5.16)$$

Using those expressions,

$$V/(\sigma\sqrt{2}) = \sqrt{\left[\frac{E_s}{N_o}\right]} \quad (5.17)$$

Then, equation 4.10 has the same form

$$P_e = \frac{1}{2}erfc\left[\sqrt{\left(\frac{E_s}{N_o}\right)}\right] = Q\left[\sqrt{\left(2\frac{E_s}{N_o}\right)}\right] \quad (5.18)$$

As can be seen, energy per symbol to noise density ratio,  $E_s/N_o$ , provides a measurement for a required error probability. A value of  $10^{-5}$  results suitable on wireless communications systems and is used in this work to obtain the link margin. Since in this point  $C/N$  has been calculated,  $E_s/N_o$  is derived from this value. For binary modulation, as contemplated for NUTS link,  $E_s/N_o$  is the same to energy per bit to noise density ratio  $E_b/N_o$ . Energy per bit is directly related to carrier power  $C$  by the period of time which  $C$  is transmitted,  $E_b = C T_b$ . Involving rate and noise concepts within noise bandwidth, yields to

$$\frac{E_b}{N_o} = \frac{B_n}{R_b} \left(\frac{C}{N}\right) \quad (5.19)$$

Where  $C$  and power noise  $N$  are expressed in watts,  $R_b$  the bit rate in bits per second and noise bandwidth  $B_n$  in Hz. Although both ratios, describe system performance in a similar form where a larger ratio corresponds a better performance, here  $E_b/N_o$  is used for the analysis, it results more common on digital links since it involves noise power spectral density. Employing a bit rate of 9600 bps and noise bandwidth of 25 KHz, the received  $(E_b/N_o)_{rec}$  corresponds to 24.58 dB. Decreasing bit rate, of course, produce a greater energy per bit to noise ratio, a value of 31.85 dB is obtained for 1800 bps bit rate. It means that, decreasing bit rate yields to improve the error probability, in contrast, a low bit rate reduces transfer capacity, an important fact in NUTS system, since visibility time must be maximized by downloading as much images as possible within a reasonable bit error. So, both scenarios are presented here and now link margin is obtained. Is necessary to know the required  $(E_b/N_o)_{req}$  as the limit value which guarantees an error probability of  $1 \times 10^{-5}$  and obtain the difference between both ratios to know the link margin allowed for NUTS communication system. This

value will change depending of modulation scheme used. For Binary PSK and according to 5.18, error probability is given by

$$P_{e\_PSK} = \frac{1}{2} \operatorname{erfc} \left( \sqrt{\frac{E_b}{N_0}} \right) \quad (5.20)$$

And for FSK

$$P_{e\_FSK} = \frac{1}{2} \operatorname{erfc} \left( \sqrt{\frac{E_b}{2N_0}} \right) \quad (5.21)$$

From these expressions and applying to NUTS communications systems is seen that the lowest error rate will occurs for PSK detection and demands 3 dB less signal power than FSK, nevertheless PSK requires a local oscillator for synchronization and a wider signal bandwidth. Those given equations represent a theoretical form to known the bit error probability. Generated graph shows that coherent PSK derives in a  $(E_b/N_0)_{req}$  roughly to 9.5 dB whereas that coherent FSK requires a ratio of 12.5 dB to meet a probability error of  $1 \times 10^{-5}$ . Figure 5.7 depicts curves for BFSK and BPSK coherent detection.

Required ratio just gives a reference for the expected value, and of course the received must be greater to ensure a safety operating point. The difference between both ratios leads to link margin, which results in 12.08 dB for BFSK modulation and data rate of 9600 bps, and 15.08 dB for BPSK. Under the same conditions, a link margin of 4.06 dB is reached on UHF band for BFSK. It is known that along the path errors are introduced in the transmitted symbols, this fact, combined with the low power levels handled by NUTS could derive in wrong decision in the demodulator. Implementation of error control should be used in those cases.

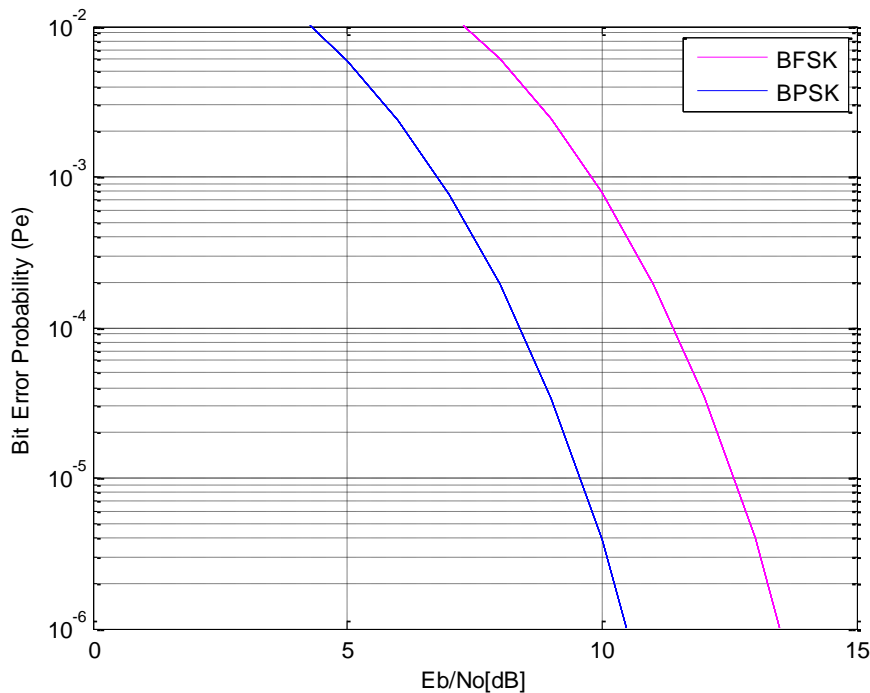


Figure 5.7: Bit error rate as a function of  $E_b/N_0$ .



## 5.8 Error control

Error control implies two functions, detection and correction and is implemented by adding redundant code bits to the uncoded bit stream; this process is denoted as encoding. The contrary process is called decoding, when the original bit stream is recovered, the combination of both is usually denoted as codec. Depending of the code both functions can be implemented or only one. Using Automatic Repeat Request, ARQ, for instance, the receiver can request for a repeat transmission but not allows correction such that this code only includes error detection. Another common code is FEC, that unlike ARQ, Forward Error Correction can correct errors without retransmission. On satellite communications ARQ does not result useful since retransmissions asked imply more time and consequently more errors, so, FEC results a suitable option for NUTS. Figure 5.8 shows the basic block diagram with FEC process implemented.

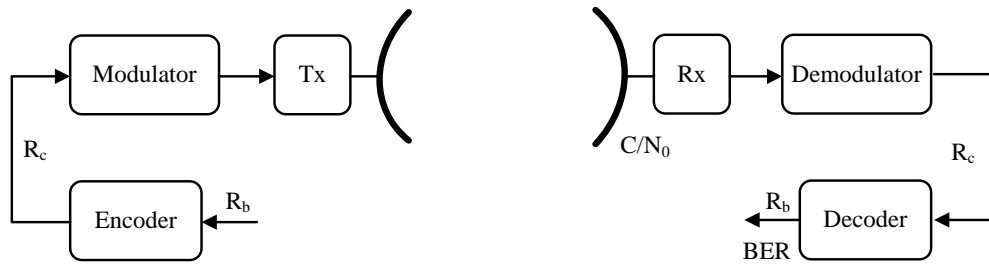


Figure 5.8: Block diagram for a coded message with FEC.

$R_c$  refers to the bit rate of the coded message at the modulator input and  $R_b$  corresponds to the bit rate of uncoded message. Block codes and convolutional codes are the options to implement error control. Errors on fading conditions occur mostly in burst and since block codes results less sensitive to burst errors it is a suitable option for NUTS system. This process consists in to group the bits of the stream into blocks; each block contains  $k$  bits also called datawords. Then datawords are encoded into codewords consisting of  $n$  bits, the ratio between those parameters is denoted as  $r_c$  and this in turns determines the relation between both bit rates

$$\frac{R_b}{R_c} = r_c \quad 5.22$$

Where it can be seen that  $R_c$  is higher than  $R_b$  since  $r_c$  is less than 1. then for PSK and FSK, with constant carrier power, is valid to express that  $r_c$  is inversely proportional to the bit energy  $E_b$  of the uncoded bit stream and results directly proportional to an energy  $E_c$  which corresponds to the bit energy of the coded bit stream, it means

$$E_c = r_c E_b \quad 5.23$$

Then from expressions given in Section 5.7 is possible deduct the error probability for the coded bit stream for BPSK and BFSK modulation schemes

$$P_{ec\_PSK} = \frac{1}{2} \operatorname{erfc} \left( \sqrt{\frac{r_c E_b}{N_0}} \right) \quad 5.24$$

$$P_{ec\_FSK} = \frac{1}{2} \operatorname{erfc} \left( \sqrt{\frac{r_c E_b}{2N_0}} \right) \quad 5.25$$

Here, it is important to clarify that probability of bit error  $P_e$  is a consequence of noise conditions at the input of the receiver and BER is the bit error rate at the output of the detector, then error control reduces the error probability of the output respect the input. A comparison between error probabilities with and without code implementation show that coded bit stream yield in a higher error probability, so, an effective control coding means that output BER should be better. In addition, an important consideration for this analysis is the bandwidth and in NUTS system it is limited, under the consideration that it is already fixed at 25 KHz, the alternative could be playing with the transmission time, nevertheless it is also a restriction in NUTS scenario. Then, considering that  $B = 2 R_b$ , the maximum transmission rate should not exceed 12500bps. It means that for a message rate of 9600 bps the condition is that  $r_c \geq 0.768$ . In order to know the efficiency of error control implementation, coding gain is developed. In this work Hamming and Reed Solomon codes have been analyzed.

### 5.8.1 Coding Gain

This section analyzes a way to figure out the coding gain if Hamming code and a binary modulation scheme are implemented. Under these considerations, the bit error rate after demodulation is equivalent to error probability of uncoded message, in BPSK, case to equation 5.20, and can be expressed as

$$BER_U = P_{eU} \quad 5.26$$

The BER for coded stream is obtained under the assumption that Hamming is considered as a perfect code, then, the BER is defined by [40]

$$BER_C = \frac{(n-1)!}{!(n-1-t)!} P_{ec}^{t+1} \quad 5.27$$

Since for perfect codes  $t=1$ , equation reduces to

$$BER_C = (n-1)P_{ec}^2 \quad 5.28$$

### 5.8.2 Block code

In order to implement a code, values for  $n$  and  $k$  that meet the given  $r_c$ ; besides it should be within the NUTS bandwidth and modulation scheme considerations. A review of typical combinations yields to values in the Table 5.6 for Hamming and Reed Solomon codes that fulfill the condition  $r_c \geq 0.768$ , nevertheless those combinations cannot be reached with binary modulation schemes since  $n$

depends on the symbols  $m$  in the form  $n = 2^m - 1$ . Table 5.7 indicate code rate when  $m$  is equal to 2 and 4, for Hamming code  $k = n - m$  and for Reed Solomon  $k < n - 1$ .

Table 5.6: Typical combinations for Hamming and Reed Solomon codes with  $r_c \geq 0.768$ .

Code	n	k	$r_c=k/n$	$R_c$
Hamming	31	26	0.8387	11446.1538
Hamming	63	57	0.9048	10610.5263
Reed Solomon	204	188	0.9216	10417.0213
Reed Solomon	236	216	0.9153	10488.8889

Table 5.7: Values reached with Binary and 4-ary modulation.

Code	m	$n = 2^m - 1$	k	$r_c=k/n$	$R_c$
Hamming	2	3	1	0.3333	28800
Hamming	4	15	11	0.7333	13090.9091
Reed Solomon	2	3	1	0.3333	28800
Reed Solomon	4	15	13	0.8667	11076.9231

It is seen, on one hand, that from binary modulation schemes a higher coded rate is required since the ratio  $r_c$  is lower than the limit defined for 25 KHz. In the other hand, implementing a high level scheme, that would reduce the required bandwidth, represents an alternative, it require a further analysis implying NUTS restrictions. Here some proposals are presented and summarized in the Table 5.8, just to analyze how the implementation of error control could improve the transmission.

Table 5.8: Proposed combinations for NUTS system.

Code	m	$n = 2^m - 1$	k	$r_c=k/n$	$R_c$
Hamming	2	3	1	0.3333	28800
Reed Solomon	2	3	1	0.3333	28800
Reed Solomon	4	15	13	0.8667	11076.9231
Hamming	4	15	11	0.7333	13090.9091
Hamming	5	31	26	0.8387	11446.1538

The script `ber_coded.m` gathers those codes and generates a graph of  $E_b/N_0$  vs BER, as is shown in Figure 5.9. Then for 4-PSK a  $E_b/N_0$  of 9.8 dB is required to meet a BER of  $10^{-5}$  when not code is used, and for coded message using 15/11 Hamming code corresponds a  $E_b/N_0$  of 8.8 dB which means that implementing this code imply a coding gain of 1 dB. It is illustrated in Figure 5.10. In addition, the small circle in this graph indicates the point where the traces cross and corresponds to  $E_b/N_0$  of 4.6 dB, it means that values above this one will ensure that code is effective for the system.

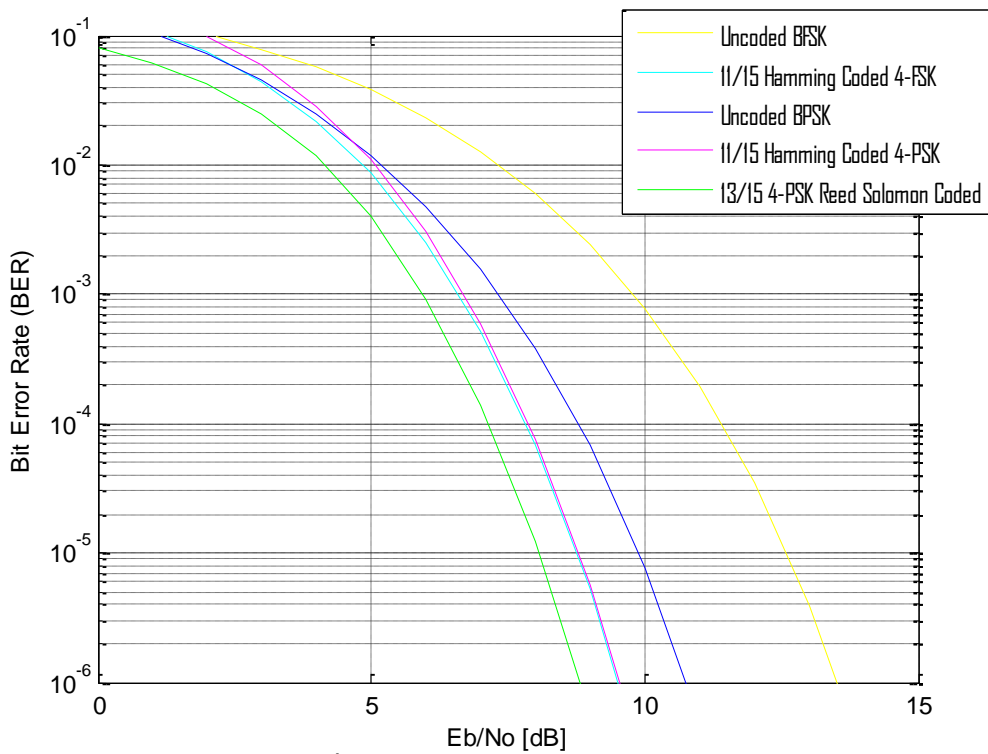


Figure 5.9:  $E_b/N_0$  vs BER for different codes and modulations. Traces corresponding to FSK are coherent and differential for PSK. Hard decision was considered for both.

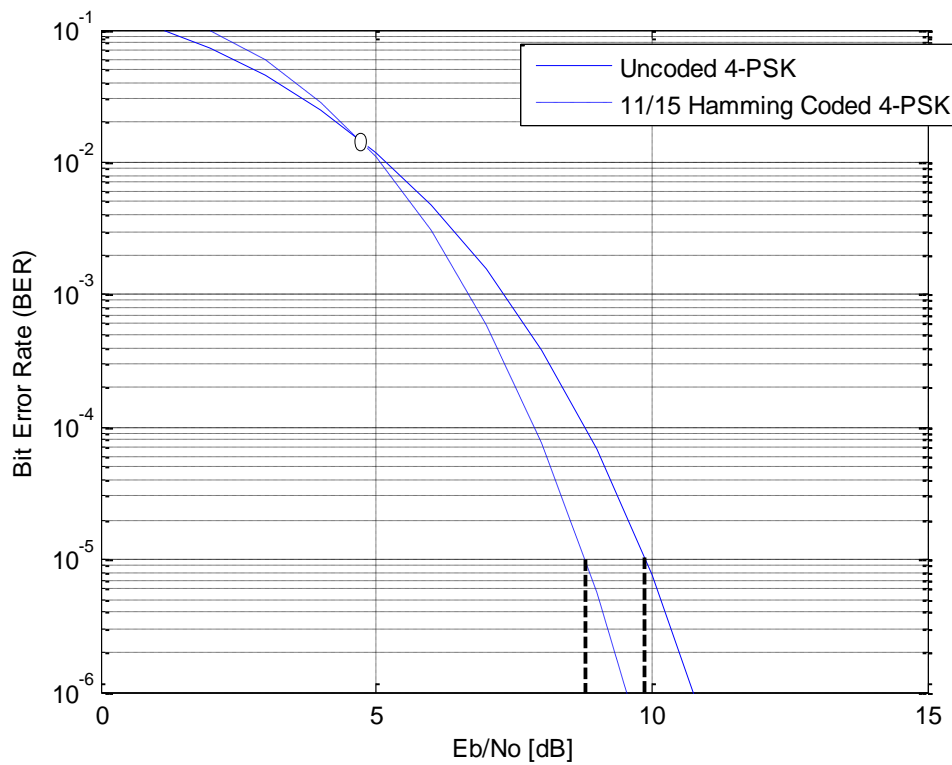


Figure 5.10:  $E_b/N_0$  vs BER for 4-PSK.

## 5.9 Results and discussion

Now, from link budget calculations and using the new required  $E_b/N_0$ , the link margin enhance and the difference result important overall on UHF band where before it had a link margin of 4 dB. Even 4 dB could be considered a good result on communications systems, for NUTS case, is better obtain a higher margin since environment condition varying continuously affecting to radiowave propagation in different manner, this fact in addition to assumptions related to orbit, components or even propagation models, demand a higher link margin as system restrictions allow.

The Table 5.9 summarizes the results for an elevation of  $90^\circ$  under consideration and analysis described in this Chapter using uncoded BFSK and BPSK schemes. Next, Link Margin for coded message with Hamming indicates values obtained on the Table 5.10.

Table 5.9: Link Margin for NUTS using uncoded binary modulation.

Parameter	Description	Unit	DL VHF		UL VHF	
BdB	Noise bandwidth	[dBHz]	43.98		43.98	
G/T	System G/T	[dBK]	-17.80		-12.95	
C/N	Signal to Noise ratio received	[dB]		20.42		12.40
R	Data rate	[dB-bits]	39.82		39.82	
(Eb/No)rec	Eb/No received	[dB]		24.58		16.56
(Eb/No)req_bfsk	Eb/No BFSK	[dB]	12.50		12.50	
Lmebno_bfsk	Link margin BFSK	[dB]		12.08		4.06
(Eb/No)req_bpsk	Eb/No BPSK	[dB]	9.50		9.50	
Lmebno_bpsk	Link margin BPSK	[dB]		15.08		7.06

Table 5.10: Link Margin for NUTS using 4-PSK and Hamming code.

Parameter	Description	Unit	DL VHF		DL UHF	
BdB	Noise bandwidth	[dBHz]	44.77		44.77	
G/T	System G/T	[dBK]	-17.80		-12.95	
C/N	Signal to Noise ratio received	[dB]		19.63		11.61
R	Data rate	[dB-bits]	39.82		39.82	
(Eb/No)rec	Eb/No received	[dB]		24.58		16.56
(Eb/No)req_cqpsk	Eb/No required 4-PSK, 11/15 Hamming	[dB]	8.70		8.70	
LM	Link margin	[dB]		15.88		7.86

Values obtained for link margin results wide enough for tolerances to put up with inaccuracies made, assumptions or changes in losses due to ionospheric conditions, nevertheless, analysis along the trajectory does not bring about the same results at low elevations angles, as expected. Graph 5.11 depicts the  $E_b/N_0$  received under tracking, traces corresponding to required threshold for different modulation schemes are shown as well, an is clear that for an elevation angle of  $20^\circ$ ,  $E_b/N_0$  received is not enough to reach the required for BFSK modulation

neither for BPSK. The option of 4-PSK coded with Hamming results highly close although not sufficiently dependable, a value of 0.1 cannot be consider as link margin. If an elevation angle of  $30^\circ$  as minimum is selected  $E_b/N_0$  for three cases of modulation are above the required, nevertheless it will decrease the visibility time. For  $El=25^\circ$ , only Phase Shift Keying schemes are above the threshold, reaching a link margin of 1.5 for BPSK. Such as, two options will be treated in next chapter in order to know the visibility time and then downlink capacity. Figure 5.12 corresponds to the plot generated for LM, left graph show the traces when BFSK is used, right one refers to LM with BPSK.

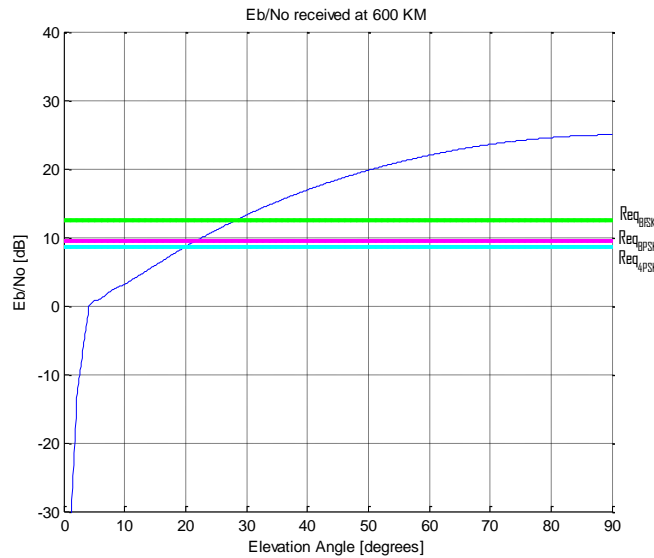


Figure 5.11:  $E_b/N_0$  received at 600km. Green trace corresponds to  $E_b/N_0$  required to reach a BER of  $10^{-5}$  when BFSK is implemented, magenta line is for BPSK and cyan refers to PSK Hamming coded.

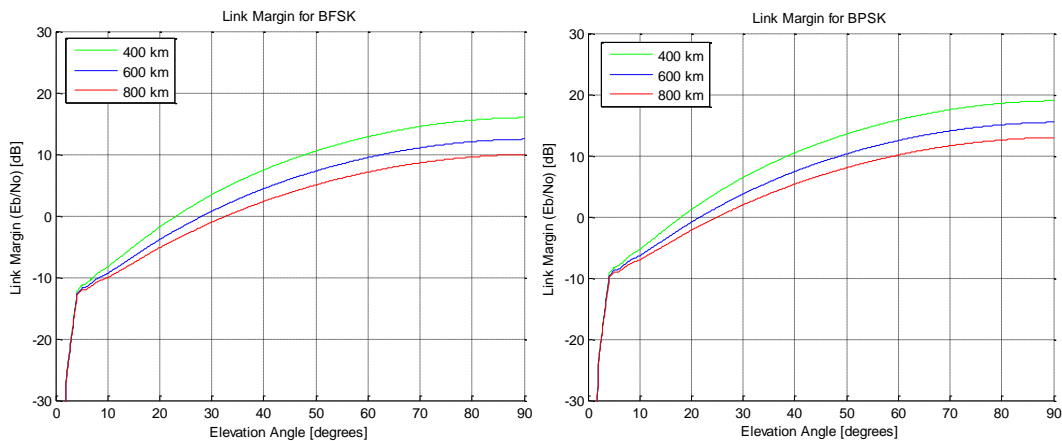


Figure 5.12: Link Margin along NUTS trajectory. Left plot depict traces when BFSK is used and right one is for BPSK.

Some important considerations to meet those results is to guarantee 1 Watt of transmitted power from satellite, for uplink an LNA with NF of 1.5 dB that was used for noise system calculations, in general taking into consider values given on sections 5.6.1 and 5.6.2. Detailed link budget table is included in the Appendix A for VHF and UHF band in both directions. Chapter 7 includes resulting plots of the  $E_b/N_0$  reached.



# Chapter 6

## Communication System Overview

A compilation of NUTS communication system is presented in this Chapter. At first, installed ground stations are briefly introduced and later the system in spacecraft end is described by using proposed commercial devices according to requirements treated on the previous Chapter. End part includes downlink capacity calculations starting from visibility time, compression image resulting from previous work and the radio packet distribution.

### 6.1 NUTS Communication Layer

The NUTS communication system is conformed by the two segments, station on board. It consists of two full duplex radio links in different amateur frequencies. In addition, a simple link transmitting a morse code is also considered. This beacon will be used to locate the satellite can be activated 15 minutes after deployment from the P-POD [41]. For the downlink, the modulation implemented will be binary with non-return to zero NRZ, 9600 bps is here assumed. Next figure roughs out the Communication System arranged in layers.

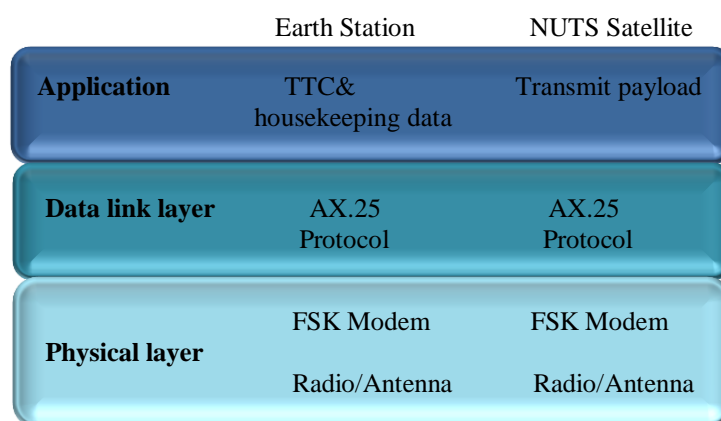


Figure 6.1: NUTS Communication System layers

### 6.2 Earth Communication System

The ground station has been installed at Faculty of Information Technology, Mathematics and Electrical Engineering, the equipment includes [3],



- 5 meter antenna mast
- Tonna 2x9 crossed Yagi-Uda for VHF
- Tonna 2x19 crossed Yagi-Uda for UHF
- Yaesu 5500 antennae rotor
- ICom IC-9100 radio
- ICom PCR-1500 radio for weather data download
- SP-200 Mast-Mounted Preamplifier
- SP-7000 Mast-Mounted Preamplifier

Basic operation will be explained imagining that a command will be sent to spacecraft. This command is requested by the operator through the Earth station computer which generates data to transmit and forwards it to the ICom IC-9100 radio. This radio modulates the incoming data at 9600 bps using FSK scheme<sup>1</sup> at 438 MHz using a protocol, the AX.25 is planned for NUTS. Then, modulated signal is passed to the antenna; the maximum power in the IC-9100 radio is of 75 W in this transmission band. The 2x19 crossed Yagi-Uda antenna has a gain of 16.2 dB. Dipole pattern is shown in respective datasheet. A Yaesu 5500 antenna is the azimuth-elevation rotor system that support the crossed-Yagis and according to instruction manual it can turning range of 450° on azimuth and a rotation range of 180° for elevation, following the NUTS tracking by the control computer. Signal is then transmitted to the space where is captured by the antenna satellite. NUTS communication system is in charge of processing the request and transmitting a response, in case. Then, signal is received in the Earth station by the crossed-Yagi antenna, with 16.2 dB of gain and amplified by the SP-7000 Low Noise Amplifier a LNA with a noise figure of 0.9 dB. IC-9100 radio receives and demodulates the signal. Demodulated data is sent to the Earth station computer to be processed.

### 6.3 On board Communication System

According to results obtained from link budget in Chapter 5, some devices have been proposed, to meet the requirements of operation. Some elements, like antennas, have been taken from previous analysis [6].

- $\lambda/2$  Dipole antenna
- ADF7020-1 radio
- RF5110G power amplifier
- ADG918 switch
- 2884 Low Noise Amplifier

In addition, miscellaneous devices has been selected to use practical values for on STK simulations.

- SMA Connector Jack Receptacle Right Angle PCB, 50 Ohms
- SMA Connector Plug Straight Crimp/Crimp RG-58 Cable, 50 Ohms
- SMA Connector Plug Right Angle Solder/Crimp RG-58 Cable, 50 Ohms
- RG-58 Coaxial cable

---

<sup>1</sup> Defined parameters in this section are in order to show the process. Other modulation schemes are available for use with this radio and the range of VHF and UHF frequencies as well. All specifications related can be consulted on datasheet included in Appendix.

The block diagram of the spacecraft communication system is depicted.

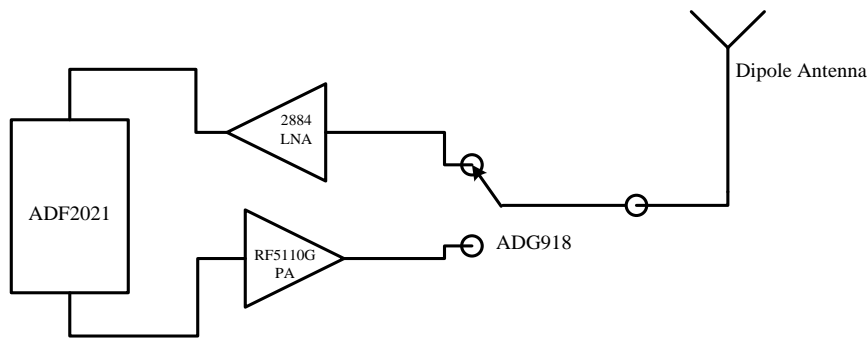


Figure 6.2: NUTS Satellite communication system diagram

In the same way as explanation described in the section before, satellite picks up the signal from ground station through a dipole antenna with a gain of 2.15 dB. Switch ADG918 commutes the circuit to receive producing an attenuation of 0.5 dB in the signal, then, it is sent to RF5110G power amplifier that has a gain of 15.9 dB with a noise figure of 1.5 dB. Then, received signal is passed to ADF7020-1 transceiver, a sensitivity of -112.5 dBm for 9600 bps is reached by the receiver and which also includes an LNA in its front end with a noise figure of 1.5 dB. Following the LNA, a quadrature down conversion mixer passes the signal from RF to IF frequency of 200 kHz. Then, signal is detected by ADF7020 internal demodulators, offering two options, through FSK correlator/demodulator or by linear demodulator. Second one is less probable to be implemented, so, FSK demodulator takes the quadrature outputs,  $I$  and  $Q$ , from the front end limiting them, and sends to a pair of digital frequency correlators, BFSK frequencies are band-pass filtered and original data is obtained by establishing a comparison of the output levels between the two correlators. This frequency discriminator meets optimum detection within AWG noise since its behavior is close to a matched filter detector. Figure 6.3 illustrates the block diagram of demodulation process.

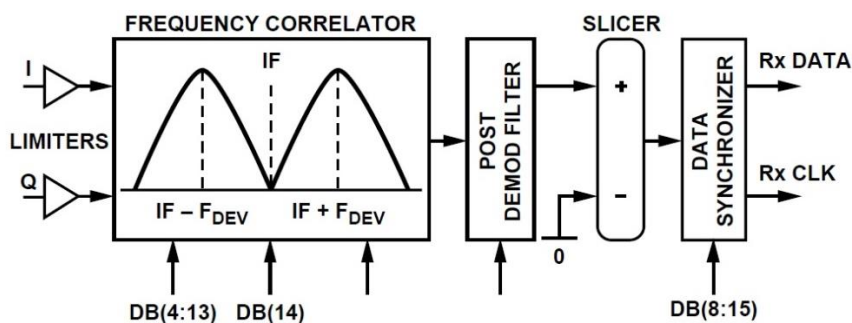


Figure 6.3: ADF7020-1 FSK Correlator/Demodulator Block Diagram. From Analog Devices datasheet.

Above diagram also shows that after discrimination, excessive noise is eliminated by a digital low pass filter that should be programmed according to data rate, nevertheless intersymbol interference, ISI, could be present since NUTS bandwidth will be narrow, then an appropriate performance is met setting the 3 dB bandwidth near 0.75 times the data rate as manufacturer suggests on the

respective datasheet. To improve robustness on data recovery results, a slicer block let fix a threshold level to zero and since output signal levels of the frequency discriminator are centered on zero, demodulator response will not depend on the run-length constraints of the transmitted stream. Finally, the bit stream is resynchronized to a local clock by a digital PLL. In addition, is important to mention that front end design of the ADF7020-1 avoid an external matching network and even the switch for Receiver/Transmitter. Nevertheless, here, switch is considered due to losses have been taking into account for the link budget calculation, so if in the future another transceiver is used which requires the switch, it will not implies changes in noise system equation defined in Chapter 5.

For downlink case when satellite transmits, the on board computer forwards the data to ADF7020-1, which modulates the stream, in this case by FSK scheme. A frequency value  $N$  is selected as center frequency, then, it is toggled by a TxDATA line, as figure 6.4 illustrates.

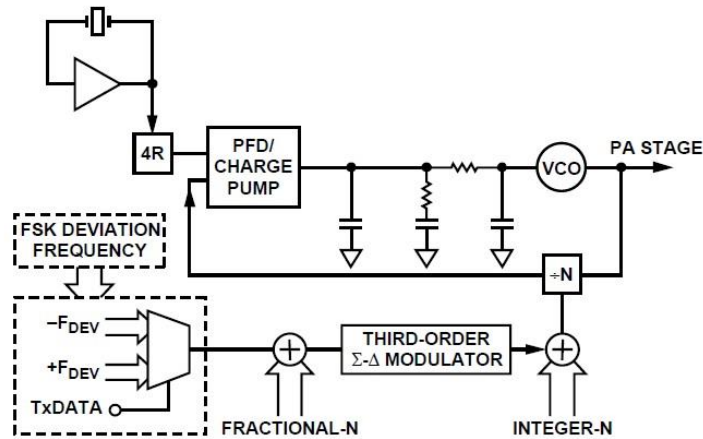


Figure 6.4: ADF7020-1 FSK Modulator Block Diagram. From Analog Devices datasheet.

The maximum transmitter power of ADF7020-1 corresponds to 13 dBm, the modulated signal is sent to the RF5110G power amplifier which has a gain of 21 dB, both gains are added to dipole gain of 2.15 dB, and, of course, passing through ADG918 switch, coaxial cable, and connectors implies losses. Signal is transmitted and a degraded waveform is picked out at the earth station whose receiver process was described before.

## 6.4 Communication Protocol

Most of existing CubeSat have implemented AX.25 protocol for its Communication System [42] and is also planning for NUTS satellite. This protocol is based in the wired network protocol X.25 which was enhancement and adapted for using in amateur radio. All facilities of this protocol are full explained in the reference manual [8], on satellite communications just a part of them are employed. AX.25 transmission is executed by organizing information in blocks of data, denoted frames and there are three types of them. Information frame is used in amateur satellite communications. Next figure shows the AX.25 basic structure of this frame where the first bit to be transmitted is on the left side.

Flag	Address	Control	PID	Info	FCS	Flag
01111110	112/224 bits	8/16 bits	8 bits	N*8 bits	16 bits	01111110

Figure 6.5 Information AX.25 frame.

Flag: Indicates the beginning and end of a frame.

Address: Includes the destination and transmitter address.

Control: Identifies the type of frame. Information frame is used in this case.

PID: Identifies the kind of protocol used in Network layer.

Info: Contains user data with having a default length of 256 bytes. This information is transmitted transparently across the link.

FCS: Is a Frame Check Sequence which ensures that the frame was not corrupted by the transmission medium. The cyclic redundancy check CRC standard code is used to calculate the FCS and is based on a 16-bit polynomial so that  $G(x) = x^{16} + x^{12} + x^5 + 1$ .

Nevertheless, implementation of pure AX.25 protocol is not totally confident since using CRC for radio packet transmission and detection does not provide a safe level of security, it results attractive due to its simplicity and less overhead in transmission. Algorithm is based on cyclic code generating the bit sequence; those bits are attached to the original stream and sent in the same packet, such data maintain a certain level of wholeness. Nevertheless this level could be improved to protect the data in case of attacker interventions, for instance. This issue was tackled on [43] for uplink case where HMAC code was included to protect the integrity of the data by implementation of a sequence number or time stamp. Hash based Message Authentication Code, HMAC, is a mechanism based on cryptographic hash functions, the key length for HMAC can be of any size. Hash function is an algorithm that maps the length of message to a smaller one, so, hash value or hash function corresponds to the returned value [43]. The interesting characteristic of this mechanism in security aspect is that results similar to encryption, where encryption algorithm and authentication algorithm are combined to obtain authentic encryption, in this form protection integrity of the data is reached. Since a deeper analysis of the protocol is required to define the radio packet, results from [43] have been used here for the downlink frame as a base to obtain the downlink capacity.

AX.25 radio packet will contain a frame of CubeSat Space Protocol CSP, which in turn contains the information data. CSP refers to a network layer delivery protocol whose improved Version 1+ present a frame conformed by 32 bit header and 0 to 65535 bytes for payload. Therefore, when sequence number is implemented, the NUTS radio packet has the structure shown in next figure.

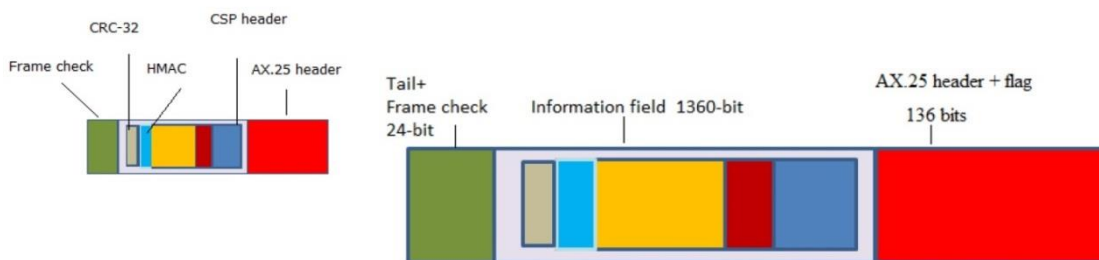


Figure 6.6: NUTS AX.25 Radio Packet. From [43]

Distribution is as follow.

AX.25 FC and tail:	24 bits
Modified CSP header:	32 bits
Sequence Number:	16 bits
Command:	64 bits x16 commands
CRC:	2 bits
HMAC code:	256 bits
Total information field:	1360 bits
AX.25 header and flag:	136 bits

Such that, the maximum size for NUTS radio frame is of 1520 bits. AX.25 tail, header and flag occupy 160 bits. Having these values about the radio packet, visibility time has been obtained in order to know the downlink capacity.

### 6.5 Downlink Capacity

NUTS link have been simulated on Satellite Tool Kit software, a file containing information about the access time was generated, it was done for each height. File presents the information in columns as follow.

```
FromElevationAngle (deg)      15/15/2013 10:25:52.322 -0.111
```

First column is just an identifier not useful here, second one refers to the number of samples that corresponds to an instant time which depends on the simulation parameters configured, next column shows the date simulation and the last one is the elevation angle in degrees that is reached in the hour indicated by fourth column. File is read in Matlab by using `read_stk_elev(file_name).m` code, then `plot_data_down_day.m` processes the data to obtain the visibility time, some modifications from [6] scripts was done according to recent simulations. Graph obtained is shown in Figure 6.7.

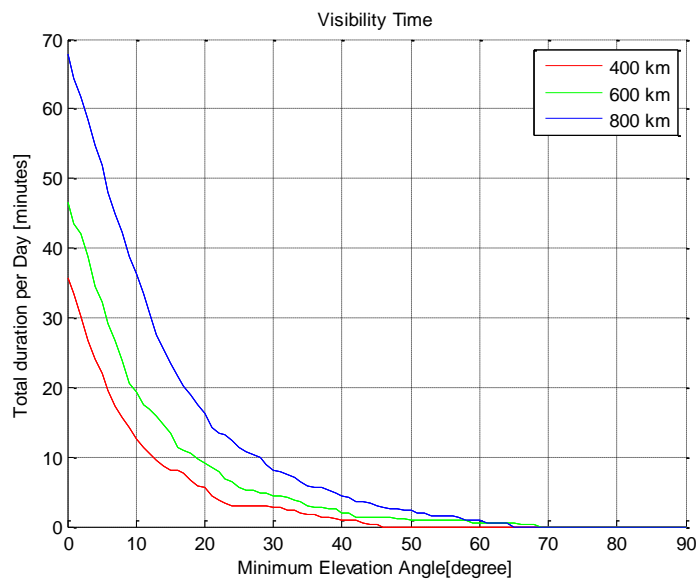


Figure 6.7: Visibility time at 145.9 MHz.

Traces above depict the access time for different minimum elevation angle. A time roughly to 5.5 minutes is reached for a height of 600 km when  $25^\circ$  is chosen as minimum elevation angle. Considering that AX.25 header bits corresponds to 11% of the complete frame downlink capacity can be calculated. Nevertheless, the Information Field includes information from all satellite subsystem, assuming that a 50% of the total packet is available for data; results yield that around 28 images per day can be transferred at height of 600 km and rate of 9600 bps. Images of  $256 \times 256$  pixels has been assumed for transferring, video compression proposed before which reach 0.83 bit per pixel [4] is also taking in account. Results are summarized in the Tables 6.1 and 6.2 for 9600 bps and 1800 bps respectively. Downlink capacity can also be calculated by using `plot_data_down_day.m` Matlab code. It traces the capacity per day for the three heights for different minimum elevation angles, from 0 to  $90^\circ$ .

Table 6.1: Data budget with a rate of 9600 bps.

Parameter	Unit	DL 400 km	DL 600 km	DL 800 km
Rate	[bps]	9600	9600	9600
Visibility time/day	[min]	3	5.57	11.43
Maximum data transferred per day	[bps]	1728000	3208320	6583680
AX.25 frame overhead	[%]	50.00%	50.00%	50.00%
Effective data transferred/day	[bits]	864000	1604160	3291840
Effective data transferred/day	[MBytes]	0.102996826	0.191230774	0.392417908
Data image	[MBytes]	0.00675	0.00675	0.00675
Images transferred/day	[num img]	15.25878906	28.33048503	58.13598633

Table 6.2: Data budget with a rate of 1800 bps.

Parameter	Unit	DL 400 km	DL 600 km	DL 800 km
Rate	[bps]	1800	1800	1800
Visibility time/day	[min]	3	5.57	11.43
Maximum data transferred per day	[bps]	324000	601560	1234440
AX.25 frame overhead	[%]	50.00%	50.00%	50.00%
Effective data transferred/day	[bits]	162000	300780	617220
Effective data transferred/day	[MBytes]	0.019311905	0.03585577	0.073578358
Data image	[MBytes]	0.00675	0.00675	0.00675
Images transferred/day	[num img]	2.861022949	5.311965942	10.90049744

Finally, next Table summarizes the number of images transferred per day for different data rate and minimum elevation angles. On Chapter 5, it was seen that to reach the confident values of link margin  $30^\circ$  results suitable for the three modulations, chosen  $25^\circ$  will imply discard BFSK as an option.

Table 6.3: Images transferred per day for different minimum elevation angles.

Minimum $EI$	Img (9600 bps)	Img (1800 bps)
$20^\circ$	46.49	8.72
$25^\circ$	28.33	5.31
$30^\circ$	22.48	4.22



# Chapter 7

## Software Tools

A set of scripts in Matlab were used to obtain link margin results, some of them was modified from the original implemented in [6] and other were created to improve the accuracy on calculations. A brief description is done in the first part of this Chapter. After that, additional simulations were running on Satellite Tool Kit, remarkable input data used on implementation of NUTS scenario are indicated and relevant results are presented here.

### 7.1 Matlab Implementation

Since all codes include a header with explanations, only main functions are mentioned and briefly described.

`bfsk.m` Implements the error probability for BFSK modulation by using Monte Carlo simulation method and shows the trace compared with theoretical value.  $E_b/N_0$  are vectors called from `link_budget.m` such that  $P_e$  is calculated for two different data rates.

`bpsk.m` Same function as above except that this has been implemented for BPSK modulation scheme. Graphs generated with those codes were taken as a criterion to use theoretical equations for error probabilities due to theoretical and simulated traces are proximate; they are shown in Figure 7.1.

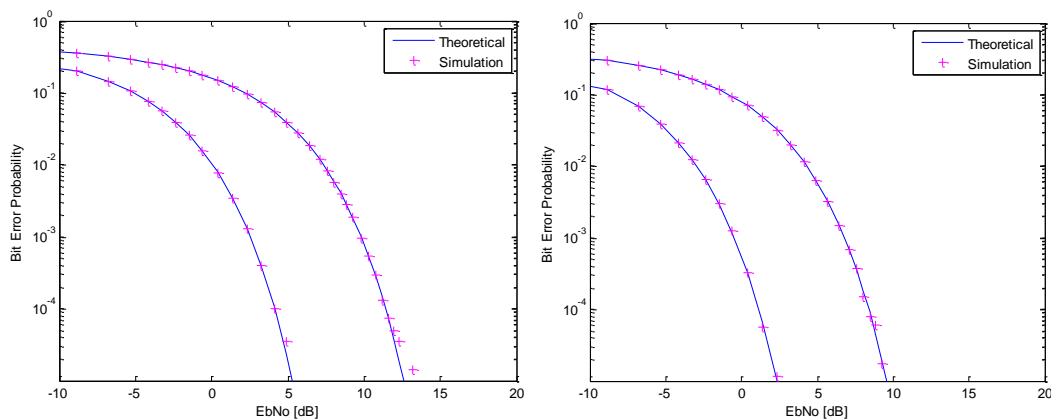


Figure 7.1:  $E_b/N_0$  vs Bit Error Probability for FSK and PSK modulation.



`ber_coded.m` Bit error probability for proposed modulations schemes and block codes are obtained by functions of Matlab Communication ToolBox. `barcoding` function is used for Reed Solomon code and `berawgn` to obtain theoretical uncoded probabilities. Output graph was used in Chapter 5 to analyze coding gain.

`link_budget.m` Calculates the link budget using the input data from `link_data.txt`, the file included in Appendix B contains parameters values according to Chapter 5, not the commercial ones. Output data are presented in graphs of Elevation angle vs  $E_b/N_0$  and Elevation angle vs. Link Margin. This template was implemented on [6], nevertheless necessary modifications have been done in the present work overall to enable the calculations for two data rates and modulations schemes, then graphs generated are focused to compare  $E_b/N_0$  and Link Margin under different modulation and rate conditions in a range of  $0^\circ$  to  $90^\circ$  Elevation angle. Link budget output information is generated for the three different heights, 400 km, 600 km and 800 km, so, several useful traces can be obtained for them just adding the respective plot commands. The first line of the script refers the function that read the link data, input parameters for this function are `file_name.txt` and a number which corresponds to the column selected in the text file and that user want to analyze, a value of 1 corresponds UHF downlink, for instance. Next line read the data of VHF downlink.

```
import_vars('link_data.txt',3) ;
```

Graphs depicted in Figure 7.2 show the  $E_b/N_0$  for downlink along the satellite track according to the analysis from Section 3.5. Losses and antenna gain introduced in the file text are replaced by values given for several functions called on `link_budget.m` script.

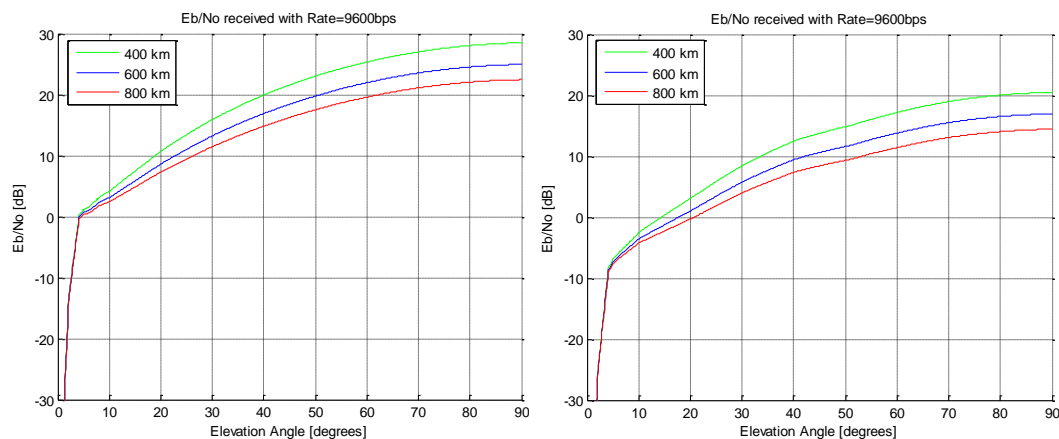


Figure 7.2: Output graphs generated by `link_budget.m`. Left plot depicts the  $E_b/N_0$  received at Earth Station along a range of elevation angles at different height on VHF band. Right graph corresponds to UHF band.

`atmloss_vs_elevation(e1,f)` Executes the interpolation of table 5.3 to obtain atmospheric losses for elevation angles between  $0^\circ$  and  $90^\circ$ . Elevation and frequency are the input data taken from text file.

`ionloss_vs_elevation(e1, f)` Executes the interpolation of tables 5.4 to obtain ionospheric losses for elevation angles between  $0^\circ$  and  $90^\circ$ . The main loss contribution is due to scintillation phenomenon which affects mainly at low elevations.

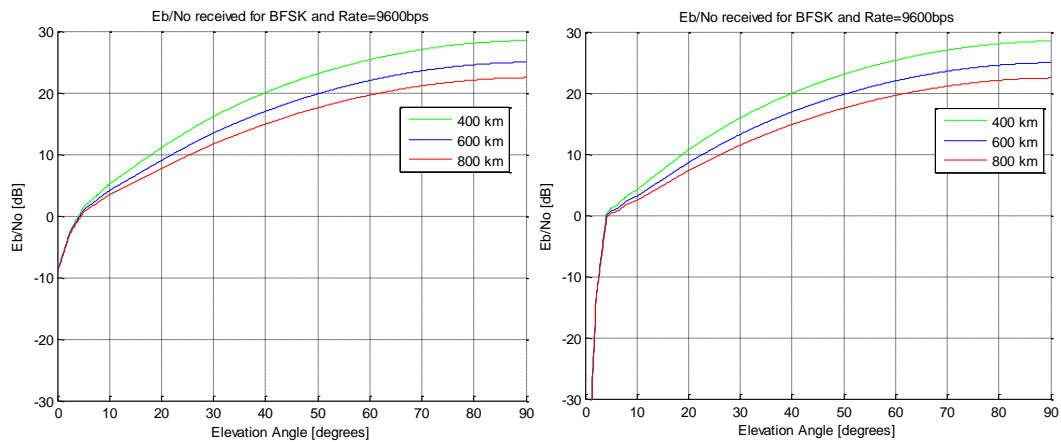


Figure 7.3: Elevation angle vs.  $E_b/N_0$ , left graph was traced before scintillation losses were obtained. Right graph includes these losses where attenuation is considerable in the first 10 angles.

`exec_link_budget.m` This script is run once variables along tracking have been replaced on `link_budget.m` and is a variant from [6], here lines to calculate  $E_b/N_0$  and Link Margin for different data rate were added.

`noise_system.m` Calculates the effective noise temperature for receivers, at Earth station and on board, according to analysis exposed in Section 5.3.

Next functions used in `link_budget.m` template were taken from [6] and are not included in the appendix of this work since not relevant modifications were done. However, modifications or additions implemented are specified in the header of scripts denoted as `===NOTES===`, if applies.

<code>los=los_vs_elevation(e1,h(i))</code>	Calculates Slant range
<code>theta=offset_angle_vs_elevation(e1,h(i))</code>	Obtains Antenna off set angle
<code>G_tx=pattern_dipole(theta,true,true)</code>	Estimates Dipole gain pattern
<code>L_fspl=fspl_vs_los(los,f)</code>	Implement FSL along trajectory

Finally, scripts to calculate the visibility time were explained in Chapter 6, respective codes are attached at the end.

## 7.2 Satellite Tool Kit Simulation

STK is a software program that allows modeling and performing analysis of real space, defense and intelligence systems in real or simulated time based on physics geometry engine. It incorporates environmental conditions and inherent constraints to the equipment, in this case at ground station and on board. Due to its wide functions is divided on modules to establish restrictions that lead to a more accuracy analysis, in this work, communications module was mainly used to define NUTS scenario conditions. Several input data and selection of appropriate

mathematical models are required to acquire adequate results; these are indicated then as well as brief description of criteria that STK considers to make calculations related to noise and losses along the trajectory.

### 7.2.1 Losses and propagation models

#### Propagation Models

ITU-R P.618-8 is the model used as default by STK to calculate scintillation losses and is based on the signal fluctuations due to scintillation. Since this model employs a RF energy model in a beam with a certain beamwidth STK use a dipole antenna of 1 meter and efficiency of 70% to apply this method, however it does not affect the link budget calculations.

ITU-R P.840-3 Attenuation due to clouds and fog is calculated by knowing the content of liquid water contained in a column ( $\text{kg/m}^2$ ). Losses will vary with the elevation angle and the mass absorption coefficient. STK does not allow activate Rain model and Clouds&Fog model simultaneously, separate simulations were executed to confirm theory support that rain does not have influence at VHF and UHF, then final link budget taking account just Clouds&Fog model. Related graphs were used in Chapter 5.

ITU-R P.676-5. It performs the ITU model by tracing a ray on the path to obtain the atmospheric absorption. Trajectory is divided in concentric layers where a number of line segments are computed per layer. Attenuation per segment is obtained by multiplying by the length segment. Total attenuation is the result of adding all attenuation segments. Simulations gave results of 0.5 dB for an elevation angle of  $20^\circ$  and 0.2 dB for  $90^\circ$  confirming that under NUTS system conditions ionospheric losses does not represents a great impact if an elevation angle upper  $20^\circ$  is chosen .

#### Polarization Losses

STK calculates the angle between the vertical references of transmitter and receiver along the line of sight, then, this angle is used to represent states rotation on Poincaré Sphere [21] of the transmitter in the receiver coordinate system. Loss is calculated by the cosine of twice the angle between the two polarization states as was mentioned in Propagation Theory Chapter.

#### Antenna Noise Temperature

Antenna noise in Kelvin is calculated as a function of the elevation angle, STK interpolates values from a table to obtain the noise temperature to each angle, a lower elevation angle a greater noise. A sample file is provided by STK, noise temperature of the first point is taken if elevation angle is below the given values and the last point if elevation is up above.

Table 7.1: Sample file of Antenna Noise Temperature as function of the Elevation angle.

$El$ [°]	0	5	10	20	30	45	60	70	80	90
$T_a$ [K]	100	80	70	60	55	50	45	43	41	40

## 7.2.2 Equipment Considerations

Relevant information related to input data specified for simulations are summarized.

### Earth Station

- Circular antenna ITU-R S1528 1.2 model.
- Antenna efficiency of 70%
- RHCP
- Modulation FSK<sup>2</sup>
- Bandwidth 25 MHz
- Data rate 9600bps
- Sensor implemented to simulate tracking system.

### On board

- Dipole  $\lambda/2$ .
- Antenna efficiency of 70%
- J2 Perturbation
- Mass satellite 2.66 kg
- Inertia matrix for a double CubeSat according to standard specifications [2].
- Antenna Orientation [5 -5 10], in Euler angles.
- Digital transmission parameters as on Earth Station.

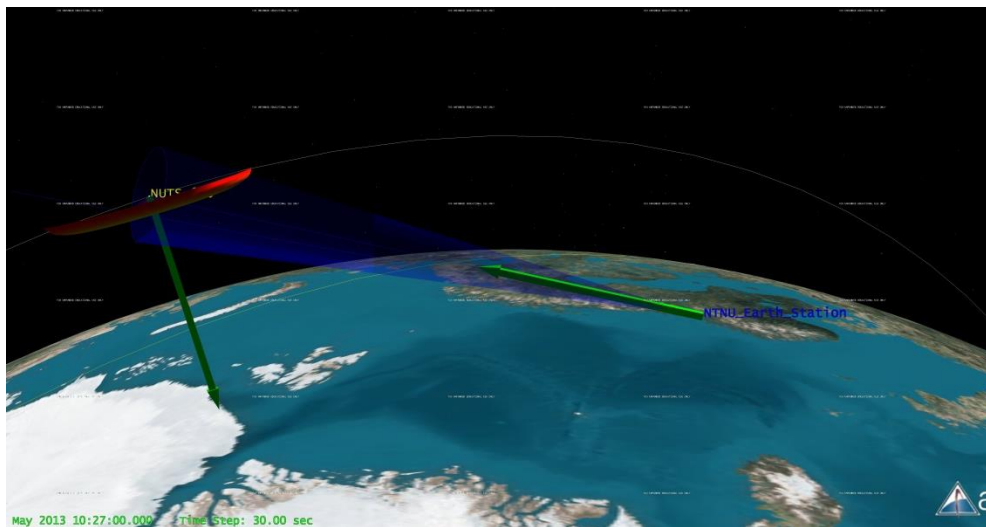


Figure 7.4: NUTS satellite tracking simulated on STK.

STK provides a variety of options to show the output information. Figure 7.5 depicts the  $E_b/N_0$  reached in a pass at 145.9 MHz and 438 MHz respectively, this parameter is also traced for different elevation angles in Figure 7.6 where is seen that  $E_b/N_0$  remains in a range of angles. A report of link budget generated from STK simulations can be found in the Appendix C.

---

<sup>2</sup> Higher modulation schemes and codification techniques are available in the STK menu; nonetheless they are beyond NUTS scope and were not used for simulations.

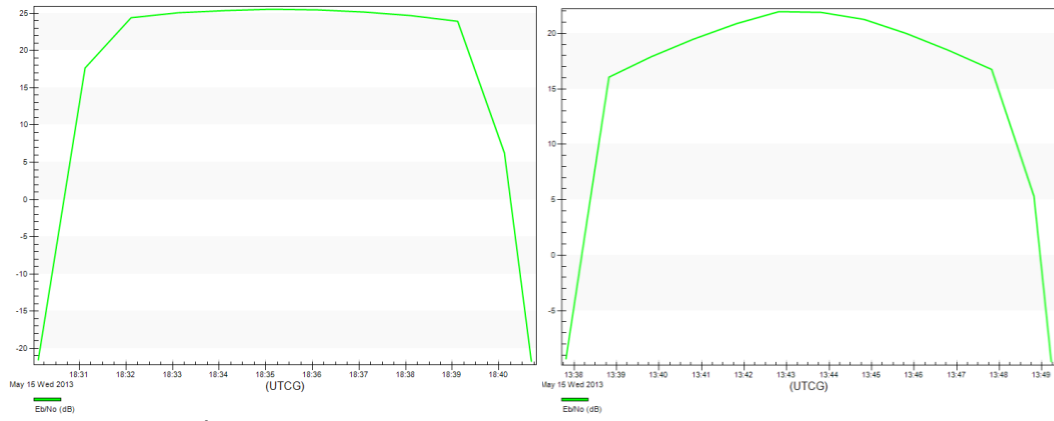


Figure 7.5:  $E_b/N_0$  along the pass for height of 600 km, left graph corresponds to VHF band simulation and right trace is from UHF.

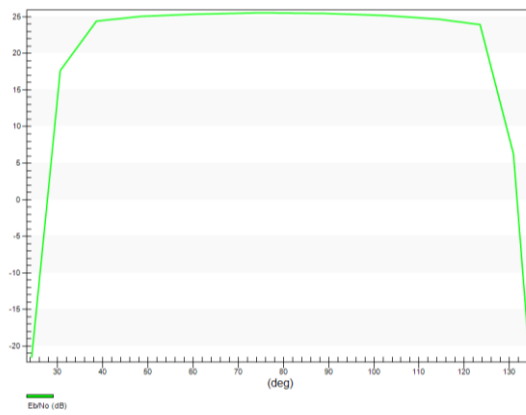


Figure 7.6:  $E_b/N_0$  vs elevation angle at height of 600 km and VHF band.



# Chapter 8

## Conclusions and Future work

### 8.1 Conclusions

Several factors have been taken into consideration for the link budget analysis. NUTS project is formed by different areas working on each subsystem, all of them involves parameters that are directly related with the communication system and become necessary for link budget calculation, power system for transmitted power, ADCS for accuracy tracking, antennas performance, etc. This results in proposed and defined parameters, underway and assumptions, in addition, advances of the project and conditions are changing due to interrelation between subsystems. Such this work implied to collect all of them at the present stage of NUTS and figure out an actualized budget involving digital treatment of the signal, modulation and proposed block codes.

According to results from Chapter 5, link margin obtained to meet a BER of  $10^{-5}$  with binary modulation schemes are enough to cover possible unsteadiness of the link. Values of 12.08 dB and 15.08 dB for BFSK and BPSK at  $90^\circ$  on VHF band provides an ample range to take up of approximations on the calculus, changes on environment conditions depending on the year and epoch since exact date of launching for NUTS is not yet defined, or future changes on devices selected for spacecraft. For low elevations, an angle of  $25^\circ$  as minimum is proposed; it will provide a link margin of 1.5 for BPSK. As was seen with  $20^\circ$ , energy per bit to noise ratio received is not enough for the threshold required, BFSK is not available at least if  $30^\circ$  is chosen. In the case of UHF band, link margin is not as wide as in VHF, however values of 4.06 dB for BFSK and 7.06 dB for BPSK can be considered acceptable and confident to establish communication at  $90^\circ$ ; minimum elevation angle nonetheless is reduced considerably. This last fact means that visibility time is also reduced and consequently the downlink capacity which suggests UHF for transferring of payload data.

The fact of fading environment necessitates of error correction implementation, then, different combinations for block codes were presented varying data rates, modulations schemes, and codes like Hamming and Reed-Solomon. Implementing of 11/15 Hamming code and PSK modulation results suitable for NUTS in terms of error control and desirable link margin, as values on the Table 5.10 summarized, a weakness here is that it requires a bandwidth of 30 kHz, higher than planned for NUTS, although in comparison with Reed-Solomon

results, this last one aims to wide bandwidth derived of higher modulation schemes.

Results from STK simulations are consistent with values reached with the methodology developed in this work, energy per bit to noise ratio of 25 dB is met with an elevation angle of 70 ° and link margin of 13 dB under the same BER conditions and binary FSK modulation on VHF band.

Downlink data rate obtained in the sixth Chapter is only reached if compression techniques are implemented, whereas not, images transferred will decrease considerably from 28 images per day to 3 at 600 km and 9600 bps. Since a high important factor corresponds to visibility time, it can be enhanced if minimum elevation angle is redefined.

## **8.2 Future Work**

Perform an analysis of the time during which the link remains on certain angles could be a new variable to involve and define a minimum elevation. A shorter time at minimum angle a less impact on link performance. This parameter in conjunction with modulation, error control codes and derived implications should provide a higher downlink capacity. Up to now, satellite position along tracking has been considered pointing to the center of the Earth; an interesting analysis will be to simulate tracking if satellite points to ground station during the pass. It is clear that this change will imply an improvement on energy per bit to noise ratio received, nevertheless since it involves additional work for ADCS team, results important to know how much the enhancement is, and depending on results evaluate if it is worth to make changes. Respect to images, transferring analysis per day results of cumulative time from different passes during one day which is well to know capacity, since is also desirable obtain lengthy sequences a review of time per pass and respective downlink will result useful to determine effectiveness on transferring.





# References

- [1] H. J. Kramer & A. P. Cracknell, “An overview of small satellites in remote sensing”, *International Journal of Remote Sensing*, 2008.
- [2] The CubSat Program, “CubeSat Design Specification”, Rev. 12, Cal Poly SLO, 2011.
- [3] Roger Birkeland, “NUTS-1 Mission Statement”, NTNU, 2011
- [4] M. Bakken, “Master’s thesis: Signal processing for communicating gravity wave images from the NTNU test satellite”, NTNU, 2012.
- [5] Roger Birkeland & Odd Gutteberg, “Overview of the NUTS CubeSat Project”, 2nd IAA Conference On University Satellite Missions And Cubesat Workshop, 2013.
- [6] Sigvald Marholm ,“Master’s Thesis: Antenna Systems for NUTS”, NTNU, 2012.
- [7] R. Birkeland, E. K. Blom, and E. Narverud, “Small student satellite,” NTNU, 2006.
- [8] W. A. Beech, D. E. Nielsen, J. Taylor. “AX.25 Link Access Protocol for Amateur Packet Radio”, Version 2.2, American Radio Relay League and the Tucson Amateur Packet Radio Corporation, 1998.
- [9] G. Málal & M. Bousquet, “Satellite Communications Systems”, Fifth Edition 2009.
- [10] T. Pratt, C. Bostian & J. Allnutt, “Satellite Communications”, Second Edition. 2003.
- [11] L. Ippolito, “Satellite Communications Systems Engineering”, 2008.
- [12] F. Solar. “Master’s thesis: Design of Attitude Estimation and Control System for a Cube Satellite”, NTNU, 2012.

- [13] M. Nygren, "Project work: Using Solar Panels as Sun Sensors on NTNU Test Satellite", NTNU, 2012.
- [14] T. Rinnan, "Master's thesis: Development and Comparison of Estimation Methods for Attitude Determination", NTNU, 2012.
- [15] F. Alvenes, "Project work: Satellite Attitude Control System", NTNU, 2012.
- [16] F. Alvenes, Oral Statement, NTNU, 2013.
- [17] F. Solar. "Final Year Project: Optimal attitude control of a double CubeSat using magnetorquers", NTNU, 2011.
- [18] S. Marholm, "Specialization project: Antenna Systems for NUTS", NTNU, 2012.
- [19] S.R. Saunders and A. A. Zavala, "Antennas and Propagation for Wireless Communication Systems", Second Edition, 2007.
- [20] ITU R-P.531-11, In force.
- [21] J. D. Kraus. "Antennas".
- [22] J. S. Hollis, T. J. Lyon, and L. Clayton, "Microwave Antenna Measurements", 1970.
- [23] L. J. Ippolito, "Modeling and prediction of atmospheric propagation effects from satellite beacons", Stanford Telecom, 1994.
- [24] C. A. Balanis, "Antenna Theory: Analysis Design". Third Edition, 2005.
- [25] J.S. Seybold, "Introduction to RF Propagation", 2005.
- [26] David. M. Pozar "Microwave and RF Design of Wireless Systems", 2001.
- [27] J. Y. Stein. "Digital Signal Processing", 2000.
- [28] NEO NASA Earth Observations. <http://neo.sci.gsfc.nasa.gov/ICETray.html>
- [29] B. Sklar. "Digital Communication Fundamentals and Applications", Second Edition, 2001.
- [30] ITU R R-REC-P.618-6, In force.
- [31] ITU R R-REC-P.618-10, In force.
- [32] ITU R R-REC-P.676, In force.
- [33] ITU R-REC-P.1239-3, In force.

- [34] C. G. Little, W. M. Rayton, and R. B. Roof, "Review of Ionospheric Effects at VHF and UHF", Proceedings of the Institute of Radio Engineers Journal 1956, Version, 2007.
- [35] L. J. Ippolito, Jr., V. Nostrand-Reinhold, "Radiowave Propagation in Satellite Communications", First Edition, 1986.
- [36] A. Dahl. et. al., "Nuts link budgets", NTNU.
- [37] K. M. Cheung, C. Ho, C. H. Lee, et. al., "Wallops' Low Elevation Link Analysis for the Constellation Launch/Ascent Links", IEEE Aerospace Conference, 2011.
- [38] Mohd-Yusoff, N. Sengupta, C. Alder, C., I.A. Glover, et. al., "Analysis of low elevation slant path scintillation", Eighth International Conference on Antennas and Propagation, 1993.
- [39] K. M. Cheung, C. Ho and C. H. Lee "A unified low elevation angle scintillation model", IEEE International Symposium on Antennas and Propagation, 2011.
- [40] D. Roddy, "Satellite Communications", Fourth Edition, 2006.
- [41] R. Birkeland, E. Blom and E. Narverud. "Design of a Small Student Satellite", NTNU, 2006
- [42] Bryan Klofas and Jason Anderson. "A Survey of CubeSat Communication Systems", California Polytechnic State University, 2008.
- [43] S. Prasai, "Master's Thesis: Access control of NUTS uplink", NTNU, 2012.

# Appendix A

## Link Budget

Following tables correspond to link budget calculations in both directions for an elevation angle of  $90^\circ$ . Modulation schemes are involved to determine link margin. Last table implicate FEC.

NUTS Link Budget on VHF band					
Parameter	Description	Unit	DL VHF	UL VHF	
f	Frequency	[MHz]	145.90	145.90	
l	Height	[km]	600.00	600.00	
$\theta$	Elevation angle	[ $^\circ$ ]	90.00	90.00	
Pt	Tx Power	[dBW]	0.00	20.00	
Ltx_p	Tx passive losses	[dB]	5.90	6.26	
Gt	Tx Gain	[dBi]	2.15	13.10	
EIRP	EIRP	[dBW]		-3.75	26.84
PLF	Polarization loss	[dB]	3.00	3.00	
FSPL	Free space propagation loss	[dB]	131.18	131.18	
Latm	Atmosferic loss	[dB]	0.30	0.30	
Lion	Ionosferic loss	[dB]	1.01	1.01	
Ltxpt	Tx pointing loss	[dB]	0.20	0.70	
PrxIso	Isotropically Received Power	[dBW]		-139.44	-109.35
Gr	Rx antenna gain peak	[dBi]	13.10	2.15	
Lrxpt	Rx pointing loss	[dB]	0.70	0.20	
Lrx_p	Rx passive losses	[dB]	6.26	5.90	
PrxIso	Receiver signal power	[dBW]		-133.30	-113.30
T	Noise System Temperature	[K]	1229.20	261.00	
TdB	System Temperature in dB	[dBK]	30.90	24.17	
BdB	Spectral (noise) bandwidth in receiver in dB	[dBHz]	43.98	43.98	
G/T	System G/T	[dBK]	-17.80	-22.02	
C/N	Signal to Noise ratio received	[dB]		20.42	47.15
R	Data rate	[dB-bits]	39.82	39.82	
(Eb/No)rec	Bit energy to noise density ratio received	[dB]		24.58	51.31
(Eb/No)req	Bit energy to noise density ratio required BFSK	[dB]	12.50	12.50	
LM_bfsk	Link margin BFSK	[dB]		12.08	38.81
(Eb/No)req	Bit energy to noise density ratio required BPSK	[dB]	9.50	9.50	
LM_bpsk	Link margin BPSK	[dB]		15.08	41.81

NUTS Link Budget on UHF band					
Parameter	Description	Unit	DL UHF	UL UHF	
f	Frequency	[MHz]	438.00	438.00	
l	Height	[km]	600.00	600.00	
θ	Elevation angle	[ ° ]	90.00	90.00	
Pt	Tx Power	[dBW]	0.00	18.75	
Ltx_p	Tx passive losses	[dB]	6.70	8.48	
Gt	Tx Gain	[dBi]	2.15	16.00	
EIRP	EIRP	[dBW]		-4.55	26.27
PLF	Polarization loss	[dB]	3.00	3.00	
FSPL	Free space propagation loss	[dB]	140.73	140.73	
Latm	Atmospheric loss	[dB]	0.30	0.30	
Lion	Ionospheric loss	[dB]	1.30	1.30	
Ltxpt	Tx pointing loss	[dB]	0.20	0.70	
PrxIso	Isotropically Received Power	[dBW]		-150.08	-119.76
Gr	Rx antenna gain peak	[dBi]	16.00	2.15	
Lrxpt	Rx pointing loss	[dB]	0.70	0.20	
Lrx_p	Rx passive losses	[dB]	8.48	6.70	
PrxIso	Receiver signal power	[dBW]		-143.26	-124.51
T	Noise System Temperature	[K]	786.04	522.00	
TdB	System Temperature in dB	[dBK]	28.95	27.18	
BdB	Spectral (noise) bandwidth in receiver in dB	[dBHz]	43.98	43.98	
G/T	System G/T	[dBK]	-12.95	-25.03	
C/N	Signal to Noise ratio received	[dB]		12.40	32.93
R	Data rate	[dB-bits]	39.82	39.82	
(Eb/No)rec	Bit energy to noise density ratio received	[dB]		16.56	37.09
(Eb/No)req	Bit energy to noise density ratio required BFSK	[dB]	12.50	12.50	
LM_bfsk	Link margin BFSK	[dB]		4.06	24.59
(Eb/No)req	Bit energy to noise density ratio required BPSK	[dB]	9.50	9.50	
LM_bpsk	Link margin BPSK	[dB]		7.06	27.59

NUTS Link Budget with FEC						
Parameter	Description	Unit	DL VHF	UL VHF	DL UHF	UL UHF
BdB	Spectral (noise) bandwidth in receiver in dB	[dBHz]	44.77	44.77	44.77	44.77
G/T	System G/T	[dBK]	-17.80	-22.02	-12.95	-25.03
C/N	Signal to Noise ratio received	[dB]		19.63	46.36	11.61
R	Data rate	[dB-bits]	39.82	39.82	39.82	39.82
(Eb/No)rec	Bit energy to noise density ratio obtained	[dB]		24.58	51.31	16.56
(Eb/No)req	Eb/No required 4-PSK, 11/15 Hamming	[dB]	8.70	8.7000	8.7000	8.7000
LM	Link margin	[dB]		15.88	42.61	7.86

# Appendix **B**

## Matlab Scripts

### B.1 Bit Error Probability

#### **bfsk.m**

```
%  
% Present script estimates Error probability for BFSK Modulation  
% by means of iterations based on Monte Carlo simulation method,  
Eb/No is a  
% vector called from link_budget.m template. Then, it makes a  
comparision  
% between simulated and theoretical BER.  
  
clear all  
close all  
  
link_budget  
  
ebnodB_aux1=EbNo_96;  
ebnodB_aux2=EbNo_18;  
  
ebnodB1=ebnodB_aux1(1:25:length(ebnodB_aux1)); %Eb/No for  
9600bps from Link budget template  
ebnodB2=ebnodB_aux2(1:25:length(ebnodB_aux2)); %Eb/No for  
1800bps from Link budget template  
nbits1=10000;  
  
ebno1=10.^(ebnodB1/10) ;  
ebno2=10.^(ebnodB2/10) ;  
  
h=waitbar(0, 'SNR Iteration');  
lebno=length(ebnodB1);  
  
for j=1:lebno  
    waitbar(j/lebno);  
    sigma1=sqrt(1/(2*ebno1(j)));  
    sigma2=sqrt(1/(2*ebno2(j)));  
    nerrors1=0;  
    nerrors2=0;  
    for k=1:(nbits1+(lebno*10000))  
  
        d1=round(rand(1));
```

```

% Transmitter
if d1==0
    xd1=1;
    xq1=0;
else
    xd1=0;
    xq1=1;
end

% AWGN Noise
nd1=sigma1*randn(1);
nq1=sigma1*randn(1);

nd2=sigma2*randn(1);
nq2=sigma2*randn(1);

% Receiver
yd1=xd1+nd1;
yq1=xq1+nq1;

yd2=xd1+nd2;
yq2=xq1+nq2;

% Detection
if yd1>yq1
    dest1=0;
else
    dest1=1;
end
if(dest1 ~=d1)
    nerrors1=nerrors1+1;
end

%1800
if yd2>yq2
    dest2=0;
else
    dest2=1;
end
if(dest2 ~=d1)
    nerrors2=nerrors2+1;           % Errors counter
end

end

errors1(j)=nerrors1;
errors2(j)=nerrors2;
end
close(h)

% Calculate BER by counting generated errors from iterations.
ber_s1=errors1/(nbits1+(lebno*10000));
ber_s2=errors2/(nbits1+(lebno*10000));

% Calculate BER by using theoretical form.
ber_t1=0.5*erfc(sqrt(0.5*ebno1));
ber_t2=0.5*erfc(sqrt(0.5*ebno2));

% Plot BER

```



```

figure
semilogy(ebnodB1,ber_t1,'b')
hold on
semilogy(ebnodB1,ber_s1,'m+')
hold on
semilogy(ebnodB1,ber_t2,'b')
hold on
semilogy(ebnodB1,ber_s2,'m+')
hold on
axis([-10 20 0.00001 1])
xlabel('EbNo [dB]')
ylabel('Bit Error Probability')
legend('Theoretical', 'Simulation')

```

## bpsk.m

```

%
% Present script estimates Error probability for BPSK Modulation
% by means of iterations based on Monte Carlo simulation method,
Eb/No is a
% vector called from link_budget.m template. Then, it makes a
comparision
% between simulated and theoretical BER.

clear all
close all

link_budget

ebnodB_aux1=EbNo_96;
ebnodB_aux2=EbNo_18;
ebnodB1=ebnodB_aux1(1:25:length(ebnodB_aux1)); %Eb/No for
9600bps from Link budget template
ebnodB2=ebnodB_aux2(1:25:length(ebnodB_aux2)); %Eb/No for
1800bps from Link budget template
nbits1=100000;
ebno1=10.^(ebnodB1/10) ;
ebno2=10.^(ebnodB2/10) ;

h3=waitbar(0, 'Executing iterations');
lebno=length(ebnodB1);
for i=1:lebno
    waitbar(i/lebno)

    sigma1=sqrt(1/(2*ebno1(i))); % Noise deviation
    sigma2=sqrt(1/(2*ebno2(i))); % Noise deviation

    error_count1=0 ;
    error_count2=0 ;

    for j=1:(nbits1+(lebno*10000))

        % Transmitted signal
        bits1=round(rand(1));
        s1=2*bits1-1; %Transmitted signal

        % AWGN noise
        noise1=sigma1*randn(1);
        noise2=sigma2*randn(1);
    end
end

```

```

    % Received signal
    ns1=s1+noise1;
    ns2=s1+noise2;

    % Detection for signal to 9600 bps
    if ns1>0
        dbits1=1;
    else
        dbits1=0;
    end
    if (dbits1 ~=bits1)
        error_count1=error_count1+1;
    end

    % Detection for signal to 1800 bps
    if ns2>0
        dbits2=1;
    else
        dbits2=0;
    end
    if (dbits2 ~=bits1)
        error_count2=error_count2+1;    % Errors counter
    end

    end
    errors1(i)=error_count1;
    errors2(i)=error_count2;
end
close(h3)

% Calculate BER by counting generated errors from iterations.
ber_s1=errors1/(nbits1+(lebno*10000));
ber_s2=errors2/(nbits1+(lebno*10000));

% Calculate BER by using theoretical form.
ber_t1=0.5*erfc(sqrt(10.^(ebnodB1/10)));
ber_t2=0.5*erfc(sqrt(10.^(ebnodB2/10)));

% Plot BER
figure
semilogy(ebnodB1,ber_t1,'b')
hold on
semilogy(ebnodB1,ber_s1,'m+')
hold on
semilogy(ebnodB1,ber_t2,'b')
hold on
semilogy(ebnodB1,ber_s2,'m+')
hold on
axis([-10 20 0.00001 1])
xlabel('EbNo [dB]')
ylabel('Bit Error Probability')
legend('Theoretical', 'Simulation')

```

## B.2 Link Budget

### link\_budget.m

```
%  
% GENERIC LINK BUDGET CALCULATIONS TEMPLATE  
%  
% This template implements the basic link budget in MATLAB and can  
be  
% further extended in order to extract parameters in the link  
budget and to  
% tweak parameters in the link budget. All the link budget  
parameters will  
% be available in this workspace for manipulation. Without further  
% manipulations the two lines of code will compute the link budget  
as is  
% the excel sheet provided by ØAsbjørn Dahl .  
%  
% Example of use 1: Extract SNR link margin  
% It is found in exec_link_budget.m that the SNR link margin is  
stored in  
% the variable LM_snr. This will be stored to workspace and can  
simply by  
% read by executing "LM_snr" on the end of the script .  
%  
% Example of use 2: Compare different budgets  
% Add a loop around the whole script and iterate through all  
budgets of  
% interest. The link budget variable names will be over written in  
each  
% iteration so store the variables of interest into an array that  
will  
% contain them after the loop has run. NB: import_link_vars( ) can  
also  
% take the budget number as argument instead of two text strings  
% describing which budget it is. It plays nicer with loops.  
%  
% Example of use 3: Plot link budget variable versus elevation  
% Create a vector of different elevation angles. Import link  
budget  
% variables with import_link_vars() as usual but over write the  
% elevation-dependent variables with vectors corresponding to the  
% different elevations afterwards. There are functions created for  
this.  
% Run exec_link_budget as usual and plot elevation versus the  
variable of  
% interest, i.e. link margin.  
%  
% Example of use 4: Plot link budget variables versus time  
% Assume circular orbit. Compute elevation angles versus time and  
follow  
% example 3 but plot versus time instead of elevation. There are  
% function screated for this .  
%  
% Example of use 5: Synthesize ideal antenna gain (advanced)  
% Load variables and replace the satellite antenna with an  
isotropic one  
% and compute link margin for a sweep of elevation angles. De fine  
the  
% ideal link margin to be constant (at least above some cut-off  
elevation
```

```

% angle) and take the difference between ideal and isotropic link
margin
% to be the preliminary antenna gain versus elevation. Convert to
gain
% versus theta. Antenna gain will be unphysical as the ideal link
% margin is arbitrarily chosen. Normalize such that average gain
is 1.
% Recompute link budget with exec_link_budget with new parameters
to get
% actual link margin
%
% Overview of different budgets:
%
% 1-UHF Downlink
% 2-UHF Uplink
% 3-VHF Downlink
% 4-VHF Uplink
% 5-Beacon Downlink
% 6-Beacon Uplink
%
% import_vars() can take either budget numer or strings as
arguments
%
% LOAD NECESSARY VARIABLES WITH DEFAULT VALUES
%
% See link_data.txt for details about the variables .
% All variables are converted to SI-units .
%
%clear all
%close all
%clc
%===== NOTES =====
% Threshold values for BFSK and BPSK were added to link_data.txt
file to figure out the right Link Margin. In addition, rates of
9600 and 1800 also have been included. Lines codes to download
Eb/No for both cases have been added, to calculate Link Margin
calculation and generate graphs as well. link_budget.m is called
on bfsk.m and bpsk.m since Eb/No is required to figure out Error
Probability.
%=====

import_vars('link_data.txt',3) ;           % Select frequency%
evalin('caller','f=f*1e6;') ;             % MHz > Hz
evalin('caller','A_h = A_h*1e3 ; ') ;     % km > m
evalin('caller','B=B*1e3; ') ;           % kHz > Hz

h=[400 600 800]*1e3 ;                     % Heights
t=0:1000 ;                                 % Time after rise [s]
el=0:0.09:90;

h0=waitbar(0,'Executing Link Budget');

for i=1:3
waitbar(i/3);
adcs_acc = 2 ;                             % Accuracy of ADCS [degree]

los=los_vs_elevation(el,h(i)) ;           % Slant range [m]
theta=offset_angle_vs_elevation(el,h(i)); % Antenna off set angle
[degree]

```

```

theta=theta+adcs_acc ; % Add ADCS uncertainty
[degree]

% Replace Link Budget variables
L_plf=3 ;
L_tx_pnt=0 ; % Included in G_tx

if dir==1
    G_tx=pattern_dipole(theta,true,true); % Diagram(normalized)
    G_tx=G_tx+2.15; % Denormalize
else
    G_tx=G_tx;
end

L_fspl=fspl_vs_los(los,f) ; % FSPL [dB]

atmloss_vs_elevation(el,f) ;
L_atm=atmloss_vs_elevation(el,f) ; % Atmosferic losses [dB]

L_ion=ionloss_vs_elevation(el,f) ; %
Ionospheric losses [dB]

exec_link_budget ; % Run link budget

% Load some useful results from exec_link_budget for both rates.
E_ebno_96(1,i,:)=EbNo_96 ;
E_ebno_18(1,i,:)=EbNo_18;

E_LM_ebno_96_fsk(1,i,:)=LM_ebno96_fsk ;
E_LM_ebno_18_fsk(1,i,:)=LM_ebno18_fsk ;

E_LM_ebno_96_psk(1,i,:)=LM_ebno96_psk ;
E_LM_ebno_18_psk(1,i,:)=LM_ebno18_psk ;

end
close(h0);

% Plot Eb/No vs. Elevation and Eb/No Threshold BER=10e-5
figure
hold on
title('Eb/No received with Rate=9600bps') ;
plot(el(1,:),squeeze(E_ebno_96(1,1,:)), 'g') ;
plot(el(1,:),squeeze(E_ebno_96(1,2,:)), 'b') ;
plot(el(1,:),squeeze(E_ebno_96(1,3,:)), 'r') ;
legend('400 km', '600 km', '800 km') ;
xlabel('Elevation Angle [degrees]') ;
ylabel('Eb/No [dB]') ;
axis([ 0 90 -30 30 ]) ;
grid on

% Plot LM vs Elevation for both modulations
figure
hold on
title('Link Margin for BFSK') ;
plot(el(1,:),squeeze(E_LM_ebno_96_fsk(1,1,:)), 'g') ;
plot(el(1,:),squeeze(E_LM_ebno_96_fsk(1,2,:)), 'b') ;
plot(el(1,:),squeeze(E_LM_ebno_96_fsk(1,3,:)), 'r') ;
legend('400 km', '600 km', '800 km') ;

```

```

xlabel('Elevation Angle [degrees]') ;
ylabel('Link Margin (Eb/No) [dB]') ;
axis([ 0 90 -30 30 ]) ;
grid on

figure
hold on
title('Link Margin for BPSK') ;
plot(el(1,:),squeeze(E_LM_ebno_96_psk(1,1,:)), 'g') ;
plot(el(1,:),squeeze(E_LM_ebno_96_psk(1,2,:)), 'b') ;
plot(el(1,:),squeeze(E_LM_ebno_96_psk(1,3,:)), 'r') ;
legend('400 km', '600 km', '800 km') ;
xlabel('Elevation Angle [degrees]') ;
ylabel('Link Margin (Eb/No) [dB]') ;
axis([ 0 90 -30 30 ]) ;
grid on

% Plot Eb/No vs. Elevation and Eb/No Threshold BER=10e-5
figure
hold on
title('Eb/No received at 600 KM') ;
plot(el(1,:),squeeze(E_ebno_96(1,2,:)), 'b') ; %Eb/No, Rate=9600
plot(el(1,:),EbNo_thr_fsk, 'g') ;
plot(el(1,:),EbNo_thr_psk, 'm') ;
plot(el(1,:),EbNo_thr_cqpsk, 'c') ;
xlabel('Elevation Angle [degrees]') ;
ylabel('Eb/No [dB]') ;
axis([ 0 90 -30 40 ]) ;
%legend('Eb/No Received R=9600bps', 'Eb/No Threshold FSK', 'Eb/No
Threshold PSK' , 'Eb/No Threshold Coded 4-PSK' ) ;
grid on

```

## Atmospheric Losses

### atmloss\_vs\_elevation.m

```

%
function latm=atmloss_vs_elevation(el,f)
% Given empirical values from "Radiowave Propagation in Satellite
% Communications" by L. J. Ippolito, Jr., V. Nostrand-Reinhold,
this
% function make an interpolation to obtain losses for different
angles.

ellist=el ;
for i=1:length(el)
    el=ellist(i) ;
    % Given preset values
    list_el=[0 2.5 5 10 30 45 90 ] ;
    list_loss=[10.2 4.6 2.1 1.1 0.4 0.3 0] ;
    % a and b are indices for values to interpolate between
    a=find(list_el<el,1,'last') ;
    b=find(list_el>=el,1,'first') ;
    if (el<=list_el(1))
        loss=list_loss(1) ;
    elseif (el>list_el(end))
        loss=list_loss(end) ;
    else

```

```

        slope=(list_loss(b)-list_loss(a))/(list_el(b)-list_el(a)) ;
        loss=list_loss(a)+slope*(el-list_el(a)) ;
    end
    latm(i)=loss ;

end

end

```

## Ionospheric Losses

### ionloss\_vs\_elevation.m

```

%
function lion=ionloss_vs_elevation(el,f)
% Given values from STK simulation, this function make an
% interpolation to obtain ionospheric losses for different angles.
% List values includes losses due to Scintillation and Cloud&Fog.
ellist=el ;
for i=1:length(el)
    el=ellist(i) ;

% Given preset values for 145.9 MHz
if f==145.9*1e6
    list_el=[0.1 2.12 4.12 6.10 7.98 10.13 20.14 29.68 40.27 49.7
63.39 70.87 80 90] ;
    list_loss=[44.18 11.17 0.9 1.65 1.52 2.01 1.36 1.23 1.07 1.04
1.02 1.01 1.01 1.01] ;
    % a and b are indices for values to interpolate between
    a=find(list_el<el,1,'last') ;
    b=find(list_el>=el,1,'first') ;
    if (el<=list_el(1))
        loss=list_loss(1) ;
    elseif (el>list_el(end))
        loss=list_loss(end) ;
    else
        slope=(list_loss(b)-list_loss(a))/(list_el(b)-list_el(a)) ;
        loss=list_loss(a)+slope*(el-list_el(a)) ;
    end
    lion(i)=loss ;
end

% Given preset values for 438 MHz
if f==438*1e6
    list_el=[0.1 2.12 4.12 6.10 7.98 10.13 20.66 31.75 40.27 51.11
63.39 70.87 80 90] ;
    list_loss=[47.95 15.05 1.72 1.33 1.17 0.93 1.26 0.95 0.82 1.56
1.42 1.3 1.3 1.3] ;
    % a and b are indices for values to interpolate between
    a=find(list_el<el,1,'last') ;
    b=find(list_el>=el,1,'first') ;
    if (el<=list_el(1))
        loss=list_loss(1) ;
    elseif (el>list_el(end))
        loss=list_loss(end) ;
    else
        slope=(list_loss(b)-list_loss(a))/(list_el(b)-list_el(a)) ;

```

```

        loss=list_loss(a)+slope*(el-list_el(a)) ;
    end
    lion(i)=loss ;
end

end

end

```

## Link budget calculations

### exec\_link\_budget.m

```

%
%=====NOTES=====
% This script make the main operations for link_budget.m, is
% called from that template and yields result that are used for
% plots. It can also be run byitself whether link data has been
% loaded. Lines to calculate Eb/No for two different data rate and
% respective operations to obtain both Link Margin have been added.
%=====
%SIGNAL PATH
%
P_tx=10*log10(P_tx_w) ; % Transmitted Power [dBW]

P_eirp=P_tx-L_tx_tl+G_tx ;
% EIRP[dBW]=
% Transmitted Power[dBW]-TX Transmission Line Losses[dB]+TX
% Antenna Gain [dBi]

P_rx_iso=P_eirp-L_tx_pnt-L_rain-L_fspl-L_plf-L_atm-L_ion ;
% Isotropically Received Power[dBW]=
% EIRP [dBW]-TX Pointing Loss[dB]-Rain Loss [dB]-FSPL[dB]-
% PLF [dB]-Atmospheric Loss[dB]-Ionospheric Loss[dB]

P_rx=P_rx_iso+G_rx-L_rx_pnt-L_rx_tl ;
% Received Power [dBW]=
% Isotropically Received Power[dBW]+RX Antenna Gain[dBi]-RX
% Pointing Loss[dB]-RX Transmission Line Losses [dB]
%
% NOISE PATH
%
K=-228.6 ; % Boltzman's constant [dBW/K/Hz]
T_db=10*log10(T) ; % Effective Noise Temperature [dBK]
B_db=10*log10(B) ; % RX (Noise) Bandwidth [dBHz]

No=K+T_db ; % (No=kT)
% Noise density[dBW/Hz]=
% Boltzman's constant[dBW/K/Hz] + Effective Noise
% Temperature[dBK]

N=No+B_db ; % (N=kTB)
% Received Noise Power [dBW]=
% Noise density[dBW/Hz]+RX (Noise) Bandwidth[dBHz]

%
% SNR

```



```

%
SNR=P_rx-N ; % Signal to Noise ratio[dB]
%LM_snr=SNR-SNR_thr ; % Link Margin (in SNR) [dB]

%
% Eb/No
%
R1_db=10*log10(R1) ; % Data rate 9600 [dBHz]
R2_db=10*log10(R2) ; % Data rate 1800 [dBHz]

SNo=P_rx-No ; % Signal to noise density ratio [dBHz]
% 9600
EbNo_96=SNo-R1_db ; % Bit energy to noise density ratio, 9600bps
[dB]
% 1800
EbNo_18=SNo-R2_db; % Bit energy to noise density ratio, 1800bps
[dB]

%
% Link Margin
%
% FSK
LM_ebno96_fsk=EbNo_96-EbNo_thr_fsk ; % Link Margin (in Eb/No) [dB]
LM_ebno18_fsk=EbNo_18-EbNo_thr_fsk ; % Link Margin (in Eb/No) [dB]

% PSK
LM_ebno96_psk=EbNo_96-EbNo_thr_psk ; % Link Margin (in Eb/No) [dB]
LM_ebno18_psk=EbNo_18-EbNo_thr_psk ; % Link Margin (in Eb/No) [dB]
%
% G/T
%
GT=G_rx-L_rx_tl-T_db ; % G/T Figure of Merit

```

## Noise System Calculations

### noise\_system.m

```

%
% This script calculates effective noise temperature at Earth
Station
% and On board receiver considering that
% System Temperature= Antenna temperature + Composite temperature
% Composite temperature=
%   % Line antenna to lna temperature...
%   % + LNA temperature
%   % + Line from LNA to front end receiver temperature

B=25000 ; % Bandwidth [Hz]
k=1.38e-23 ; % Boltzman's constant
B_db=10*log10(B) ; % RX (Noise) Bandwidth [dBHz]
Tsky_VHF=1000 ; % Sky temperature for 145.9 MHz at elevation
of 0 degrees [K]
Tsky_UHF=150 ; % Sky temperature for 438.5 MHz at elevation
of 0 degrees [K]
n=0.7 ; % Antenna efficiency
To=290 ; % Reference Temperature [k]

% Antenna Noise Temperature
Ta_es_VHF=Tsky_VHF*n+(To*(1-(1/3)))*(1-n)+(Tsky_VHF*(1/3)*(1-n)) ;

```

```

Ta_es_UHF=Tsky_UHF*n+(To*(1-(1/3))*(1-n))+(Tsky_UHF*(1/3)*(1-n)) ;

% DOWNLINK (Rx at Earth Station)
Ts= 274.02 ;           % Surface Temperature [K]
To_es=(1.12*Ts)-50 ;   % Enviroment Temperature [k]

Ll1_VHF= 1.48 ;        % Loss line antenna-lna. Actual value.
Ll2_VHF=3.28 ;        % Loss line lna-front receiver. Actual value.

Ll1_UHF=1.9 ;         % Loss line antenna-lna. Actual value.
Ll2_UHF=5.08 ;       % Loss line lna-front receiver. Actual value.

NFlna_es=1.5 ;        % LNA Noise figure. Actual value.
Glna_es=15 ;          % LNA gain. Actual value.

%Composite temperature
Tcomp_es_VHF=To_es*(Ll1_VHF-1)+(To_es*(NFlna_es-
1)/(1/Ll1_VHF))+(To_es*(Ll2_VHF-1)/((1/Ll1_VHF)*Glna_es)) ;
Tcomp_es_UHF=To_es*(Ll1_UHF-1)+(To_es*(NFlna_es-
1)/(1/Ll1_UHF))+(To_es*(Ll2_UHF-1)/((1/Ll1_UHF)*Glna_es)) ;

%System Temperature=Antenna temperature+Composite temperature
Ts_dl_VHF=Ta_es_VHF+Tcomp_es_VHF
Ts_dl_UHF=Ta_es_UHF+Tcomp_es_UHF

% UPLINK (Rx at Satellite)
To_sat=To ;
Ta_sat=To ;           % Antena temperature On board
Ll_VHF=1.5 ;          % Loss line antenna-switch (2 connector+
0.5dB cable)
Ll_UHF=3 ;            % Loss line antenna-switch (2 connector+ 1 dB
cable)
Lsw=0.5 ;             % Switch loss
NFlna_sat=1.2 ;       % Noise figure, proposed value.
Glna_sat=15 ;         % LNA Gain, proposed value.

%Composite temperature
Tcomp_sat_VHF=To_sat*(Ll_VHF-1)+(To_sat*(Lsw-
1)/(1/Ll_VHF))+(To*(NFlna_sat-1)/((1/Ll_VHF)*(1/Lsw))) ;
Tcomp_sat_UHF=To_sat*(Ll_UHF-1)+(To_sat*(Lsw-
1)/(1/Ll_UHF))+(To*(NFlna_sat-1)/((1/Ll_UHF)*(1/Lsw))) ;

%System Temperature=Antenna temperature+Composite temperature
Ts_up_VHF=Ta_sat+Tcomp_sat_VHF
Ts_up_UHF=Ta_sat+Tcomp_sat_UHF

```

### B.3 Visibility time

#### plot\_data\_visibility\_time.m

```

%
% This is a script that plots the downloaded data per average day
for
% different orbital heights and threshold elevation angles.
% =====NOTES=====
% Modifications to read three files from STK simulations that
corresponds to different heights, have been done. Present

```

```

simulations was run in a period of time of 1 week, equations was
adapted to it.
% =====

close all

% SIMULATION INPUT GOES HERE (AND IN STK)
altitudes=[400 600 800] ; % different orbital altitudes
thresholds=0:90 ; % different threshold elevation angles

% D and I is hold the average kB downloaded during an average day
and an
% average pass , respectively , for various altitudes and
thresholds .
W=zeros(length(altitudes),length(thresholds)) ;
D=W;
I=D;
T4=I;
T6=I;
T8=I;
% Read access information from fname.dat files.
data4=read_stk_elev(fname_400) ;
data6=read_stk_elev(fname_600) ;
data8=read_stk_elev(fname_800) ;

for alt=1:length(altitudes)

    for thr=1:length(thresholds)

        % 400 %

        intervals=threshold_stk_elev(data4,thresholds(thr)) ;

        if (isempty(intervals)) % Elevation never passes threshold
            start4=0;
            stop4=0;
        else % Elevation is bigger than interval
            start4=datenum(intervals(:,1:6)) ;
            stop4=datenum(intervals(:,7:12)) ;
        end

        duration_d4=stop4-start4; % This is the duration of the
passes in ...days .
        duration_h4=duration_d4*24; % . . . and in hours
        duration_m4=duration_h4*60; % . . . and in minutes.
        duration_s4=duration_m4*60; % . . . and in seconds.

        T4(alt,thr)=sum(duration_m4) ; % Total duration of pass in MIN
T4(alt,thr)=(T4(alt,thr))/7 ; % Total duration of pass in MIN
PER DAY

        % 600 %

        intervals=threshold_stk_elev(data6,thresholds(thr)) ;

        if (isempty(intervals)) % Elevation never passes threshold
            start6=0;
            stop6=0;
        else % Elevation is bigger than interval

```

```

        start6=datetime(intervals(:,1:6)) ;
        stop6=datetime(intervals(:,7:12)) ;
    end

    duration_d6=stop6-start6; % This is the duration of the passes
in ...days .
    duration_h6=duration_d6*24; % . . . and in hours
    duration_m6=duration_h6*60; % . . . and in minutes.
    duration_s6=duration_m6*60; % . . . and in seconds.

    T6(alt,thr)=sum(duration_m6) ; % Total duration of pass in MIN
    T6(alt,thr)=(T6(alt,thr))/7 ; % Total duration of pass in MIN
PER DAY

    % 600 %

    intervals=threshold_stk_elev(data8,thresholds(thr)) ;

    if (isempty(intervals)) % Elevation never passes threshold
        start8=0;
        stop8=0;
    else % Elevation is bigger than interval
        start8=datetime(intervals(:,1:6)) ;
        stop8=datetime(intervals(:,7:12)) ;
    end

    duration_d8=stop8-start8; % This is the duration of the passes
in ...days .
    duration_h8=duration_d8*24; % . . . and in hours
    duration_m8=duration_h8*60; % . . . and in minutes.
    duration_s8=duration_m8*60; % . . . and in seconds.

    T8(alt,thr)=sum(duration_m8) ; % Total duration of pass in MIN
PER WEEK
    T8(alt,thr)=(T8(alt,thr))/7 ; % Total duration of pass in MIN
PER DAY

    end

end

% Plot Visibility time per Day
figure
hold on
grid on
for alt=1:length(altitudes)
    plot(thresholds,T4(alt,:), 'r') ;
    plot(thresholds,T6(alt,:), 'g') ;
    plot(thresholds,T8(alt,:), 'b') ;

end
xlabel ('Minimum Elevation Angle[degree]') ;
ylabel ('Total duration per Day [minutes]') ;
legend('400 km', '600 km', '800 km') ;
title ('Visibility Time' ) ;

```

## B.4 Link Data Text File

Variable Name	UHF		VHF		BEACON		UNIT	DESCRIPTION
	Down	Up	Down	Up	Down	Up		
dir	1		2	1	2	1	2	na Auxiliary line to define Direction selected
f	438	438	145.9	145.9	438	438	MHz	Carrier frequency
A_el	90	90	90	90	90	90	degree	Assumed elevation angle throughout calculations
A_h	600	600	600	600	600	600	km	Assumed height above ground the satellite will orbit in
P_tx_w	1	75	1	100	0.1	75	W	Transmitted power (in linear scale)
L_tx_tl	6.7	8.48	5.9	6.26	6.7	8.48	dB	Transmitter passive losses
G_tx	2.15	16	2.15	13.1	2.15	16	dBi	Transmitter antenna gain
L_tx_pnt	0.2	0.7	0.2	0.7	0.2	0.7	dB	Transmitter antenna misalignment/pointing loss
L_plf	3	3	3	3	3	1.9	dB	Polarization loss factor (PLF)
L_fspl	140.73	140.73	131.18	131.18	148.69	148.69	dB	Free-Space Loss (FSPL)
L_atm	0.3	0.3	0.3	0.3	0.3	0.3	dB	Atmospheric loss (gases etc.)
L_ion	1.3	1.3	1.01	1.01	1.3	1.3	dB	Ionospheric loss
L_rain	0	0	0	0	0	0	dB	Rain loss
L_rx_pnt	0.7	0.2	0.7	0.2	0.7	0.2	dB	Receiver antenna misalignment/pointing loss Rx+Tx
G_rx	16	2.15	13.1	2.15	16	2.15	dBi	Receiver antenna gain
L_rx_tl	6.7	6.26	5.9	8.48	6.7	6.7	dB	Receiver transmission passive losses
T	786.04	522	1229.2	261	786.04	522	K	Effective Noise Temperature in receiver
R1	9600	9600	9600	9600	100	9600	bps	Data rate
R2	1800	1800	1800	1800	100	1200	bps	Data rate
B	25	25	25	25	1.2	25	kHz	Spectral (noise) bandwidth in receiver
EbNo_thr_fsk	12.5	12.5	12.5	12.5	12.5	12.5	dB	Required/minimum/threshold Eb/No for FSK
EbNo_thr_psk	9.5	9.5	9.5	9.5	9.5	9.5	dB	Required/minimum/threshold Eb/No for PSK
EbNo_thr_cqpsk	8.7	8.7	8.7	8.7	8.7	8.7	dB	Required/minimum/threshold Eb/No for Coded PSK

-----  
Syntax :

Everything between the two bars are interpreted as variables, and the rest as comments. The following syntax is used for the variable names:

f – Frequency

P – Power

L – Loss

G – Gain

T – Temperature

R – Datarate

B – Bandwidth

A – Parameters that are assumed to be something

SNR – Signal-to-noise ratio

EbNo – Bit-energy-to-noise-density ratio

Moreover descriptive subscripts are used to further specify what it is.

The following abbreviations are common:

rx – receiver

tx – transmitter

For downlink the spacecraft is the transmitter and the ground station

is the receiver. Note that for the uplink it's the other way around. First line is just an auxiliary y

for reader script that assigns 1 for Downlink and 2 for Uplink, values should not be changed.

Note: Values indicated are according to Analysis developed mainly in Chapter 3 of this work.

Nevertheless BEACON Uplink budget has been made according previous link budget information.

# Appendix C

## STK Link Budget

This appendix presents a summary of the Link Budget obtained on STK simulation. It corresponds to downlink execution for VHF band, only some passes, as a sample, are presented here due to size of entire file.

El(deg)	Rcvd. Iso. Power (dBW)	g/T (dB/K)	C/N (dB)	Eb/No (dB)	LM (dB)
0.111	-193.434	-15.56627	-24.5704	-21.4137	-34.114
3.16	-151.759	-14.200356	17.9601	21.1168	8.5192
6.691	-148.624	-13.515449	21.7806	24.9373	12.3396
10.398	-147.909	-13.486991	22.5241	25.6808	13.831
13.948	-147.527	-13.47438	22.9184	26.751	13.4774
16.558	-147.452	-13.468726	22.9987	26.1554	13.5577
17.2	-147.5	-13.4676	22.9521	26.1088	13.5111
15.536	-147.567	-13.470647	22.8816	26.383	13.4407
12.333	-147.813	-13.479033	22.6277	25.7844	13.1867
8.598	-148.368	-13.497311	22.541	25.2108	12.6131
4.905	-149.24	-13.54419	21.136	24.2926	11.695
1.452	-166.917	-15.11074	1.9915	5.1482	-7.4495
0.111	-193.546	-15.53184	-24.6798	-21.5232	-34.1208
0.111	-192.925	-15.56677	-24.617	-20.905	-33.5027
3.839	-151.272	-14.264178	18.3832	21.5399	8.9422
8.681	-147.339	-13.497072	23.838	26.2405	13.6429
14.971	-146.137	-13.471948	24.311	27.4677	14.87
23.988	-145.599	-13.459784	24.8607	28.174	15.4197
38.626	-147.834	-13.452805	22.6327	25.7894	13.1917
63.387	-163.1	-13.44908	7.3712	10.5278	-2.698
65.983	-167.662	-13.448898	2.809	5.9657	-6.6319
40.315	-148.93	-13.452343	21.537	24.6937	12.96
24.835	-145.964	-13.459071	24.4963	27.653	15.553
15.418	-146.311	-13.470837	24.1375	27.2941	14.6965
8.924	-147.453	-13.495005	22.9718	26.1285	13.5309
3.968	-152.13	-14.375741	17.5311	20.6878	8.902
0.101	-193.29	-15.52815	-24.1616	-21.49	-33.6026
0.111	-193.32	-15.52945	-24.1656	-21.89	-33.6065
1.334	-167.105	-15.21496	1.7931	4.9498	-7.6479
5.286	-147.624	-13.537114	22.7588	25.9154	13.3178
9.914	-146.191	-13.489497	24.2391	27.3957	14.7981
15.405	-144.985	-13.471014	25.4637	28.6204	16.227
21.66	-144.134	-13.461884	26.3243	29.481	16.8833
27.235	-143.838	-13.457506	26.624	29.7807	17.183
28.559	-143.88	-13.456733	26.5832	29.7399	17.1422
24.364	-144.63	-13.459462	26.3977	29.5544	16.9567
18.47	-144.707	-13.466262	25.7467	28.9034	16.3057
12.122	-145.791	-13.479774	24.6491	27.8058	15.2082
7.104	-147.133	-13.510363	23.276	26.4327	13.835
2.854	-152.828	-14.534014	16.5582	19.7148	7.1172
0.111	-192.492	-15.53755	-23.6263	-20.4696	-33.673
4.345	-147.558	-13.559465	22.8019	25.9586	13.3609
7.19	-146.549	-13.509891	23.8604	27.17	14.4194
9.643	-145.812	-13.490992	24.6167	27.7734	15.1758
11.154	-145.41	-13.483628	25.26	28.1827	15.5851
11.258	-145.401	-13.483179	25.357	28.1924	15.5947
9.916	-145.785	-13.489427	24.6451	27.8018	15.2041
7.552	-146.507	-13.50616	23.9066	27.633	14.4657
4.694	-147.509	-13.54976	22.8611	26.178	13.4201
1.706	-162.538	-14.986728	6.3954	9.5521	-3.456
0.111	-192.103	-15.55067	-23.2379	-20.812	-32.6789

# Appendix D

## Datasheets

Datasheets included in this part corresponds to proposed devices for On board system. Main features of installed elements at Earth station are attached as well; they were used to determines losses and noise system.



**RF5110G**

**3V GSM POWER AMPLIFIER**

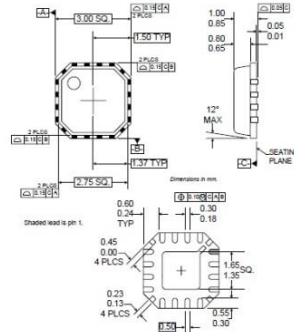
*RoHS & Pb-Free Product*

### Typical Applications

- 3V GSM Cellular Handsets
- 3V Dual-Band/Triple-Band Handsets
- GPRS Compatible
- Commercial and Consumer Systems
- Portable Battery-Powered Equipment
- FM Radio Applications: 150MHz/220MHz/450MHz/865MHz/915MHz

### Product Description

The RF5110G is a high-power, high-efficiency power amplifier module offering high performance in GSM OR GPRS applications. The device is manufactured on an advanced GaAs HBT process, and has been designed for use as the final RF amplifier in GSM hand-held digital cellular equipment and other applications in the 800MHz to 950MHz band. On-board power control provides over 70dB of control range with an analog voltage input, and provides power down with a logic "low" for standby operation. The device is self-contained with 50Ω input and the output can be easily matched to obtain optimum power and efficiency characteristics. The RF5110G can be used together with the RF5111 for dual-band operation. The device is packaged in an ultra-small 3mmx3mmx1mm plastic package, minimizing the required board space.



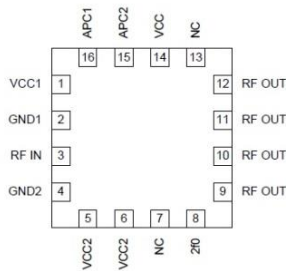
### Optimum Technology Matching® Applied

- |                                     |  |                                       |
|-------------------------------------|--|---------------------------------------|
| <input type="checkbox"/> Si BJT     | <input checked="" type="checkbox"/> GaAs HBT | <input type="checkbox"/> GaAs MESFET  |
| <input type="checkbox"/> Si Bi-CMOS | <input type="checkbox"/> SiGe HBT            | <input type="checkbox"/> Si CMOS      |
| <input type="checkbox"/> InGaP/HBT  | <input type="checkbox"/> GaN HEMT            | <input type="checkbox"/> SiGe Bi-CMOS |

**Package Style: QFN, 16-Pin, 3x3**

### Features

- Single 2.7V to 4.8V Supply Voltage
- +36dBm Output Power at 3.5V
- 32dB Gain with Analog Gain Control
- 57% Efficiency
- 800MHz to 950MHz Operation
- Supports GSM and E-GSM



**Functional Block Diagram**

### Ordering Information

RF5110G 3V GSM Power Amplifier  
RF5110GPCBA-410 Fully Assembled Evaluation Board

RF Micro Devices, Inc.  
7628 Thorndike Road  
Greensboro, NC 27409, USA

Tel (336) 664 1233  
Fax (336) 664 0454  
<http://www.rfmd.com>



# RF5110G

## Absolute Maximum Ratings

Parameter	Rating	Unit
Supply Voltage	-0.5 to +6.0	V <sub>DC</sub>
Power Control Voltage (V <sub>APC1,2</sub> )	-0.5 to +3.0	V
DC Supply Current	2400	mA
Input RF Power	+13	dBm
Duty Cycle at Max Power	50	%
Output Load VSWR	10:1	
Operating Case Temperature	-40 to +85	°C
Storage Temperature	-55 to +150	°C

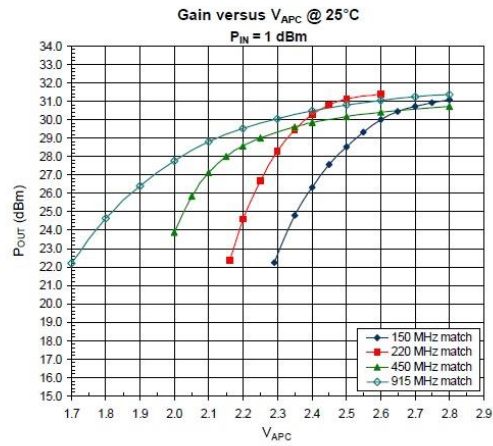
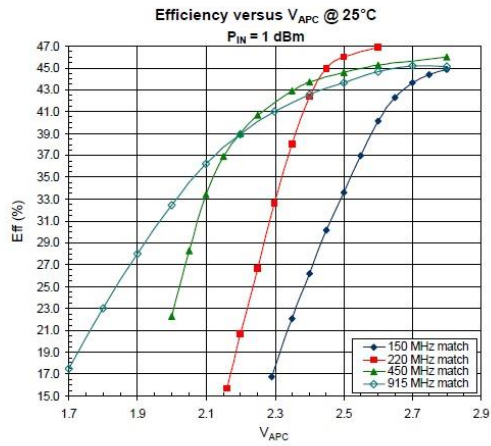
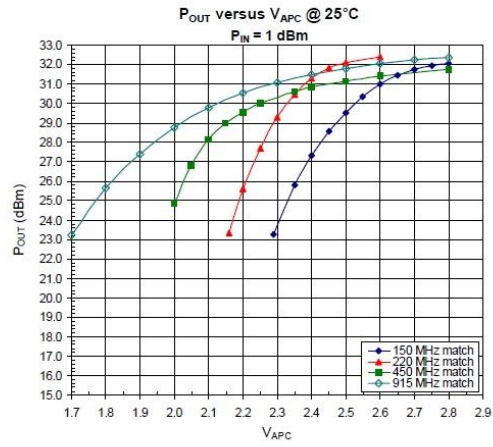
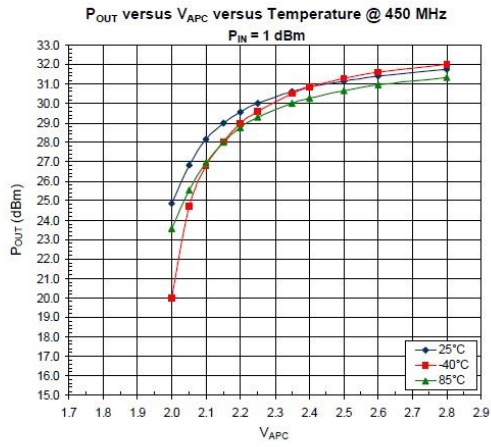


Caution! ESD sensitive device.

RF Micro Devices believes the furnished information is correct and accurate at the time of this printing. RoHS marking based on EU Directive 2002/95/EC (at time of this printing). However, RF Micro Devices reserves the right to make changes to its products without notice. RF Micro Devices does not assume responsibility for the use of the described product(s).

Parameter	Specification			Unit	Condition
	Min.	Typ.	Max.		
<b>Overall</b>					Temp=25°C, V <sub>CC</sub> =3.6V, V <sub>APC1,2</sub> =2.8V, P <sub>IN</sub> =+4.5dBm, Freq=880MHz to 915MHz, 37.5% Duty Cycle, pulse width=1731µs See evaluation board schematic. Using different evaluation board tune.
Operating Frequency Range		880 to 915		MHz	
Usable Frequency Range		800 to 950		MHz	
Maximum Output Power	33.8	34.5		dBm	Temp=25°C, V <sub>CC</sub> =3.6V, V <sub>APC1,2</sub> =2.8V
	33.1			dBm	Temp=+60°C, V <sub>CC</sub> =3.3V, V <sub>APC1,2</sub> =2.8V
Total Efficiency	50	57		%	At P <sub>OUT,MAX</sub> ; V <sub>CC</sub> =3.6V
		12		%	P <sub>OUT</sub> =+20dBm
		5		%	P <sub>OUT</sub> =+10dBm
Input Power for Max Output	+4.5	+7.0	+9.5	dBm	
Output Noise Power			-72	dBm	RBW=100kHz, 925MHz to 935MHz, P <sub>OUT,MIN</sub> <P <sub>OUT</sub> <P <sub>OUT,MAX</sub> , P <sub>IN,MIN</sub> <P <sub>IN</sub> <P <sub>IN,MAX</sub> , V <sub>CC</sub> =3.3V to 5.0V
			-81	dBm	RBW=100kHz, 935MHz to 960MHz, P <sub>OUT,MIN</sub> <P <sub>OUT</sub> <P <sub>OUT,MAX</sub> , P <sub>IN,MIN</sub> <P <sub>IN</sub> <P <sub>IN,MAX</sub> , V <sub>CC</sub> =3.3V to 5.0V
Forward Isolation			-22	dBm	V <sub>APC1,2</sub> =0.3V, P <sub>IN</sub> =+9.5dBm
Second Harmonic		-20	-7	dBm	P <sub>IN</sub> =+9.5dBm
Third Harmonic		-25	-7	dBm	P <sub>IN</sub> =+9.5dBm
All Other Non-Harmonic Spurious			-36	dBm	
Input Impedance		50		Ω	
Optimum Source Impedance		40+j10		Ω	For best noise performance
Input VSWR			2.5:1		P <sub>OUT,MAX</sub> -5dB<P <sub>OUT</sub> <P <sub>OUT,MAX</sub>
			4:1		P <sub>OUT</sub> <P <sub>OUT,MAX</sub> -5dB
Output Load VSWR					
Stability	8:1				Spurious<-36dBm, V <sub>APC1,2</sub> =0.3V to 2.6V, RBW=100kHz
Ruggedness	10:1				No damage
Output Load Impedance		2.6-j1.5		Ω	Load Impedance presented at RF OUT pad
<b>Power Control</b> V <sub>APC1</sub> V <sub>APC2</sub>					
Power Control "ON"	2.6			V	Maximum P <sub>OUT</sub> . Voltage supplied to the input
Power Control "OFF"	0.2	0.5		V	Minimum P <sub>OUT</sub> . Voltage supplied to the input
Power Control Range	75			dB	V <sub>APC1,2</sub> =0.2V to 2.6V
Gain Control Slope	5	100	150	dB/V	P <sub>OUT</sub> =-10dBm to +35dBm
APC Input Capacitance			10	pF	DC to 2MHz
APC Input Current		4.5	5	mA	V <sub>APC1,2</sub> =2.8V
			25	µA	V <sub>APC1,2</sub> =0V
Turn On/Off Time			100	ns	V <sub>APC1,2</sub> =0 to 2.8V

# RF5110G



## ADG918/ADG919

### FEATURES

- Wideband switch:  $-3$  dB @ 4 GHz
- Absorptive/reflective switches
- High off isolation (43 dB @ 1 GHz)
- Low insertion loss (0.8 dB @ 1 GHz)
- Single 1.65 V to 2.75 V power supply
- CMOS/LVTTL control logic
- 8-lead MSOP and tiny 3 mm  $\times$  3 mm LFCSP packages
- Low power consumption ( $<1$   $\mu$ A)

### APPLICATIONS

- Wireless communications
- General-purpose RF switching
- Dual-band applications
- High speed filter selection
- Digital transceiver front end switch
- IF switching
- Tuner modules
  - Antenna diversity switching

### GENERAL DESCRIPTION

The ADG918/ADG919 are wideband switches using a CMOS process to provide high isolation and low insertion loss to 1 GHz. The ADG918 is an absorptive (matched) switch having 50  $\Omega$  terminated shunt legs, whereas the ADG919 is a reflective switch. These devices are designed such that the isolation is high over the dc to 1 GHz frequency range. They have on-board CMOS control logic, thus eliminating the need for external controlling circuitry. The control inputs are both CMOS and

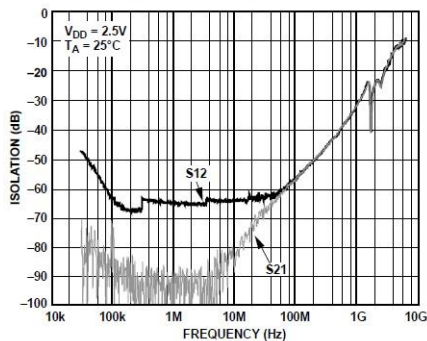


Figure 2. Off Isolation vs. Frequency

### Rev. C

Information furnished by Analog Devices is believed to be accurate and reliable. However, no responsibility is assumed by Analog Devices for its use, nor for any infringements of patents or other rights of third parties that may result from its use. Specifications subject to change without notice. No license is granted by implication or otherwise under any patent or patent rights of Analog Devices. Trademarks and registered trademarks are the property of their respective owners.

### FUNCTIONAL BLOCK DIAGRAMS

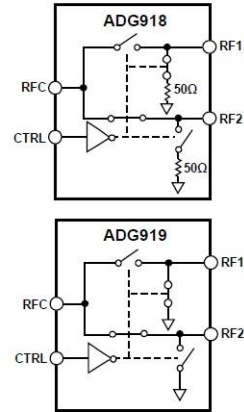


Figure 1.

LVTTL compatible. The low power consumption of these CMOS devices makes them ideally suited to wireless and general-purpose high frequency switching applications.

### PRODUCT HIGHLIGHTS

1.  $-43$  dB off isolation @ 1 GHz.
2. 0.8 dB insertion loss @ 1 GHz.
3. Tiny 8-lead MSOP/LFCSP packages.

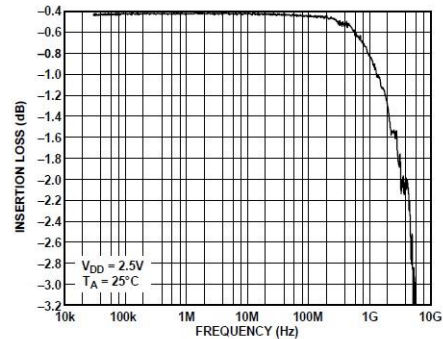


Figure 3. Insertion Loss vs. Frequency

## SPECIFICATIONS

$V_{DD} = 1.65\text{ V to }2.75\text{ V}$ ,  $GND = 0\text{ V}$ , input power = 0 dBm, all specifications  $T_{MIN}$  to  $T_{MAX}$ , unless otherwise noted. Temperature range for B Version:  $-40^{\circ}\text{C to }+85^{\circ}\text{C}$ .

Table 1.

Parameter	Symbol	Conditions	B Version			Unit
			Min	Typ <sup>1</sup>	Max	
<b>AC ELECTRICAL CHARACTERISTICS</b>						
Operating Frequency <sup>2</sup>			dc		2	GHz
3 dB Frequency <sup>2</sup>					4	GHz
Input Power <sup>3</sup>		0 V dc bias			7	dBm
		0.5 V dc bias			16	dBm
Insertion Loss	$S_{21}, S_{12}$	DC to 100 MHz; $V_{DD} = 2.5\text{ V} \pm 10\%$		0.4	0.7	dB
		500 MHz; $V_{DD} = 2.5\text{ V} \pm 10\%$		0.5	0.8	dB
		1000 MHz; $V_{DD} = 2.5\text{ V} \pm 10\%$		0.8	1.25	dB
Isolation—RFC to RF1/RF2 (CP Package)	$S_{21}, S_{12}$	100 MHz	57	60		dB
		500 MHz	46	49		dB
		1000 MHz	36	43		dB
Isolation—RFC to RF1/RF2 (RM Package)	$S_{21}, S_{12}$	100 MHz	55	60		dB
		500 MHz	43	47		dB
		1000 MHz	34	37		dB
Isolation—RF1 to RF2 (Crosstalk) (CP Package)	$S_{21}, S_{12}$	100 MHz	55	58		
		500 MHz	41	44		
		1000 MHz	31	37		
Isolation—RF1 to RF2 (Crosstalk) (RM Package)	$S_{21}, S_{12}$	100 MHz	54	57		
		500 MHz	39	42		
		1000 MHz	31	33		
Return Loss (On Channel) <sup>3</sup>	$S_{11}, S_{22}$	DC to 100 MHz	21	27		dB
		500 MHz	22	27		dB
		1000 MHz	22	26		dB
Return Loss (Off Channel) <sup>3</sup> ADG918	$S_{11}, S_{22}$	DC to 100 MHz	18	23		dB
		500 MHz	17	21		dB
		1000 MHz	16	20		dB
On Switching Time <sup>3</sup>	$t_{ON}$	50% CTRL to 90% RF		6.6	10	ns
Off Switching Time <sup>3</sup>	$t_{OFF}$	50% CTRL to 10% RF		6.5	9.5	ns
Rise Time <sup>3</sup>	$t_{RISE}$	10% to 90% RF		6.1	9	ns
Fall Time <sup>3</sup>	$t_{FALL}$	90% to 10% RF		6.1	9	ns
1 dB Compression <sup>3</sup>	$P_{-1\text{ dB}}$	1000 MHz		17		dBm
Third Order Intermodulation Intercept	$IP_3$	900 MHz/901 MHz, 4 dBm	28.5	36		dBm
Video Feedthrough <sup>4</sup>				2.5		mV p-p
<b>DC ELECTRICAL CHARACTERISTICS</b>						
Input High Voltage	$V_{INH}$	$V_{DD} = 2.25\text{ V to }2.75\text{ V}$	1.7			V
	$V_{INH}$	$V_{DD} = 1.65\text{ V to }1.95\text{ V}$	$0.65 V_{CC}$			V
Input Low Voltage	$V_{INL}$	$V_{DD} = 2.25\text{ V to }2.75\text{ V}$			0.7	V
	$V_{INL}$	$V_{DD} = 1.65\text{ V to }1.95\text{ V}$			$0.35 V_{CC}$	V
Input Leakage Current	$I_I$	$0\text{ V} \leq V_{IN} \leq 2.75\text{ V}$		$\pm 0.1$	$\pm 1$	$\mu\text{A}$

## ADG918/ADG919

Parameter	Symbol	Conditions	B Version			Unit
			Min	Typ <sup>1</sup>	Max	
CAPACITANCE <sup>3</sup>						
RF On Capacitance	C <sub>RF ON</sub>	f = 1 MHz		1.6		pF
CTRL Input Capacitance	C <sub>CTRL</sub>	f = 1 MHz		2		pF
POWER REQUIREMENTS						
V <sub>DD</sub>			1.65		2.75	V
Quiescent Power Supply Current	I <sub>DD</sub>	Digital inputs = 0 V or V <sub>DD</sub>		0.1	1	μA

<sup>1</sup> Typical values are at V<sub>DD</sub> = 2.5 V and 25°C, unless otherwise stated.

<sup>2</sup> Point at which insertion loss degrades by 1 dB.

<sup>3</sup> Guaranteed by design, not subject to production test.

<sup>4</sup> The dc transience at the output of any port of the switch when the control voltage is switched from high to low or low to high in a 50 Ω test setup, measured with 1 ns rise time pulses and 500 MHz bandwidth.



### FEATURES

- Low power, low IF transceiver
- Frequency bands
  - 135 MHz to 650 MHz, direct output
  - 80 MHz to 325 MHz, divide-by-2 mode
- Data rates supported
  - 0.15 kbps to 200 kbps, FSK
  - 0.15 kbps to 64 kbps, ASK
- 2.3 V to 3.6 V power supply
- Programmable output power
  - 20 dBm to +13 dBm in 63 steps
- Receiver sensitivity
  - 119 dBm at 1 kbps, FSK, 315 MHz
  - 114 dBm at 9.6 kbps, FSK, 315 MHz
  - 111.8 dBm at 9.6 kbps, ASK, 315 MHz
- Low power consumption
  - 17.6 mA in receive mode
  - 21 mA in transmit mode (10 dBm output)

- On-chip VCO and fractional-N PLL
- On-chip 7-bit ADC and temperature sensor
- Fully automatic frequency control loop (AFC) compensates for lower tolerance crystals
- Digital RSSI
- Integrated TRx switch
- Leakage current <1  $\mu$ A in power-down mode

### APPLICATIONS

- Low cost wireless data transfer
- Wireless medical applications
- Remote control/security systems
- Wireless metering
- Keyless entry
- Home automation
- Process and building control

FUNCTIONAL BLOCK DIAGRAM

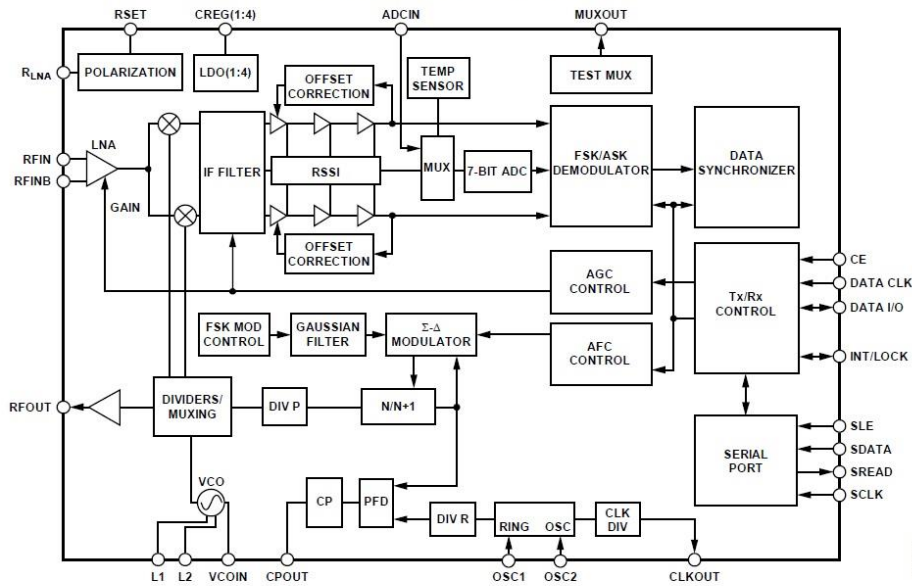


Figure 1.

Rev. 0  
Information furnished by Analog Devices is believed to be accurate and reliable. However, no responsibility is assumed by Analog Devices for its use, nor for any infringements of patents or other rights of third parties that may result from its use. Specifications subject to change without notice. No license is granted by implication or otherwise under any patent or patent rights of Analog Devices. Trademarks and registered trademarks are the property of their respective owners.

One Technology Way, P.O. Box 9106, Norwood, MA 02062-9106, U.S.A.  
Tel: 781.329.4700 [www.analog.com](http://www.analog.com)  
Fax: 781.461.3113 © 2005 Analog Devices, Inc. All rights reserved.

# ADF7020-1

## SPECIFICATIONS

$V_{DD} = 2.3\text{ V to }3.6\text{ V}$ ,  $GND = 0\text{ V}$ ,  $T_A = T_{MIN}$  to  $T_{MAX}$ , unless otherwise noted. Typical specifications are at  $V_{DD} = 3\text{ V}$ ,  $T_A = 25^\circ\text{C}$ . All measurements are performed using the EVAL-ADF7020-1-DBX and PN9 data sequence, unless otherwise noted.

Table 1.

Parameter	Min	Typ	Max	Unit	Test Conditions
<b>RF CHARACTERISTICS</b>					
Frequency Ranges (Direct Output)	135		650	MHz	See Table 5 for VCO bias settings at different frequencies
Frequency Ranges (Divide-by-2 Mode)	80		325	MHz	
VCO Frequency Range	1.1	1.2		Ratio	$F_{MAX}/F_{MIN}$ , using VCO bias settings in Table 5
Phase Frequency Detector Frequency	RF/256		20.96	MHz	PFD must be less than direct output frequency/31
<b>TRANSMISSION PARAMETERS</b>					
Data Rate					
FSK/GFSK	0.15		200	kbps	
OOK/ASK	0.15		64 <sup>1</sup>	kbps	
OOK/ASK	0.3		100	kbaud	Using Manchester biphas-L encoding
Frequency Shift Keying					
GFSK/FSK Frequency Deviation <sup>2,3</sup>	1		110	kHz	PFD = 3.625 MHz
	4.88		620	kHz	PFD = 20 MHz
Deviation Frequency Resolution	100			Hz	PFD = 3.625 MHz
Gaussian Filter BT		0.5			
Amplitude Shift Keying					
ASK Modulation Depth			30	dB	
OOK-PA Off Feedthrough		-50		dBm	
Transmit Power <sup>4</sup>	-20		+13	dBm	$V_{DD} = 3.0\text{ V}$ , $T_A = 25^\circ\text{C}$ , $FRF > 200\text{ MHz}$
Transmit Power	-20		+11	dBm	$V_{DD} = 3.0\text{ V}$ , $T_A = 25^\circ\text{C}$ , $FRF < 200\text{ MHz}$
Transmit Power Variation vs. Temp.		$\pm 1$		dB	From $-40^\circ\text{C}$ to $+85^\circ\text{C}$
Transmit Power Variation vs. $V_{DD}$		$\pm 1$		dB	From 2.3 V to 3.6 V at 315 MHz, $T_A = 25^\circ\text{C}$
Programmable Step Size					
-20 dBm to +13 dBm		0.3125		dB	See Figure 13 for how output power varies with PA setting
Integer Boundary		-55		dBc	50 kHz loop BW
Reference		-65		dBc	
<b>Harmonics</b>					
Second Harmonic		-27		dBc	Unfiltered conductive
Third Harmonic		-21		dBc	
All Other Harmonics		-35		dBc	
VCO Frequency Pulling, OOK Mode		30		kHz rms	DR = 9.6 kbps
Optimum PA Load Impedance <sup>5</sup>		79.4 + j64			FRF = 140 MHz
		109 + j64			FRF = 320 MHz
		40 + j47.5			FRF = 590 MHz

Parameter	Min	Typ	Max	Unit	Test Conditions
<b>RECEIVER PARAMETERS</b>					
FSK/GFSK Input Sensitivity					
Sensitivity at 1 kbps		-119.2		dBm	At BER = $1E-3$ , FRF = 315 MHz, LNA and PA matched separately <sup>6</sup>
Sensitivity at 9.6 kbps		-114.2		dBm	FDEV = 5 kHz, high sensitivity mode <sup>7</sup>
OOK Input Sensitivity					
Sensitivity at 1 kbps		-118.2		dBm	At BER = $1E-3$ , FRF = 315 MHz
Sensitivity at 9.6 kbps		-111.8		dBm	High sensitivity mode
LNA and Mixer, Input IP <sub>3</sub> <sup>7</sup>					
Enhanced Linearity Mode		6.8		dBm	Pin = -20 dBm, 2 CW interferers,
Low Current Mode		-3.2		dBm	FRF = 315 MHz, F1 = FRF + 3 MHz,
High Sensitivity Mode		-35		dBm	F2 = FRF + 6 MHz, maximum gain
Rx Spurious Emissions <sup>8</sup>					
			-57	dBm	<1 GHz at antenna input
			-47	dBm	>1 GHz at antenna input
AFC					
Pull-In Range		±50		kHz	IF_BW = 200 kHz
Response Time		48		Bits	Modulation index = 0.875
Accuracy		1		kHz	
<b>CHANNEL FILTERING</b>					
Adjacent Channel Rejection (Offset = ±1 × IF Filter BW Setting)					
		27		dB	IF filter BW settings = 100 kHz, 150 kHz, 200 kHz; desired signal 3 dB above the input sensitivity level; CW interferer power level increased until BER = $10^{-3}$ ; image channel excluded
Second Adjacent Channel Rejection (Offset = ±2 × IF Filter BW Setting)					
		50		dB	
Third Adjacent Channel Rejection (Offset = ±3 × IF Filter BW Setting)					
		55		dB	
Image Channel Rejection					
		35		dB	Image at FRF - 400 kHz
<b>CO-CHANNEL REJECTION</b>					
Wideband Interference Rejection					
		-2		dB	
		70		dB	Swept from 100 MHz to 2 GHz, measured as channel rejection
<b>BLOCKING</b>					
±1 MHz					
		60		dB	Desired signal 3 dB above the input sensitivity level, CW interferer power level increased until BER = $10^{-2}$
±5 MHz					
		68		dB	
±10 MHz					
		65		dB	
±10 MHz (High Linearity Mode)					
		72		dB	
Saturation (Maximum Input Level)					
		12		dBm	FSK mode, BER = $10^{-3}$
LNA Input Impedance					
		237 - j193		Ω	FRF = 130 MHz, RFIN to GND
		101.4 - j161.6		Ω	FRF = 310 MHz
		49.3 - j104.6		Ω	FRF = 610 MHz
RSSI					
Range at Input		-100 to -36		dBm	
Linearity		±2		dB	
Absolute Accuracy		±3		dB	
Response Time		150		μs	See the RSSI/AGC section



Parameter	Min	Typ	Max	Unit	Test Conditions
<b>POWER SUPPLIES</b>					
Voltage Supply V <sub>DD</sub>	2.3		3.6	V	All V <sub>DD</sub> pins must be tied together FRF = 315 MHz, V <sub>DD</sub> = 3.0 V, PA is matched to 50 Ω
Transmit Current Consumption 433 MHz, 0 dBm/5 dBm/10 dBm		13/16/21		mA	VCO_BIAS_SETTING = 2
Receive Current Consumption Low Current Mode		17.6		mA	VCO_BIAS_SETTING = 2
High Sensitivity Mode		20.1		mA	VCO_BIAS_SETTING = 2
Power-Down Mode Low Power Sleep Mode		0.1	1	μA	

<sup>1</sup> Higher data rates are achievable, depending on local regulations.

<sup>2</sup> For definition of frequency deviation, see the Register 2—Transmit Modulation Register (FSK Mode) section.

<sup>3</sup> For definition of GFSK frequency deviation, see the Register 2—Transmit Modulation Register (GFSK/GOOK Mode) section.

<sup>4</sup> Measured as maximum unmodulated power. Output power varies with both supply and temperature.

<sup>5</sup> For matching details, see the LNA/PA Matching section.

<sup>6</sup> Sensitivity for combined matching network case is typically 2 dB less than separate matching networks. See Table 11 for sensitivity values at various data rates and frequencies.

<sup>7</sup> See Table 6 for a description of different receiver modes.

<sup>8</sup> Follow the matching and layout guidelines to achieve the relevant FCC/ETSI specifications.

<sup>9</sup> This figure can be used to calculate the in-band phase noise for any operating frequency. Use the following equation to calculate the in-band phase noise performance as seen at the PA output:  $-198 + 10 \log(f_{\text{ref}}) + 20 \log N$ .

Parameter	Min	Typ	Max	Unit	Test Conditions
<b>POWER SUPPLIES</b>					
Voltage Supply V <sub>DD</sub>	2.3		3.6	V	All V <sub>DD</sub> pins must be tied together
Transmit Current Consumption  433 MHz, 0 dBm/5 dBm/10 dBm		13/16/21		mA	FRF = 315 MHz, V <sub>DD</sub> = 3.0 V, PA is matched to 50 Ω VCO_BIAS_SETTING = 2
Receive Current Consumption Low Current Mode		17.6		mA	VCO_BIAS_SETTING = 2
High Sensitivity Mode		20.1		mA	VCO_BIAS_SETTING = 2
Power-Down Mode Low Power Sleep Mode		0.1	1	μA	

<sup>1</sup> Higher data rates are achievable, depending on local regulations.

<sup>2</sup> For definition of frequency deviation, see the Register 2—Transmit Modulation Register (FSK Mode) section.

<sup>3</sup> For definition of GFSK frequency deviation, see the Register 2—Transmit Modulation Register (GFSK/GOOK Mode) section.

<sup>4</sup> Measured as maximum unmodulated power. Output power varies with both supply and temperature.

<sup>5</sup> For matching details, see the LNA/PA Matching section.

<sup>6</sup> Sensitivity for combined matching network case is typically 2 dB less than separate matching networks. See Table 11 for sensitivity values at various data rates and frequencies.

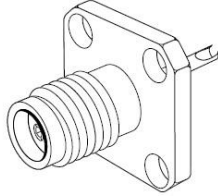
<sup>7</sup> See Table 6 for a description of different receiver modes.

<sup>8</sup> Follow the matching and layout guidelines to achieve the relevant FCC/ETSI specifications.

<sup>9</sup> This figure can be used to calculate the in-band phase noise for any operating frequency. Use the following equation to calculate the in-band phase noise performance as seen at the PA output:  $-198 + 10 \log(f_{RF}) + 20 \log N$ .

**SMA Connectors  
Jack Receptacle  
4 Hole Flange Mount  
Solder Pot**

- Overall Plating: Gold
- Body: Brass

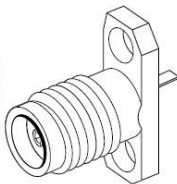


Order No.	Lead-free
73391-0040	Yes

RF/Microwave Coaxial Products

**SMA Connectors  
Jack Receptacle  
2 Hole Flange Mount  
Tab Terminal**

- Body: Stainless Steel, passivated



Order No.	Lead-free
73251-0280	Yes





**SP-6/ SP-2000/ SP-220/ SP-7000  
SUPER AMP GaAsFET SERIES  
50, 144, 220 & 432/435 MHz.  
Mast-Mounted Preamplifiers**

Thank you for purchasing this preamplifier which is manufactured by SSB ELECTRONIC GmbH. We believe that it is without a doubt the best available anywhere and would ask that you please spend a few moments to read through these notes in order to ensure that you obtain the very best possible results from this product.

The full potential of this preamplifier can only be realized when a minimum of feed line exists between the preamplifier input and the antenna feed point. Maximum lengths are: 24 ft. on 50/144MHz and 15 ft. on 432MHz assuming that a quality coax. such as AIRCOM PLUS is used. This length can usually be achieved by mounting the preamplifier on the support mast close to the antenna mounting point.

The amplification factor of this preamplifier can be adjusted so that a good system gain distribution can be maintained. This is important in order to insure that the receiver front-end as well as the mixer are not overloaded. The following table may be used as a guide for setting the preamplifier gain to overcome the feedline losses encountered from your rig to the preamp.

<u>CABLE LOSSES</u>	<u>GAIN SETTING</u>
Under 2 dB	MIN
2 - 3 dB	MID
Over 3 dB	MAX

The following table may be used as a guide to the losses for various cable types:

<u>Frequency</u>	<u>RG58U</u>	<u>RG213</u>	<u>AIRCOM PLUS</u>
144 MHz.	0.2 dB/M	0.08 dB/m	0.05 dB/M
432 MHz	0.4 dB/M	0.15 dB/m	0.08 dB/M

A good rule of thumb is to aim for 12 - 14 dB. of gain above feed line losses.

Access to the gain adjusting potentiometer is obtained by removing the four self tapping screws from the underside of the unit. This enables the plastic weather shield to be removed exposing the tin plated shielded box in which a small hole will be found. Adjustment may now be made with a small screwdriver. CAUTION: Great care should be taken when making this adjustment noting:

- The potentiometer only rotates through 270 deg.
- Do not exert any pressure on the adjuster
- Ensure the screwdriver goes to the pot, and does not slip sideways causing possible damage to any surrounding components. An insulated trimming tool would be best suited for this job!

If the tin plate box lid is removed to make this adjustment then please **DO NOT TOUCH ANY OTHER CONTROLS** as these have all been carefully set at the factory for the best noise figure.

**124 Cherrywood Drive., Mountaintop, Pa. 18707 (570)-868-5643**

**SPECIFICATIONS**

GENERAL			
• Frequency coverage (Unit: MHz)*1:			
Receive	0.030- 60.000**	136.000- 174.000**	
Transmit	420.000- 480.000**	1240.000- 1320.000**	
	1.800- 1.999	3.500- 3.999	
	5.255- 5.405**	7.200- 7.300	
	10.100- 10.150	14.000- 14.350	
	18.068- 18.168	21.000- 21.450	
	24.890- 24.990	28.000- 29.700	
	50.000- 54.000	144.000- 148.000	
	430.000- 450.000	1240.000- 1300.000**	
*1 Showing USA version, frequency coverage depends on version. ** Some frequency ranges are not guaranteed. ** With optional UX-9100.			
• Mode : USB, LSB, CW, RTTY (FSK), FM, AM*, DV (with UT-121)			
* Transmit HF/50MHz only. Cannot receive on 1200MHz band.			
• No. of memory channels : 396 Ch* (99 Ch for each HF/50, 144, 430/440, 1200MHz band)			
4 Call Ch* (1 Ch for each band)			
24 Scan edges* (6 Ch for each band)			
20 satellite and 50 GPS memories			
* With optional UX-9100.			
• Power supply requirement : 13.8V DC ±15 %			
• Operating temp. range : 0°C to +50°C; +32°F to +122°F			
• Frequency stability : Less than ±0.5ppm (0°C to +50°C)			
• Current drain (at 13.8V DC) : IC-9100 UX-9100			
TX Max. power 24.0A 9.0A			
FX Max. audio 4.5A 5.5A			
• Antenna connector : HF/50MHz SO-239 (500)×2			
144MHz SO-239 (500)			
430/440MHz Type-N (500)			
1200MHz Type-N (500) (With UX-9100)			
• Dimensions (W×H×D) : 315×116×94.3 mm; 12.4×4.57×3.5 in			
• Weight (approx.) : IC-9100 11kg; 24.3lb			
UX-9100 950g; 2.1lb			

TRANSMITTER				
• Modulation system : SSB Digital PSN modulation				
AM Digital Low power modulation				
FM Digital Phase modulation				
DV (With UT-121) GMSK Digital Phase modulation				
• Output power :				
	HF/50MHz	144MHz	440MHz	1200MHz**
SSB/CW/RTTY/FM/DV**	2-100W	2-100W	2-75W	1-10W
AM	2-30W	-	-	-
*1 With UX-9100 ** With UT-121				
• Spurious emissions (Unwanted emission) :				
1.8-29.7MHz Less than -50dB				
50, 144MHz Less than -43dB				
430/440MHz Less than -61.8dB				
1200MHz Less than -53dB (With UX-9100)				
• Carrier suppression : More than 40dB				
• Unwanted sideband : More than 55dB				
1200MHz More than 40dB (With UX-9100)				
• Microphone connector : 8-pin connector (600Ω)				

RECEIVER					
• Intermediate frequencies :					
HF/50MHz	64.455MHz, 36kHz				
144MHz	10.850MHz, 36kHz				
430/440MHz	7.125MHz, 36kHz				
1200MHz (With UX-9100)	243.950MHz, 10.950MHz, 36kHz				
• Sensitivity :					
	0.5-1.8MHz	1.8-29.7MHz	50-54MHz	144/440MHz	1200MHz**
SSB/CW	-	0.16µV**	0.13µV**	0.11µV	0.11µV
AM	12.6µV**	2.0µV**	1.6µV**	1.4µV	-
FM	-	0.5µV**	0.32µV**	0.18µV	0.18µV
DV**	-	1.0µV**	0.63µV**	0.35µV	0.35µV
SSB/CW, AM : 10dB S/N, FM : 12dB SINAD, DV : 1% BER					
** With UX-9100 ** With UT-121 ** Preamp-1 ON ** Preamp-2 ON ** 29-29.7MHz					

• Selectivity :					
SSB	More than 2.4kHz/-6dB				
(BW: 2.4kHz, sharp)	Less than 3.4kHz/-40dB				
CW	More than 500Hz/-6dB				
(BW: 500Hz, sharp)	Less than 700Hz/-40dB				
RTTY	More than 500Hz/-6dB				
(BW: 500Hz sharp)	Less than 800Hz/-40dB				
AM (BW: 6kHz)	More than 6.0kHz/-6dB				
	Less than 10.0kHz/-40dB				
FM (BW: 15kHz)	More than 12.0kHz/-6dB				
	Less than 22.0kHz/-40dB				
DV (with UT-121)	More than -50dB (12.5kHz spacing)				
1200MHz (With UX-9100)	More than 2.3kHz/-6dB				
SSB, CW	More than 15.0kHz/-6dB				
FM	More than 15.0kHz/-6dB				
• Squelch sensitivity (threshold):					
	HF	50MHz	144MHz	440MHz	1200MHz**
FM	0.3µV**	0.3µV**	0.18µV	0.18µV	0.18µV
SSB	5.6µV**	5.6µV**	1.0µV	1.0µV	1.0µV
*1 With UX-9100 ** Preamp-1 ON ** Preamp-2 ON					
• Spurious and image rejection ratio :					
HF/50MHz	More than 70dB*				
144, 430/440MHz	More than 60dB				
1200MHz	More than 50dB (With UX-9100)				
* Except IF through points on 50MHz band.					
• Audio output power : More than 2.0W at 10% distortion (at 13.8V DC)					
• EXT SP connectors : 2-conductor 3.5 (d) mm (1/4") ØQ					

Supplied accessories:	
• Hand microphone, HM-36	• Electronic keyer plug
• DC power cable	• ACC cable (13-pin)
• Spare fuses	

**OPTIONS**



**IC-PW1/IC-PW1EURO**  
HF+50MHz 1kW  
HF LINEAR AMPLIFIER

Covers all HF and 50MHz bands, provides clean, stable 1kW output. Automatic antenna tuner and compact detachable controller are standard. 2 exciter inputs are available.



**AH-2b ANTENNA ELEMENT**  
For mobile operation with the AH-4. All bands between 7-54 MHz can be matched.



**AH-4 HF+50MHz AUTOMATIC ANTENNA TUNER**  
Covers 0.5-54MHz with a 7m (23ft) or longer wire antenna.



**PS-126 DC POWER SUPPLY**  
13.8V DC, 25A max, with 4-pin type connector.



**HM-36 HAND MICROPHONE**  
Same as supplied.



**SM-50 DESKTOP MICROPHONE**  
Unidirectional, dynamic microphone. LUP/DND switches and low cut function are available.



**SM-30 DESKTOP MICROPHONE**  
Compact, lightweight electret microphone. Low cut function is available. SM-20 is also available.



**CT-17 CH-V LEVEL CONVERTER**  
For external transceiver control using a PC with an RS-232C.



**SP-21 EXTERNAL SPEAKER**  
Input impedance: 8Ω  
Max. input power: 5W



**SP-23 EXTERNAL SPEAKER**  
4 audio filters; headphone jack. Input impedance: 8Ω  
Max. input power: 5W



**UX-9100 1200MHz BAND UNIT**  
Allows you to operation on the 1200MHz band.



**UT-121 D-STAR UNIT**  
Provides D-STAR DV mode capability at 4.8kSPs (Voice + Data).



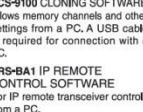
**FL-430 6kHz 1st IF FILTER**  
**FL-431 3kHz 1st IF FILTER**  
1st IF filters for HF/50MHz band.




**OPC-1529R DATA CABLE**  
For D-STAR DV mode or GPS receiver connection. (Data 1 Jack (IC-9100) to RS-232C)



**OPC-599 CABLE ADAPTER**  
Converts 13-pin ACC connector to 7-pin + 8-pin ACC connector.



**CS-9100 CLONING SOFTWARE**  
Allows memory channels and other settings from a PC. A USB cable is required for connection with a PC.



**MB-123 CARRYING HANDLE**  
Same as supplied.

Icom, Icom Inc. and the Icom logo are registered trademarks of Icom Incorporated (Japan) in the United States, the United Kingdom, Germany, France, Spain, Russia, Japan and/or other countries.

**Icom Inc.** 1-1-32, Kami-minami, Hirano-ku, Osaka 547-0003, Japan Phone: +81 (06) 6793 5302 Fax: +81 (06) 6793 0013 [www.icom.co.jp/world](http://www.icom.co.jp/world) **Count on us!**

**Icom America Inc.**  
2380 116th Avenue NE,  
Bellevue, WA 98004, U.S.A.  
Phone: +1 (425) 454-4155  
Fax: +1 (425) 454-1509  
E-mail: [sales@icomamerica.com](mailto:sales@icomamerica.com)  
URL: <http://www.icomamerica.com>

**Icom New Zealand**  
146A Harris Road, East Tamaki,  
Auckland, New Zealand  
Phone: +64 (0) 274 4062  
Fax: +64 (0) 274 4708  
E-mail: [inquiries@icom.co.nz](mailto:inquiries@icom.co.nz)  
URL: <http://www.icom.co.nz>

**Icom (UK) Ltd.**  
Blacksale House, Altra Park,  
Herne Bay, Kent, CT6 6GZ, U.K.  
Phone: +44 (0)1227 741741  
Fax: +44 (0)1227 741742  
E-mail: [info@icomuk.co.uk](mailto:info@icomuk.co.uk)  
URL: <http://www.icomuk.co.uk>

**Asia Icom Inc.**  
6F No. 88, Sec. 1 Cheng-Teh Road,  
Taipei, Taiwan, R.O.C.  
Phone: +886 (02) 2559 1899  
Fax: +886 (02) 2559 1874  
E-mail: [sales@asia-icom.com](mailto:sales@asia-icom.com)  
URL: <http://www.asia-icom.com>

**Icom Canada**  
Glenwood Centre #150-6165 Highway 17,  
Delta, B.C., V4K 5B8, Canada  
Phone: +1 (604) 952-4266  
Fax: +1 (604) 952-0090  
E-mail: [info@icomcanada.com](mailto:info@icomcanada.com)  
URL: <http://www.icomcanada.com>

**Icom (Europe) GmbH**  
Communication Equipment  
Auf der Krautweide 24  
65812 Bad Soden am Taunus, Germany  
Phone: +49 (6196) 76685-0  
Fax: +49 (6196) 76685-50  
E-mail: [info@icom-europe.com](mailto:info@icom-europe.com)  
URL: <http://www.icomeurope.com>

**Icom France s.a.s.**  
Zac de la Plaine,  
1 Rue Brédarion des Moulinets, BP 45804,  
31505 Toulouse Cedex 5, France  
Phone: +33 (5) 61 36 03 03  
Fax: +33 (5) 61 36 03 00  
E-mail: [icom@icom-france.com](mailto:icom@icom-france.com)  
URL: <http://www.icom-france.com>

**Beijing Icom Ltd.**  
10C07, Long Silver Mansion, No.88, Yong Ding  
Road, Haidian District, Beijing, 100039, China  
Phone: +86 (010) 5889 5391/5392/5393  
Fax: +86 (010) 5889 5395  
E-mail: [bjicom@bjicom.com](mailto:bjicom@bjicom.com)  
URL: <http://www.bjicom.com>

**Icom (Australia) Pty. Ltd.**  
Unit 1 / 103 Garden Road,  
Clayton, VIC 3168 Australia  
Phone: +61 (03) 9549 7500  
Fax: +61 (03) 9549 7505  
E-mail: [sales@icom.net.au](mailto:sales@icom.net.au)  
URL: <http://www.icom.net.au>

**Icom Spain S.L.**  
Ctra.Rubi, No. 88 "Edificio Can Castanyer"  
Bajos A 08174, Sant Cugat del Valles,  
Barcelona, Spain  
Phone: +34 (93) 580 26 70  
Fax: +34 (93) 589 04 48  
E-mail: [icom@icomspain.com](mailto:icom@icomspain.com)  
URL: <http://www.icomspain.com>

**Icom Polska**  
81-500 Sopot, ul.3 Maja 54, Poland  
Phone: +48 (58) 550 7135  
Fax: +48 (58) 550 7135  
E-mail: [icompolka@icompolka.com.pl](mailto:icompolka@icompolka.com.pl)  
URL: <http://www.icompolka.com.pl>

Your local distributor/dealer:



## Aircell®7

### Technical data

Centre conductor ...	stran. copper, oxy. free, 19x0,37 mm
Centre conductor Ø	1,85 mm
Dielectric	PE, low-loss compound
Dielectric Ø	5,0 mm
Outer conductor 1	copperfoil, PE-coated
Shielding factor	100 %
Outer conductor 2	copper braid
Shielding factor	70 %
Sheath	black PVC, UV-resistant
Outer diameter Ø	7,3 mm
Weight	72 g/m
Min. bending radius ...	one single bending ..... 25 mm
	15 repeated bendings..... 50 mm
Temperature range	-30 bis +80°C
Pulling strength	2 daN

### Typ. attenuation (dB/100 m @ 20°C)

5 MHz	1,6	1000 MHz	21,52
10 MHz	2,2	1296 MHz	24,84
50 MHz	4,52	1500 MHz	27,08
100 MHz	6,28	1800 MHz	30,0
144 MHz	7,6	2000 MHz	31,88
200 MHz	9,04	2400 MHz	35,6
300 MHz	11,2	3000 MHz	40,88
432 MHz	13,6	4000 MHz	49,12
500 MHz	14,72	5000 MHz	57,04
800 MHz	19,0	6000 MHz	64,9

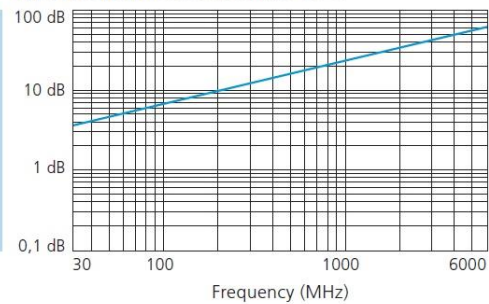
### Max. power handling (W @ 40°C)

10 MHz	2040	1000 MHz	180
100 MHz	620	2000 MHz	120
500 MHz	260	3000 MHz	90

### Electrical specifications

Impedance	50 Ω
Capacity	75 pF/m
Velocity factor	0,83
fmax	6 GHz
Screening efficiency @ 1 GHz	83 dB
DC-resistance	
Centre conductor	8,6 Ω/km
Outer conductor	8,5 Ω/km
RF peak voltage	0,7kV

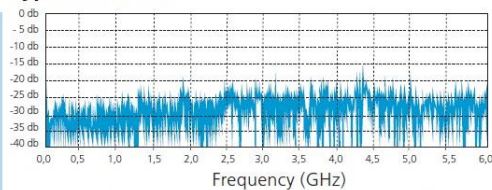
### Typ. Attenuation (dB/100 m) @ 20°C



### Aircell 7    RG 213/U    RG 58/U

Capacity	75 pF/m	101 pF/m	102 pF/m
Velocity factor	0,83	0,66	0,66
Attenuation (dB/100 m)			
10 MHz	2,2	2,0	5,0
100 MHz	6,28	7,0	17,0
500 MHz	14,72	17,0	39,0
1000 MHz	21,52	22,5	54,6
3000 MHz	40,88	58,5	118

### Typ. Return loss

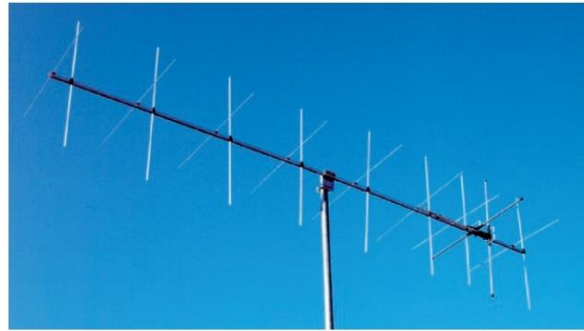


Due to production tolerances the RTL may have different characteristics.

# 2x9 elements Yagi antenna

144 to 146 MHz

Part Nr. 220818



### Electrical data

#### Radiation at 144.5 MHz

Effective electrical length .....	: 1.65 $\lambda$
Isotropic gain .....	: 13.1 dBi
Aperture angle @ -3 dB	
- E-plane .....	: 2 x 20.2°
- H-plane .....	: 2 x 23.0°
First side lobe set	
- E-plane .....	: - 20.5 dB @ 54°
- H-plane .....	: - 13.6 dB @ 58°
Rear protection .....	: - 19 dB
Average stray radiation	
- E-plane .....	: - 35 dB
- H-plane .....	: - 24 dB

### Bandwidth

Gain @ -1 dB .....	
Nominal impedance .....	: 140 to 148 MHz
Impedance match bandwidth @ SWR <1.3/1.....	: 50 $\Omega$
Acceptable RF power (continuous duty) .....	: 143.4 to 146.2 MHz
Required phase delay between frontmost and rearmost driven element .....	: 1000 W

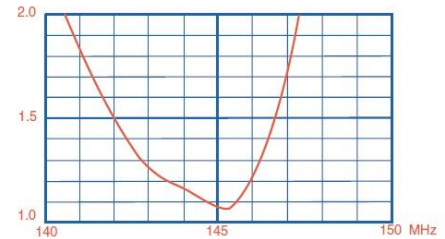
### Array of 2 or 4 antennas

.....	: 72°
(optimized stacking distance. from center to center of elements. for minimal side lobe radiation)	
- Electrical distance .....	: 1.33 $\lambda$
- Pratical distance .....	: 2.77 m

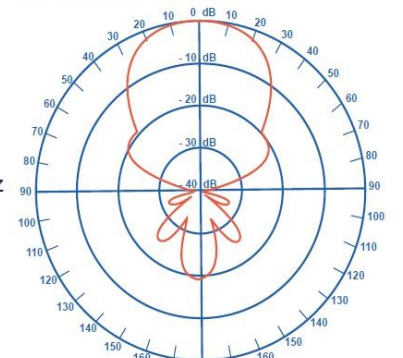
### Mechanical data

Connector .....	: N
Overall length .....	: 3.57 m
Mass .....	: 3.3 kg
Effective wind load.....	: 0.15 m <sup>2</sup>
Approximate wind load (25 m/s - 55 mph) .....	: 5.6 daN
Approximate wind load (45 m/s - 100 mph) .....	: 18.2 daN

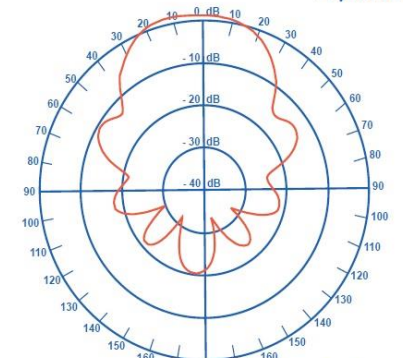
SWR curve



Radiation patterns



E plane



H plane

